Jason-3 validation and cross calibration activities (Annual report 2022)

Contract N° 200443 / Lot 1.8.1
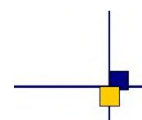
Chronology Issues:		
Issue:	Date:	Reason for change:
0.0	2022-12-15	Creation
1.0	2023-20-01	Version delivered to CNES for reviewing
1.1	2023-22-03	Version delivered to CNES after reviews

People involved in this issue :				
	AUTHORS	COMPANY	DATE	INITIALS
Written by:	B. Flamant	CLS		
Checked by:		CLS		
Approved by:		CLS		
		CLS		
Application authorised by:	F. Bignalet-Cazalet	CNES		

Index Sheet :	
Context:	
Keywords:	
Hyperlink:	

Distribution:		
Company	Means of distribution	Names
CLS/BU ENV	electronic copy	F.Mertz
CNES	electronic copy	thierry.guinle@cnes.fr
		nicolas.picot@cnes.fr
		francois.bignalet-cazalet@cnes.fr
		gerald.dibarboure@cnes.fr
		aqgp_rs@cnes.fr
		dominique.chermain@cnes.fr

List of Tables

List of Figures

Jason-3 validation and cross calibration activities (Annual report 2022)

Nomenclature : SALP-RP-MA-EA-23597-CLS   i.3

Document version: 1.1   Date : January 23, 2022
. . . .

List of items to be defined or to be confirmed

Applicable documents / reference documents

Contents

Glossary

AMR Advanced Microwave Radiometer

CLS Collecte Localisation Satellites

CNES Centre National d'Etudes Spatiales

CNG Consigne Numerique de Gain (= Automatic Gain Control)

DEM Digital Elevation Model

DIODE Détermination Immédiate d'Orbite par Doris Embarqué

ECMWF European Centre for Medium-range Weather Forecasting

GDR Geophysical Data Record

GIM Global Ionosphere Maps

GOT Global Ocean Tide

IGDR Interim Geophysical Data Record

JPL Jet Propulsion Laboratory (Nasa)

MLE Maximum Likelyhood Estimator

MOE Medium Orbit Ephemeris

MQE Mean Quadratic Error

MSS Mean Sea Surface

PLTM PayLoad TeleMetry

POE Precise Orbit Ephemeris

OGDR Operational Geophysical Data Record

SALP Service d'Altimétrie et de Localisation Précise

SSH Sea Surface Height

SLA Sea Level Anomaly

SLR Satellite Laser Ranging

SSB Sea State Bias

SWH Significant Wave Height

TM TeleMetry

1. Introduction

This document presents the synthesis report concerning validation activities of Jason-3 data (Geophysical Data Records (GDRs), as well as Interim and Operational Data Records (I/OGDR)) under SALP contract (N° 200443/Lot 1.8.1) supported by CNES at the CLS Environment & Climate Business Unit.

History

Jason-3 satellite was successfully launched on the 17th of January 2016. Since February 12th, Jason-3 is on its operational orbit to continue the long term climate data record on the primary TOPEX, Jason-1, and OSTM/Jason-2 ground track. Until October 2nd, 2016, Jason-3 and Jason-2 were in tandem flight, with only 80 seconds delay, before Jason-2 was moved to the same interleaved orbit that was used by TOPEX from 2002 to 2005 and Jason-1 from 2009 to 2012. Jason-2 was on its repetitive interleaved position until May 17th 2017, then was moved on a first Long Repeat Orbit from July 11th 2017 to July 18th 2017, and finally was on a second interleaved long repeat orbit from July 25th 2018 to the end of the mission on October 1st 2019. After tandem phase with Jason-2, Jason-3 has become the reference mission in DUACS system from mid-september 2016 onwards. On February 24th 2019 at 09:57:16, Jason-3 entered in Safe Hold Mode (SHM). This SHM ended 10 days after on March 6th 2019 at 08:44:21. On April 6th 2019 at 23:17:22, another SHM occured. This SHM lasted for around 7 days and ended on April 12th 2019 at 02:20:01. Over 2020, Jason-3 has triggered a SHM 3 times : on January 31st 2020 at 04:51:17 for 6 days until February 5th 2020 at 09:37:14 and on the same day at 21:00:53 for 8 other days until February 13th 2020 at 08:42:44. The last Safe Hold Mode of the year occured on June 15th 2020 at 21:50:42 and lasted for around 4 days until June 15th 2020 at 21:50:42. In addition, due to a DORIS anomaly, Jason-3 data are unavailable between October 27th 2020 at 13:23:01 and October 29th 2020 at 11:36:00. Jason-3 was also used as a reference to perform the tandem phase with Sentinel-6 / Michael Freilich. During the year 2022, the success of this tandem phase lead to Jason-3 orbit change to leave the place to Sentinel-6. At the end of the tandem phase, Jason-3 was moved to an interleaved orbit. The maneuver took place between April 7th 2022 and April 25th 2022 and it was decided to start over the cycle count at 300.

Over 2022, specific events observed for Jason-3 are :

- A DEM patch upload over cycle 215 (from 09/12/2021 17:25:04 to 09/12/2021 17:25:18);

- A ground segment anomaly over cycle 219 (from 20/01/2022 19:25:51 to 20/01/2022 21:13:32);

- A second ground segment anomaly over cycle 220 (from 04/02/2022 06:18:20 to 04/02/2022 07:14:33);

- A maneuver to change the satellite's orbite (from 07/04/2022to 25/04/2022);

- A DORIS restart at the end of the maneuver (18/04/2022 14:18:36);

- A radiometer restart at the end of the maneuver due to repetitive AMR errors (28/04/2022 15:55:45);

- A DEM patch upload over cycle 316 (from 27/09/2022 07:02:00 to 29/09/2022 07:48:00);

- Several DORIS restarts leading to data loss over ocean for cycles 312, 315, 319, 322 and 323.

. **CalVal activities**

Since the beginning of the mission, Jason-3 data have been analyzed and monitored in order to assess the quality of Jason-3 products. Cycle per cycle reports summarizing mission performance are generated

and made available through the AVISO web page [1]. Please note that analyses are done **over ocean** only, no assesment is done over hydrological targets. This encompasses several points, which are either part of Cal/Val routine activities or following mission events:

— mono-mission validation and monitoring,

— Jason-3/Jason-2 cross-calibration (2016),

— Sentinel-6/Jason-3 cross-calibration (2021),

— accuracy and stability of SLA measurements check,

— specific studies and investigations.

Overview

The present document assesses Jason-3 data quality and mission performance **over ocean**. After an executive summary in the following pages, dedicated sections of this report deal with:

— description of data processing,

— data coverage / availability,

— monitoring of rejected spurious data,

— analysis of relevant parameters derived from instrumental measurements and geophysical corrections.

— system performance via analyses at crossover points,

— system performance via along-track Sea Level Anomalies monitoring,

— long-term monitoring and contribution to climate surveys.

Even though Sentinel-6 became the reference mission over the year 2022, this document does not focus on Sentinel-6/Jason-3 cross-calibration since it is extensively described in Sentinel-6 2022 Annual Report.

---

[1]http://www.aviso.altimetry.fr/en/data/calval/systematic-calval/validation-reports.html

By succeeding to TOPEX/Poseidon, Jason-1 and Jason-2 on their primary ground track, Jason-3 has extended the high-precision ocean altimetry data record [1]. It was launched on January 17th 2016 and is still on orbit at this date.

Tandem Phase with Jason-2

During Jason-3 tandem phase with Jason-2 (February 12th to October 2nd 2016), both satellites were on the same ground-track (with only 80 seconds delay), which was a unique opportunity to precisely assess parameter discrepancies between both missions and detect geographically correlated biases, jumps or drifts. At the end of this tandem phase, Jason-3 was declared fully operational and became the reference mission for the GMSL computation, and Jason-2 continued its mission on another orbit.

Reference Mission Period

From October 2nd 2016 to April 7th 2022, during 5,5 years, Jason-3 was the reference mission for the GMSL computation. OGDR and IGDR products have been publicly available since June 30th 2016. OGDRs were firstly generated in version "T" for the first cycles, and then turned into "D" version. GDR products have been available in version "T" since early October 2016 (more details on products versions on Jason-3 handbook [2]). **From cycle 174 onwards (29/10/2020), respectively cycle 171 onwards (29/09/2020), IGDR and GDR have been produced in standard F. The complete reprocessing to standard "F" of the GDR data was achieved during 2021.** [see OSTST2020 dedicated presentation[3]]. GDR data have been distributed in standard F from cycle 171 onwards (16/12/2020).

During each cycle, missing measurements were monitored, spurious data were edited and relevant parameters derived from instrumental measurements and geophysical corrections were analysed for OGDR, IGDR and GDR. Please note that analysis are done **over ocean** only, no assessment is done over hydrological targets. GDR cyclic reports are publicly available [4].

Tandem Phase with Sentinel-6 / Michael Freilich

In order to insure the extension of the legacy of sea-surface height measurements, Sentinel-6 / Michael Freilich satellite was launched on November 21st 2020: it reached Jason-3 orbit at end of december 2020. From cycle 179 onwards (18/12/2020), Jason-3 is used as a reference for Sentinel-6 tandem phase. At the end of cycle 226 (07/04/2022), the tandem-phase is completed and Sentinel-6 takes the lead as the Reference Altimetry Mission.

Please note the change in orbit standard solution available in the products:

– **GDR-F data orbit solution is POE-F ;**

– **until Jason-3 cycle 094, MOE-E orbit standard is available in IGDR products (MOE-F from cycle 095 onwards) ;**

– **from Jason-3 cycle 113 onwards, MOE orbit standard uses both DORIS and GPS data.**

---

[1] https://www.aviso.altimetry.fr/?id=601&L=0
[2] https://www.aviso.altimetry.fr/fileadmin/documents/data/tools/hdbk_j3.pdf
[3] https://meetings.aviso.altimetry.fr/fileadmin/user_upload/tx_ausyclsseminar/files/CVL_J3_GDRF_ready_v02_ostst2020_02.pdf
[4] https://www.aviso.altimetry.fr/en/data/calval/systematic-calval/validation-reports/jason-3-gdr.html

Data availability

Data availability is excellent for Jason-3. Jason-3 presents 99.3% of data availability over ocean after removing specific events (99.98% for Jason-2, see figure 1). Such events occured only a few times over Jason-3 full period. **Some of these events occured during 2022**:

– during cycle 3, where 21.02% of measurements are missing due to the GPS platform upload,

– during cycle 57, where 1.76% of measurements are missing due to the DEM-onboard upload.

– during cycles 112/113, where 79.89% (for cycle 112) and 24.21% (for cycle 113) of measurements are missing due to SHM from 24/02/2019 09:57:16 until 06/03/2019 08:44:21.

– during cycle 116, where 53.19% of measurements are missing due to SHM from 06/04/2019 23:17:22 until 12/04/2019 02:20:01.

– during cycles 146/147, SHM occured from 31/01/2020 04:51:17 until 05/02/2020 09:37:14, and another time from 05/02/2020 21:00:53 until 13:02:2020 08:42:44. Due to those SHM events, missing data rate is 38.94% for cycle 146 and 88.81% for cycle 147.

– during cycle 160, SHM occured from 15/06/2020 21:50:42 until 19/06/2020 07:32:46. Due to this SHM event, missing data rate is 33.58% for cycle 160.

– during cycles 173/174, there is a DORIS anomaly from 27/10/2020 13:23:01 until 29/10/2020 11:36:00. Due to this event, missing data rate is 13.46% for cycle 173 and 7.02% for cycle 174.

– between cycle 227 and cycle 300 : Orbit change maneuver from 07/04/2022 until 25/04/2022. Over this event, the altimeter is off and the radiometer does not send any data.

– during cycle 316, where 1.4% of measurements are missing due to the DEM-onboard upload.
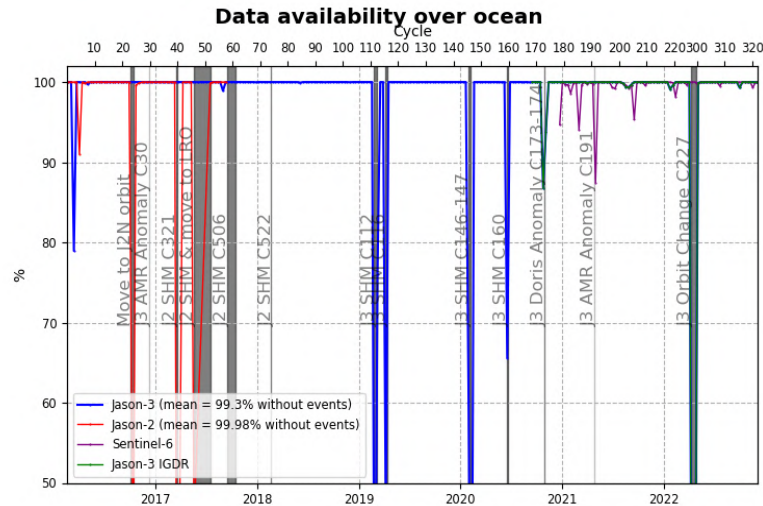
Figure 1 – Jason-2 and Jason-3 GDR data availability over ocean (per cycle)

Sea Level Anomalies

During Sentinel-6 tandem phase with Jason-3, the averaged difference of gridded SLA shows little difference between both missions as they have a very small temporal shift, similar to Jason-2/Jason-3 tandem phase. One noticeable difference between both missions is the dependency of range to SWH for Sentinel-6. This issue has been resolved, just like the equatorial band in the map difference. See Analysis of the Sentinel-6A SLA biais correction.

The daily monitoring of mean SLA for Jason-3 is computed on figure 2. The orbit change over 2022 had no impact on the SLA stability of Jason-3 mission which shows a strong consistency with what was previously observed.
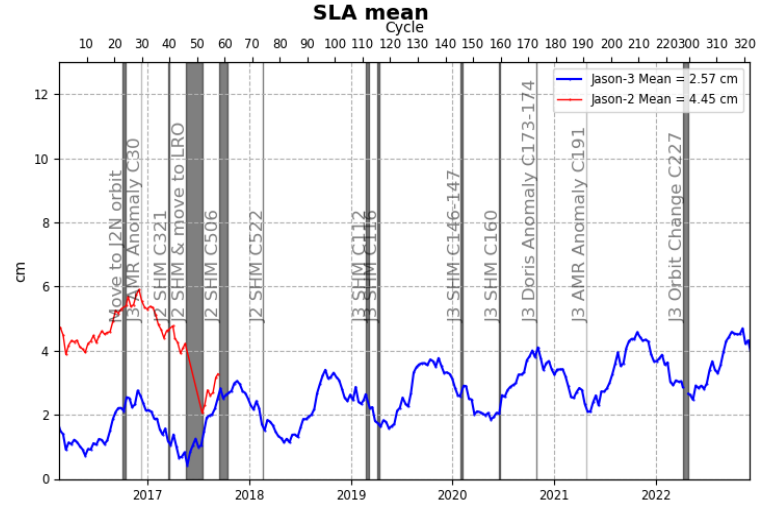
Figure 2 – Daily monitoring of SSH bias between Jason-2 and Jason-3 before Jason-2 moved to interleaved ground-track in October 2016 (using GDRD data for Jason-2 only).

Performances at crossover points

Looking at SSH difference at crossovers (red curve on figure 5), a 120 day signal is way less visible than before on the mean for Jason-3 GDR data now that the orbit standard is homogeneous for the whole record (standard-F).

Concerning SSH error at crossover points (*standard deviation* / $\sqrt{2}$), Jason-3 mission show very good and stable performances with an error of 3.39 cm (3.48 cm for Jason-2). This satisfying performance is confirmed from cycle 15 onwards for Sentinel-6.
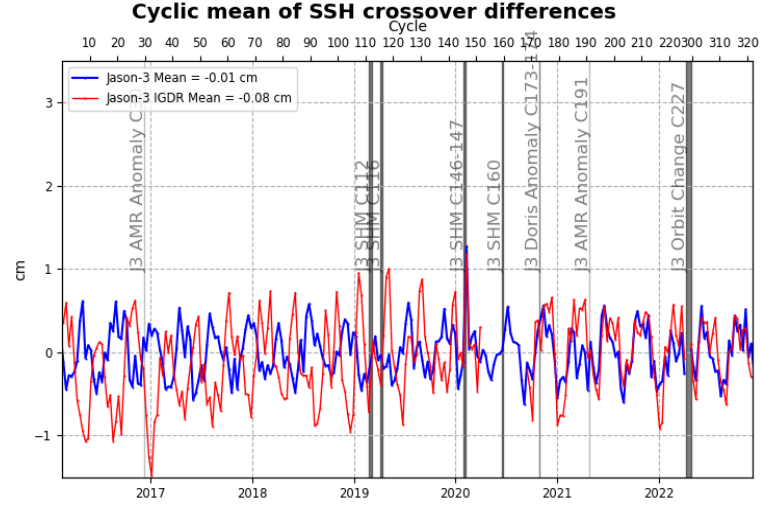
Figure 3 – Monitoring of mean of Jason-3 SSH crossover differences for IGDRs and GDRs. Only data with |latitude| < 50˚, bathymetry < -1000m and low oceanic variability were selected. (ocean_tide_sol1 = FES is used in SSH computation)
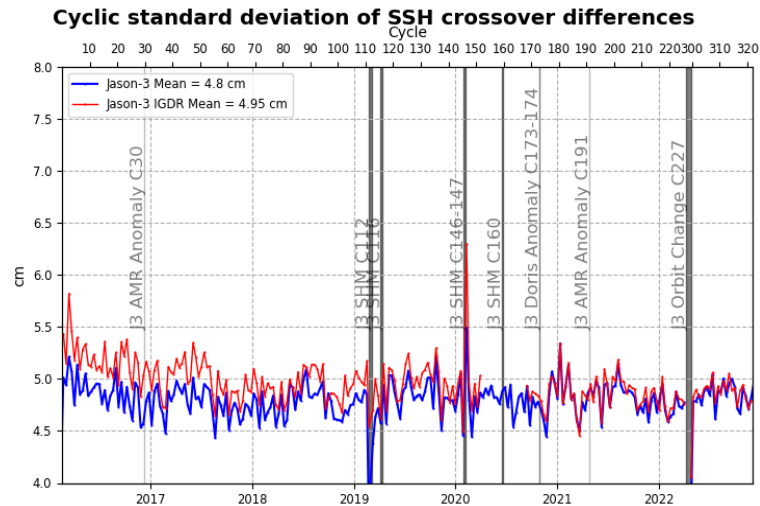
Figure 4 – Cycle by cycle standard deviation of SSH crossover differences for Jason-3. Only data with |latitude| < 50˚, bathymetry < -1000m and low oceanic variability was selected.

The mean SSH differences at Jason-3 crossovers is highly stable and around 3cm in average (figure 5), thus proving the accuracy of Jason-3 as the reference mission.
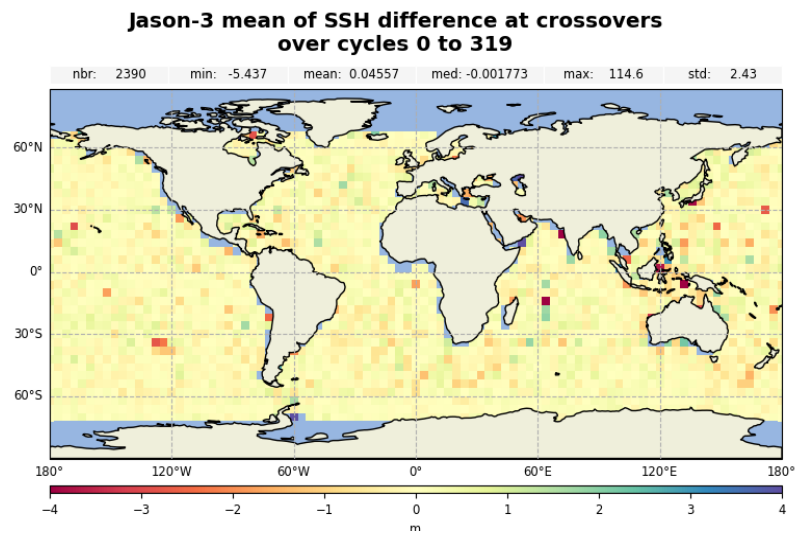
Figure 5 – Map of Jason-3 SSH crossover differences over cycles 1 to 319 (right).

Contribution to Global Mean Sea Level

From May 2016 (Jason-3 cycle 11) to April 2022, Jason-3 has been the reference altimetry mission to estimate the Global Mean Sea Level (GMSL), replacing Jason-2. Regional and global biases between missions have to be precisely estimated in order to ensure the quality of the reference GMSL serie. For more precisions, see the dedicated section on AVISO+ website [5].
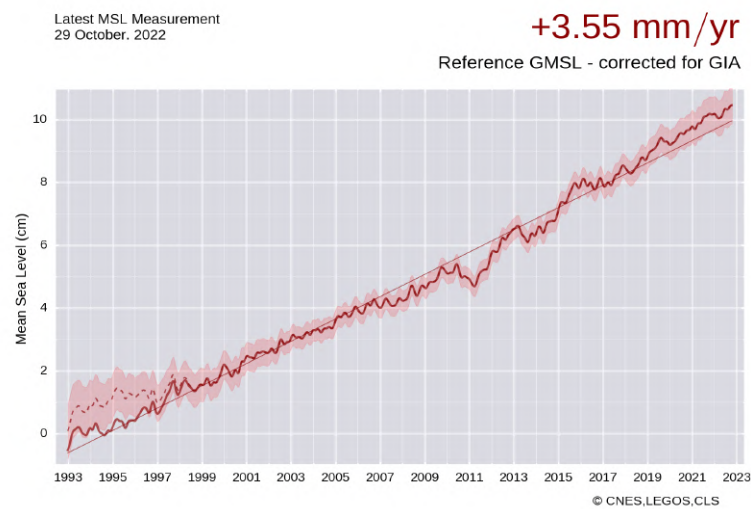
Figure 6 – Global (right) and regional (left) MSL trends from 1993 onwards.

---
[5]https://www.aviso.altimetry.fr/en/data/products/ocean-indicators-products/mean-sea-level.html

2. Processing status

2.1. Data Used

Metrics provided in this document are based on Jason-3 dataset from cycle 0 to 319 for GDR products (corresponding to February 10th 2016 to November 3rd 2022). This period extends until cycle 322 (December 3rd 2022) when IGDR data are considered. Cycle 0 is not included in many statistics because of its available data covering only 5 days. **Note that all GDR data used in this report follow standard "F", the IGDR data follow standard "F" since cycle 174 included**.

After tandem phase with Jason-2, Jason-3 has become the reference mission in *DUACS* system from mid-september 2016 right until mid-april 2022. Its orbit was then changed for Sentinel-6 to become the new reference mission. Note that in order to improve their product quality (and also to use as possible same corrections for multimission products), *DUACS* system applies some updates to IGDR data. If no precision is done, IGDR results that are presented in this document contain *DUACS* updates (also called here IGDR-L2P).

2.2. List of events

The following table shows the major events during the Jason-3 mission.

Start time → End time	Cycle	Event
15/02/2016 08:00:00 → 18:04:28	0	First calibration in DIODE + DEM mode
16/02/2016 16:07:00 → 16:38:59	0	Poseidon3B instrument CNG calibration
08/03/2016 20:00:00 → 09/03/2016 00:00:01	3	Gyro calibration
11/03/2016 05:09:50 → 05:17:14	3	AMR Cold Sky calibration maneuver
15/03/2016 → 17/03/2016	3	Platform GPS upload
21/03/2016 20:46:00 → 20:46:11	4	DEM patch upload
25/03/2016 09:30:15	4	AMR OFF / ON
06/04/2016 06:05:00 → 06:36:59	5	Poseidon3B instrument CNG calibration
07/04/2016 00:21:27 → 16:32:55	6	DIODE DEM mode

Start time → End time	Cycle	Event
08/04/2016 04:44:30 → 05:00:46 05:11:00 → 05:28:21	6	Poseidon3B instrument CAL2 calibration
27/04/2016 11:38:21 → 12:05:55	8	OPS error
02/05/2016 14:34:23 → 14:37:28	8	DEM patch upload.
06/05/2016 18:16:59 → 16/05/2016 16:15:29	9	DIODE DEM mode
12/05/2016 22:44:59 → 22:52:23	9	AMR Cold Sky calibration maneuver
16/05/2016 10:00:00 → 10:16:15	9	Poseidon3B instrument CAL2 calibration
17/05/2016 02:34:00 → 19/05/2016 03:34:16	10	Poseidon3B instrument CAL2 calibration (5 sequences)
25/06/2016 08:09:39 → 05/07/2016 06:08:10	14	DIODE DEM mode
07/07/2016 15:04:44 → 15:11:15	15	AMR internal error
12/07/2016 04:26:36 → 04:34:00	15	AMR Cold Sky calibration maneuver
05/09/2016 04:24:44 → 04:32:08	21	AMR Cold Sky calibration maneuver
10/2016	24	OSTM/Jason 2 moved to the interleaved orbit, end of the verification phase for Jason 3
07/11/2016 22:21:30 → 22:28:54	27	AMR Cold Sky calibration maneuver
27/11/2016 06:15:00 → 06:46:59	29	Poseidon3B instrument CNG calibration
08/12/2016 04:36:34 → 09/12/2016 12:58:47	30	AMR anomaly
10/01/2017 16:37:35 → 16:44:59	34	AMR Cold Sky calibration maneuver
23/02/2017 11:35:00 → 12:06:59	38	Poseidon3B instrument CNG calibration

Start time → End time	Cycle	Event
26/02/2017 17:13:07 → 17:20:31	38	AMR Cold Sky calibration maneuver
27/04/2017 04:13:16 → 04:20:40	44	AMR Cold Sky calibration maneuver
03/06/2017 15:46:00 → 16:17:59	48	Poseidon3B instrument CNG calibration
28/06/2017 05:10:04 → 05:17:28	51	AMR Cold Sky calibration maneuver
14/08/2017 05:57:05 → 06:04:29	55	AMR Cold Sky calibration maneuver
29/08/2017 13:41:14 → 31/08/2017 16:24:07	57	DEM onboard upload
31/08/2017 21:33:00 → 22:04:59	57	Poseidon3B instrument CNG calibration
04/09/2017 17:32:09 → 17:39:33	58	AMR Cold Sky calibration maneuver
14/09/2017 16:54:56 → 17:52:18	59	Gyro calibration
14/10/2017 15:30:11 → 15:37:35	62	AMR Cold Sky calibration maneuver
02/11/2017 02:05:23 → 02:12:47	63	AMR Cold Sky calibration maneuver
02/12/2017 02:30:00 → 03:01:59	66	Poseidon3B instrument CNG calibration
16/12/2017 02:03:45 → 02:11:09	68	AMR Cold Sky calibration maneuver
05/01/2018 20:45:36 → 20:53:00	70	AMR Cold Sky calibration maneuver
04/02/2018 16:46:42 → 16:54:06	73	AMR Cold Sky calibration maneuver
26/02/2018 02:36:17 → 02:43:41	75	AMR Cold Sky calibration maneuver
01/03/2018 08:17:00 → 08:48:59	75	Poseidon3B instrument CNG calibration

Start time → End time	Cycle	Event
07/04/2018 23:25:16 → 23:32:40	79	AMR Cold Sky calibration maneuver
25/04/2018 20:34:10 → 20:41:34	81	AMR Cold Sky calibration maneuver
29/05/2018 14:05:00 → 14:36:59	84	Poseidon3B instrument CNG calibration
30/05/2018 13:08:34 → 13:17:02 14:41:24 → 14:42:47	85	Poseidon BDR update (2 sequences)
10/06/2018 00:41:29 → 00:48:53	86	AMR Cold Sky calibration maneuver
07/07/2018 19:27:47 → 19:35:10	88	AMR Cold Sky calibration maneuver
31/07/2018 01:05:47 → 01:13:11	91	AMR Cold Sky calibration maneuver
22/08/2018 01:25:28 → 01:32:52	93	AMR Cold Sky calibration maneuver
29/08/2018 19:00:00 → 19:31:59	94	Poseidon3B instrument CNG calibration
02/10/2018 18:53:50 → 19:01:14	97	AMR Cold Sky calibration maneuver
21/10/2018 14:32:55 → 14:40:19	99	AMR Cold Sky calibration maneuver
01/12/2018 00:25:00 → 00:59:59	103	Poseidon3B instrument CNG calibration
04/12/2018 01:36:39 → 01:44:03	103	AMR Cold Sky calibration maneuver
25/12/2018 18:48:13 → 18:55:37	106	AMR Cold Sky calibration maneuver
22/01/2019 15:56:15 → 16:03:39	108	AMR Cold Sky calibration maneuver
28/01/2019 21:50:00	109	AMR Reset
12/02/2019 22:04:38 → 22:12:02	111	AMR Cold Sky calibration maneuver

Start time → End time	Cycle	Event
24/02/2019 09:57:16 → 06/03/2019 08:44:21	112-113	Safe Hold Mode (SHM)
27/02/2019	112	Doris Software patch update (during recovery)
28/02/2019	112	Upload of the GPS software (version N) on PMB (during recovery)
07/03/2019 14:30:00 → 15:25:00	113	Gyro calibration
27/03/2019 02:53:30 → 03:00:54	115	AMR Cold Sky calibration maneuver
06/04/2019 23:17:22 → 12/04/2019 02:20:01	116	Safe Hold Mode (SHM)
29/05/2019 05:50:23 → 05:57:47	121	AMR Cold Sky calibration maneuver
31/05/2019 11:10:00 → 11:41:59	121	Poseidon3B instrument CNG calibration
18/06/2019 18:36:47 → 18:44:11	123	AMR Cold Sky calibration maneuver
18/07/2019 00:15:34 → 00:22:58	126	AMR Cold Sky calibration maneuver
08/08/2019 21:00:06 → 21:07:30	128	AMR Cold Sky calibration maneuver
18/08/2019 11:10:00 → 11:41:59	129	Poseidon3B instrument CNG calibration
20/09/2019 20:18:57 → 20:26:21	133	AMR Cold Sky calibration maneuver
09/10/2019 15:58:18 → 16:05:42	135	AMR Cold Sky calibration maneuver
21/11/2019 19:38:16 → 19:45:40	139	AMR Cold Sky calibration maneuver
25/11/2019 22:42:00 → 23:13:59	139	Poseidon3B instrument CNG calibration
13/12/2019 20:13:34 → 20:20:58	141	AMR Cold Sky calibration maneuver

Start time → End time	Cycle	Event
09/01/2020 20:51:16 → 20:58:40	144	AMR Cold Sky calibration maneuver
31/01/2020 15:43:05 → 15:50:29	146	AMR Cold Sky calibration maneuver
31/01/2020 04:51:17 → 05/02/2020 09:37:14	146-147	Safe Hold Mode (SHM)
05/02/2020 21:00:53 → 13/02/2020 08:42:44	147	Safe Hold Mode (SHM)
04/03/2020 02:28:00 → 02:29:59	149	Poseidon3B instrument CNG calibration
14/03/2020 02:27:18 → 02:34:42	150	AMR Cold Sky calibration maneuver
01/04/2020 16:30:06 → 16:37:30	152	AMR Cold Sky calibration maneuver
15/05/2020 23:47:54 → 23:47:54	157	AMR Cold Sky calibration maneuver
29/05/2020 09:05:00 → 09:36:59	158	Poseidon3B instrument CNG calibration
06/06/2020 01:44:40 → 01:52:04	159	AMR Cold Sky calibration maneuver
15/06/2020 21:50:42 → 19/06/2020 07:32:46	160	Safe Hold Mode (SHM)
04/07/2020 01:20:01 → 01:27:25	162	AMR Cold Sky calibration maneuver
12/08/2020 17:15:00 → 17:46:59	166	Poseidon3B instrument CNG calibration
01/09/2020 17:15:00 → 03/09/2020 14:13:40	168	DEM onboard upload
07/09/2020 23:45:32 → 23:52:56	168	AMR Cold Sky calibration maneuver
09/09/2020 22:13:36 → 23:04:55	169	Gyro calibration
26/09/2020 02:38:06 → 02:45:30	170	AMR Cold Sky calibration maneuver

Start time → End time	Cycle	Event
27/10/2020 13:23:01 → 29/10/2020 11:36:00	173-174	DORIS anomaly
08/11/2020 03:52:22 → 03:59:46	175	AMR Cold Sky calibration maneuver
26/11/2020 19:50:00 → 20:21:59	176	Poseidon3B instrument CNG calibration
29/11/2020 17:23:40 → 17:31:05	177	AMR Cold Sky calibration maneuver
27/12/2020 16:32:49 → 16:40:13	180	AMR Cold Sky calibration maneuver
17/01/2021 16:46:07 → 16:53:31	182	AMR Cold Sky calibration maneuver
24/02/2021 01:35:00 → 02:06:59	185	Poseidon3B instrument CNG calibration
03/03/2021 00:24:03 → 00:31:27	186	AMR Cold Sky calibration maneuver
08/03/2021 08:19:28 → 09:27:29	187	DORIS on-board software upgrade
19/03/2021 23:06:47 → 23:14:11	188	AMR Cold Sky calibration maneuver
02/04/2021 20:46:22 → 21:12:41	189	Ground control segment anomaly
07/04/2021 13:27:46 → 13:27:59	190	DEM onboard upload
24/04/2021 15:33:15 → 25/04/2021 01:19:22	191	AMR anomaly
02/05/2021 06:05:37 → 06:13:01	192	AMR Cold Sky calibration maneuver
05/05/2021 13:54:41 → 13:54:55	193	DEM onboard upload
22/05/2021 02:02:41 → 02:10:05	194	AMR Cold Sky calibration maneuver
24/05/2021 07:22:00 → 07:53:59	194	Poseidon3B instrument CNG calibration

Start time → End time	Cycle	Event
22/06/2021 06:27:41 → 06:35:05	197	AMR Cold Sky calibration maneuver
29/06/2021 16:54:30	198	AMR Reset performed on rev 25487 due to error 32 (RAM!=ROM) and error count rising
12/07/2021 23:14:40 → 23:22:04	199	AMR Cold Sky calibration maneuver
27/08/2021 23:43:32 → 23:50:56	204	AMR Cold Sky calibration maneuver
28/08/2021 11:57:00 → 12:28:59	204	Poseidon3B instrument CNG calibration
12/09/2021 03:21:30 → 03:28:54	206	AMR Cold Sky calibration maneuver
26/10/2021 20:13:41 → 20:21:05	210	AMR Cold Sky calibration maneuver
16/11/2021 14:44:21 → 14:51:45	212	AMR Cold Sky calibration maneuver
28/11/2021 16:55:00 → 17:26:59	213	Poseidon3B instrument CNG calibration
15/12/2021 16:05:29 → 16:12:53	215	AMR Cold Sky calibration maneuver
05/01/2022 22:02:23 → 22:09:47	217	AMR Cold Sky calibration maneuver
20/01/2022 19:25:51 → 21:13:32	219	Ground segment anomaly
04/02/2022 06:18:20 → 07:14:33	220	Ground segment anomaly
19/02/2022 20:42:05 → 20:49:29	222	AMR Cold Sky calibration maneuver
25/02/2022 22:40:00 → 23:11:59	222	Poseidon3B instrument CNG calibration
08/03/2022 17:27:52 → 17:35:16	224	AMR Cold Sky calibration maneuver
23/04/2022 13:05:48 → 13:13:12	300	AMR Cold Sky calibration maneuver

Start time → End time	Cycle	Event
28/04/2022 15:55:45 → 22:07:50	300	AMR Reset
09/05/2022 02:05:32 → 02:12:56	301	AMR Cold Sky calibration maneuver
27/05/2022 03:45:00 → 04:16:59	303	Poseidon3B instrument CNG calibration
10/06/2022 01:17:54 → 01:25:18	305	AMR Cold Sky calibration maneuver
31/08/2022 08:18:00 → 08:49:59	313	Poseidon3B instrument CNG calibration
01/09/2022 20:54:57 → 21:02:21	313	AMR Cold Sky calibration maneuver
27/09/2022 07:02:00 → 07:48:00	316	DEM patch upload
13/10/2022 23:50:51 → 23:58:15	317	AMR Cold Sky calibration maneuver
03/11/2022 14:47:43 → 14:55:07	320	AMR Cold Sky calibration maneuver
28/11/2022 14:05:00 → 14:36:59	322	Poseidon3B instrument CNG calibration
03/12/2022 20:21:44 → 20:29:08	323	AMR Cold Sky calibration maneuver

Table 1 – Events on Jason-3 mission

2.3. Tracking and acquisition mode

Jason-3 can use two on-board tracking modes: Diode/DEM (open loop) and median tracker. In addition, a tracking automatic transition is possible, which means that when authorized: acquisition mode switches automatically from autonomous DIODE acquisition mode over land to Diode/DEM over ocean and referenced inland water. The status of tracking and acquisition modes are detailed in table 2.

Cycle	Acquisition Mode over land	Acquisition Mode over ocean and all referenced inland waters	Comment
Cycle 000	Median tracker + autonomous acquisition / tracking + DEM	Median tracker + autonomous acquisition / tracking + DEM	tracking automatic transition inhibited except for 7 passes
Cycles 001 to 005	Median tracker	Median tracker	tracking automatic transition inhibited.
Cycles 006	see dedicated point below	see dedicated point below	
Cycles 007	Median tracker	Median tracker	tracking automatic transition inhibited everywhere.
Cycles 008	mainly Median tracker	mainly Median tracker	autonomous acquisition / tracking for passes 144 to 148 (DEM patch upload on 2016-05-02). tracking automatic transition inhibited everywhere.
Cycle 009 Pass 001 to mid-248	Median tracker	DEM	mid-pass 248 = CAL2 event on 2016-05-16 10:00)
Cycle 009 Pass mid-248 to 254	Median tracker	Median tracker	mid-pass 248 = CAL2 event on 2016-05-16 10:00)
Cycle 010	Median tracker	Median tracker	tracking automatic transition inhibited
Cycles 011 to 019	Median tracker	DEM	tracking automatic transition authorized
Cycle 020	Median tracker	Median tracker	tracking automatic transition inhibited
Cycles 021 to 056	Median tracker	DEM	tracking automatic transition authorized
Cycle 057			DEM upload
Cycles 058 to 167	Median tracker	DEM	tracking automatic transition authorized
Cycle 168			DEM upload

Cycle	Acquisition Mode over land	Acquisition Mode over ocean and all referenced inland waters	Comment
Cycles 168 to 227	Mainly DEM (see dedicated point below)	DEM	tracking automatic transition authorized
Cycles 300 to 322	Median tracker	Median tracker	tracking automatic transition inhibited
Cycle 323	Mainly DEM (see dedicated point below)	DEM	tracking automatic transition authorized

Table 2 – Acquisition mode

- About cycle 006: Altimeter state flag for tracking mode is set to 1 by three times (=0 everywhere else):

    - for passes 018 to 029 from 2016-04-07 16:32:57 to 2016-04-08 03:13:59 :
    >DIODE Acquisition/Autonomous mode (Altimeter state flag for acquisition mode is set to 9) due to operation error after transponder calibration : back to DIODE DEM mode after the next routine calibration.

    - for passes 065 to 070, from 2016-04-09 12:46:05 to 2016-04-09 17:25:10 :
    >Auto Acquisition/Autonomous tracking mode (Altimeter state flag for acquisition mode is set to 8) due to automatic reintialisation in POS3B default mode, triggered on-board by GPS reinit : back to DIODE DEM mode after the next routine calibration

    - for passes 113 to 116, from 2016-04-11 10:03:37 to 2016-04-11 12:20:28 :
    >Auto Acquisition/Autonomous tracking mode (Altimeter state flag for acquisition mode is set to 8) due to automatic reintialisation in POS3B default mode, triggered on-board by GPS OFF-ON : back to DIODE DEM mode after the next routine calibration

- From cycle 21 to cycle 167, except during DEM upload on cycles 057 and 168, tracking automatic transition is activated.

- During cycle 057, some passes are entirely autonomous acquisition / tracking, and some passes entirely median tracker. DEM upload during this cycle is detailed in [13].

- During cycle 168, some passes are entirely autonomous acquisition / tracking, and some passes entirely median tracker. DEM upload during this cycle is detailed in [8] in the SHM investigation.

- From cycle 169 to cycle 227, tracking automatic transition is activated. Due to the new database of targets used to define onboard elevation commands over continental surfaces, a very low part of measurements are in median mode (see green points on left of Figure 2).

- From cycle 300 onwards, the acquisition mode is set once more to autonomous DIODE and the automatic switch is inhibited due to a lack of DEM fitting the new orbit (see Figure 3).
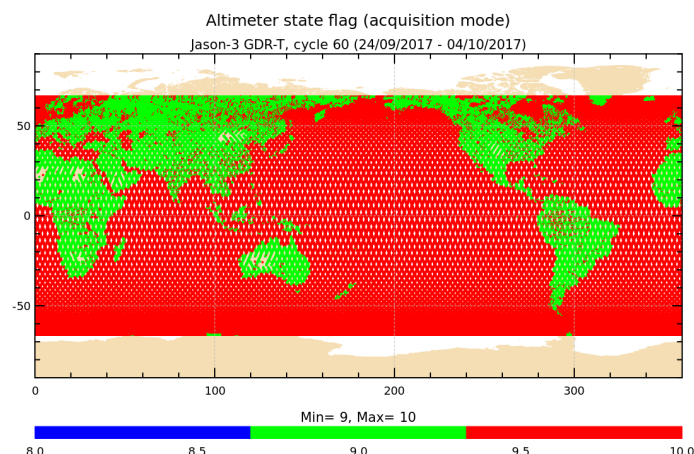
Figure 1 – Acquisition mode for cycle 060 (identical to acquisition mode automatic switch for cycles 6, 9, 11-19, 21-56,58-167). 8 = autonomous acquisition / tracking, 9 = autonomous DIODE acquisition / tracking, 10 = DIODE + Digital Elevation Model tracking
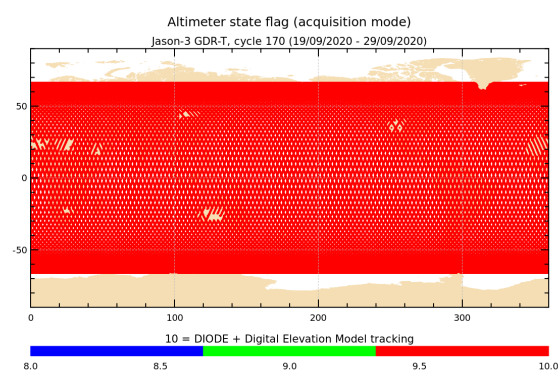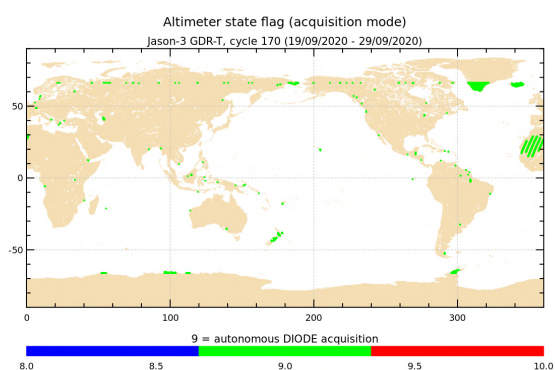
Figure 2 – Acquisition mode for cycle 170 (identical to acquisition mode automatic switch for cycles 169-322). **Left:** *9 = autonomous DIODE acquisition / tracking.* **Right:** *10 = DIODE + Digital Elevation Model tracking*
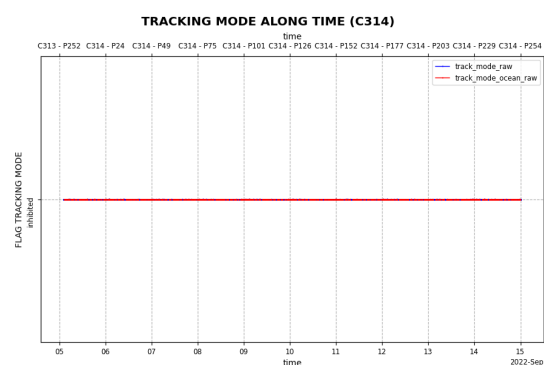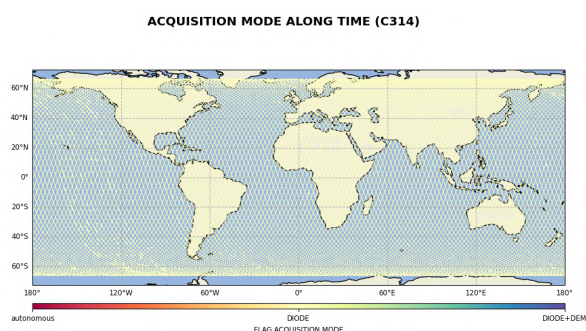
Figure 3 – Acquisition and tracking mode for cycle 314 (identical to acquisition mode from cycle 300)
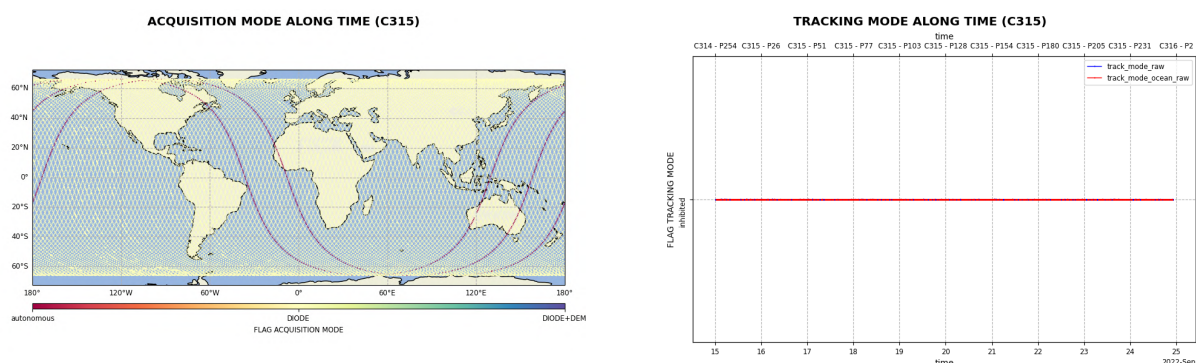
Figure 4 – Acquisition and tracking mode for cycle 315 (identical to acquisition mode for cycle 319)

- In cycles 315, 319 and 322, the acquisition passes from autonomous DIODE (9) to autonomous (8) for a few passes each time due to some lacking and expected navigation on-board instructions for the altimeter (see Figure 4).

- In cycle 316, the acquisition passes from autonomous DIODE (9) to DIODE+DEM (10) for a few passes with the tracking automatic transition re-activated but is quickly set back to autonomous DIODE (9) due to an erroneous configuration in DIODE. This should theorically be fixed over the next cycles to use the DEM uploaded after the orbit change (see Figure 5).
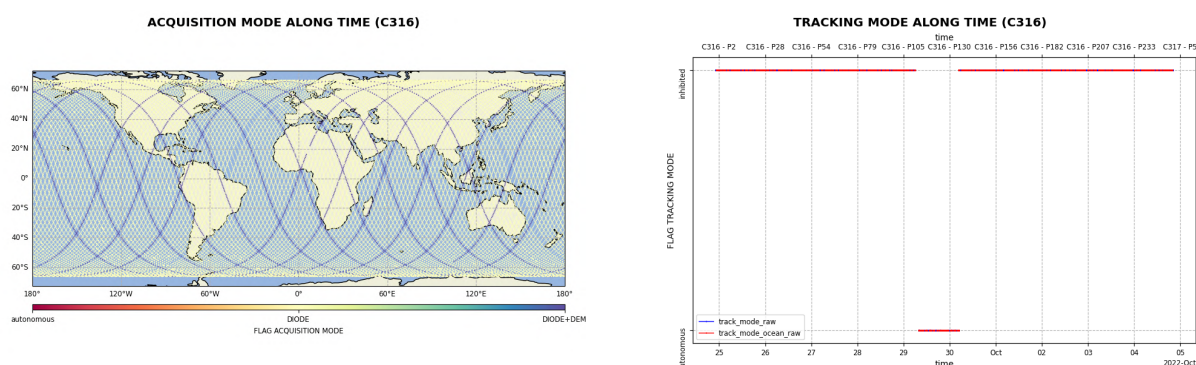
Figure 5 – Acquisition and tracking mode for cycle 316

- From cycle 323 the tracking automatic transition is finally activated. This activation awaited the upload of a correct DEM fitting the new orbit properties.

2.4. Models and standards

The standards previously used in version "D" are listed in Table 3. Now that the reprocessing of all cycles has been performed, GDR products are in standard "F". OGDR and IGDR products are in standard "F" since the cycle 174 (2020/10).

The main differences between the O/IGDRs versions "T" and "D" are summarized hereafter:

- CAL-2 calibration processing are based on typical ocean AGC values, correcting the negative squared-attitude values that were observed from the start of the mission.

- Backscatter (sigma-0) values are adjusted internally during ground processing. A calibration bias of +0.14 dB and +0.109 dB is added to the measured (and reported) MLE-4 and MLE-3 Ku-band sigma-0, respectively, prior to wind speed computation; a calibration bias of -0.231 dB and -0.012 dB is added to the measured (and reported) MLE-3 Ku- and C-band sigma-0, respectively, prior to rain flag computation and rain flag values. This ensure that they are properly aligned with the adopted algorithms, so that rain flagging and wind speed values are in-line with those from Jason-2.

The main differences between the O/IGDRs versions "D" and "F" are summarized hereafter:

- Move from TOPEX/Poseidon reference ellipsoid to WGS84.

- Precision of the CAL1 total power of the PTR from 10^{-2} to 10^{-4}.

- Change in the CAL2 (LPF) normalization.

- Backscatter (sigma-0) values are adjusted internally during ground processing. A calibration bias of +0.06 dB and +0.109 dB is added to the measured (and reported) MLE-4 and MLE-3 Ku-band sigma-0, respectively, prior to wind speed computation; no more bias to apply to sigma0 before rain flag computation as a new table based on preliminary GDR-F data is used.

Model	Product version "D"	*(version "F" for O/IGDR from cycle 174 onwards and for all GDR)*
Orbit	Based on Doris onboard navigator solution for OGDRs. DORIS tracking data for IGDRs (orbit standard MOE-E until cycle 094 and MOE-F from cycle 095 onwards). From Feb.2019 onwards, a DORIS+GPS solution is used for MOE computation DORIS and/or GPS tracking data for GDRs (orbit standard POE-E until cycle 094 and POE-F from cycle 095 onwards).	

Model	Product version "D"	*(version "F" for O/IGDR from cycle 174 onwards and for all GDR)*
Altimeter Retracking	OceanMLE4 retracking: MLE4 fit from 2nd order Brown model: MLE4 simultaneously retrieves the following 4 parameters from the altimeter waveforms: • Epoch (tracker range offset) → altimeter range • Composite Sigma → SWH • Amplitude → Sigma0 • Trailing Edge slope → Square of mispointing angle (Ku band only, a null value is used in input of the C band retracking algorithm) OceanMLE3 retracking: MLE3 fit from first orderBrown analytical model: MLE3 simultaneously retrieves the 3 parameters that can be inverted from the altimeter waveforms: • Epoch (tracker range offset) → altimeter range • Composite Sigma → SWH • Amplitude → Sigma0 "Ice" retracking: Geometrical analysis of the altimeter waveforms, which retrieves the following parameters: • Epoch (tracker range offset) → altimeter range • Amplitude → Sigma0	
Altimeter Instrument Corrections	Two sets: one set consistent with MLE4 retracking and one set consistent with MLE3 retracking	
Jason3 Advanced Microwave Radiometer (AMR) Parameters	Using parameters derived from long term calibration tool developed and operated by NASA/JPL	

Model	Product version "D"	*(version "F" for O/IGDR from cycle 174 onwards and for all GDR)*
Dry Troposphere Range Correction	From ECMWF atmospheric pressures and model for S1 and S2 atmospheric tides	Two solutions: • From ECMWF atmospheric pressures at sea level and model for S1 and S2 atmospheric tides • From ECMWF atmospheric pressures at measurement level and model for S1 and S2 atmospheric tides
Wet Troposphere Range Correction from Model	From ECMWF model	identical
Ionosphere correction from model	Based on Global Ionosphere TEC Maps from JPL	identical
Sea State Bias Model	Two empirical models: • MLE4 version derived from 1 year of MLE4 Jason-2 altimeter data with version "D" geophysical models • MLE3 version derived from 1 year of MLE3 Jason-2 altimeter data with version "D" geophysical models	Two empirical models (in IGDR): • MLE4 version derived from 1 year of MLE4 Jason-3 altimeter data with version "F" geophysical models • MLE3 version derived from 1 year of MLE3 Jason-3 altimeter data with version "F" geophysical models
Mean Sea Surface Model	MSS_CNES-CLS11 (reference 7 years)	Two models: • MSS_CNES-CLS15 (reference 20 years) • MSS_DTU-18
Mean Dynamic Topography Model	MDT_CNES-CLS09	MDT_CNES-CLS18
Geoid	EGM96	EGM2008
Bathymetry Model	DTM2000.1	ACE-2
Inverse Barometer Correction	Computed from ECMWF atmospheric pressures after removing S1 and S2 atmospheric tides	identical
Non-tidal High-frequency De-aliasing Correction	Mog2D high resolution ocean model on I/GDRs. None on OGDRs. Ocean model forced by ECMWF atmospheric pressures after removing S1 and S2 atmospheric tides.	identical

Model	Product version "D"	*(version "F" for O/IGDR from cycle 174 onwards and for all GDR)*
Tide Solution 1	GOT4.8 + S1 ocean tide. S1 load tide ignored. *Note that this solution is used in ssha computation variable.*	GOT4.10
Tide Solution 2	FES2004 + S1 and M4 ocean tides. S1 and M4 load tides ignored	FES2014B. *Note that this solution is used in ssha computation variable.*
Equilibrium long-period ocean tide model.	From Cartwright and Taylor tidal potential.	identical
Non-equilibrium long-period ocean tide model.	Mm, Mf, Mtm, and Msqm from FES2004	Mm, Mf, Mtm, Msqm, Sa and Ssa from FES2014B
Solid Earth Tide Model	From Cartwright and Taylor tidal potential.	identical
Pole Tide Model	Equilibrium model WAHR85	DESAI2015 with 2017 coefficients for mean pole location
Wind Speed from Model	ECMWF model	identical
Rain Flag	Derived from comparisons to thresholds of the radiometer-derived integrated liquid water content and of the difference between the measured and the expected Ku-band backscatter coefficient	Use of preliminary GDR-F data to compute rain flag table
Ice Flag	Derived from comparison of the model wet tropospheric correction to a dual-frequency wet tropospheric correction retrieved from radiometer brightness temperatures, with a default value issued from a climatology table	

Table 3 – List of GDR version "D" standard (version "F" for O/IGDR from cycle 174 onwards and for all GDR)

2.5.   Processing versions

OGDR and IGDR products are publicly available since June 30th 2016. OGDRs were generated in version "T" until cycle 18/pass 137, in version "D" until cycle 173/pass 222, and then turned in "F" version.
→ The first OGDR "D" file is: $JA3\_OPN\_2PdS018\_137\_20160809\_080914\_20160809\_100739.nc$
→ The first OGDR "F" file is: $JA3\_OPN\_2PfS174\_018\_20201029\_121148\_20201029\_140842.nc$

Concerning IGDRs, they turned from "T" to "D" version a few days before OGDRs on June 27th(cycle 14/pass 143). They were generated in version "D" until cycle 173/pass 222, and then turned in "F" version.
→ The first IGDR "D" file is: $JA3\_IPN\_2PdP014\_043\_20160626\_233040\_20160627\_002653.nc$
→ The first IGDR "F" file is: $JA3\_IPN\_2PfP174\_017\_20201029\_111312\_20201029\_120925.nc$

GDRs products have been computed in version "F" for the whole mission period (recomputed from version

"D" to "F" from cycles 0 to 177, see [5]).

2.6.   Cautions

Caution (see 2021 annual report [7] "Caution about qual inst corr 1hz sig0 ku")
Natural evolution of PTR results in a gradual increase of the Ku-band sigma0 instrumental correction, this correction exceeded the corresponding threshold: there was a first thereshold exceeding from cycle 72 onwards. Since IGDR data have not been reprocessed, the flag 'qual_inst_corr_1hz_sig0_ku' is thus considered unvalid for IGDR data from cycle 72 until cycle 99 and the adjustment of the threshold in the processing chain. Thanks to the GDR reprocessing, the flag for cycles 72 to 99 is considered valid into GDR-F, contrary to the IGDR. Again, a gradual increase of the Ku-band sigma0 instrumental correction leads to the exceed of this correction over the corresponding threshold from cycle 206 onwards. The threshold was once more increased in the processing chain and this change was taken into account in the beginning of April 2022.

Caution (see part "Caution about qual inst corr 1hz sig0 C" in 2020 annual report [8]):
The nominal evolution (aging) of the altimeter forced a gradual increase of the C-band sigma0 instrument correction, which has exceeded thresholds for flagging from cycle 160 onwards.
The flag 'qual_inst_corr_1hz_sig0_c' parameter has an abnormal number of points with value set to 1 over ocean and should not be used then. This has no impact on data quality or system performance.
Note that the threshold used to set the flag qual_inst_corr_1hz_sig0_c has been adjusted in the standard F processing chain. As a consequence the flag qual_inst_corr_1hz_sig0_c is back ok for a standard use from IGDR and GDR cycles.

3. Data coverage and edited measurements

3.1. Missing measurements

3.1.1. Over land and ocean

Determination of missing measurements relative to the theoretically expected orbit ground pattern is an essential tool to detect missing telemetry or satellite events for instance. Applying the same procedure for Jason-2 and Jason-3, the comparison of the percentage of missing measurements has been performed.

Figure 6 shows the percentage of available measurements for Jason-3 and Jason-2 for all kinds of surfaces observed, computed with respect to a theoretical possible number of measurements. In average Jason-3 provides 99.0% of measurements over 319 cycles (without taking into accounts cycles with explained anomalies or safe hold mode), which shows an improvement compared to Jason-2 tracking capabilities.
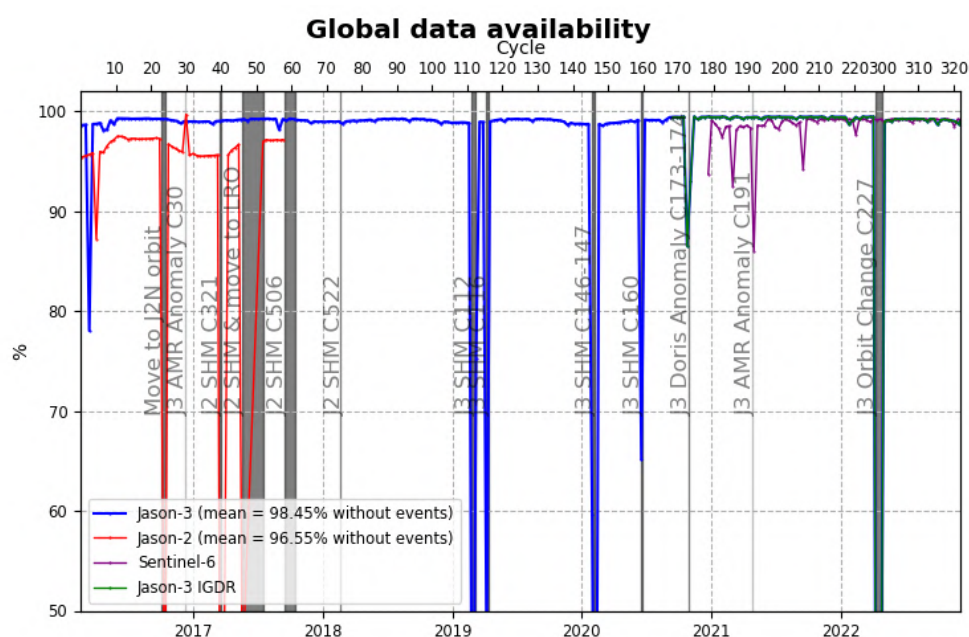
Figure 6 – Global GDRs data availability per cycle

Out of Jason-2 SHM or move of orbit, missing measurements on Jason-2 and Jason-3 since the beginning of Jason-3 mission are:

- Jason-3 Cycle 3: GPS platform upload interrupted the data production for two days.

- Jason-2 Cycle 285: Data are missing in 2016 between April, 5 at 13:35:10 and April, 6 at 12:02:40. No scientific products have been processed during this period to allow the upload of new GPS On Board software.

- Jason-3 Cycle 57: DEM onboard upload interrupted the data production for a few passes.

— Jason-3 Cycles 112-113: Jason-3 SHM (Safe Hold Mode) occured from 24/02/2019 09:57:16 until 06/03/2019 08:44:21. Over this SHM event, missing data rate is 79.89% for cycle 112 and 24.21% for cycle 113.

— Jason-3 Cycle 116: SHM occured from 06/04/2019 23:17:22 until 12/04/2019 02:20:01. Over this SHM event, missing data rate is 53.19% for cycle 116.

— Jason-3 Cycles 146-147: SHM occured from 31/01/2020 04:51:17 until 05/02/2020 09:37:14. And from 05/02/2020 21:00:53 until 13/02/2020 08:42:44. Over those SHM events, missing data rate is 38.94% for cycle 146 and 88.81% for cycle 147.

— Jason-3 Cycle 160: SHM occured from 15/06/2020 21:50:42 until 19/06/2020 07:32:46. Over this SHM event, missing data rate is 33.58% for cycle 160.

— Jason-3 Cycles 173-174: DORIS anomaly from 27/10/2020 13:23:01 until 29/10/2020 11:36:00. Over this event, missing data rate is 13.46% for cycle 173 and 7.02% for cycle 174.

— Jason-3 Cycles 227-300: Orbit change maneuver from 07/04/2022 until 25/04/2022. Over this event, the altimeter is off and the radiometer does not send any data.

— Jason-3 Cycle 316: A DEM onboard updload interrupted the data production for a few passes leading to 1.4% of missing measurements.

Table 4 gives an overview of missing passes and reasons for Jason-3.

Date	Jason-3 Cycle/Pass	Reason
Before 12/02/2016 01:11:09	C000 / P001-116	Final ground-track reached on 12-02-2016 01:11:09
	C000 / P201, 203, 236	Due to calibration events, passes 201 (∼10%), 203 (∼12%) and 236 (∼8%) partly missing
08/03/2016 20:00:00 → 09/03/2016 00:00:01	C003	Due to Gyro calibration , data gap on pass 018.
11/03/2016 05:14:00 → 05:34:00	C003	AMR Cold Sky calibration maneuver
15/03/2016 07:15:04 to 17/03/2016 08:06:13	C003 / P181-233	Due to platform GPS software upload, passes 182 to 232 are entirely missing, as well as part of passes 181 and 233
06/04/2016 06:05:00 → 06:36:59	C005 / P235	Due to Poseidon3B instrument CNG calibration, data gap on pass 235, that mainly concerns land data acquisition and a portion of Red Sea.
26/04/2016 20:18:29 → 2016-05-06 18:16:59	C008	Due to Poseidon3B instrument CAL2 calibrations , data gaps over land on passes 55, 53, 27, 5, 38, 12 and 29

Date	Jason-3 Cycle/Pass	Reason
27/04/2016 11:38:11 to 12:05:55	C008 / P017	Due to OPS error, pass 017 has 49.39% of missing measurements (42.44% over ocean)
08/04/2016 04:44:30 → 05:00:46 05:11:00 → 05:28:21	C006	Due to Poseidon3B instrument CAL2 calibration, data gaps over land
02/05/2016 10:17:04 to 10:28:14 and 14:34:22 to 14:37:28	C008 / P144,148	Due to DEM upload: • Pass 144 has 20.33% of missing measurements (13.27% over ocean, Norwegian Sea) • Pass 148 has 6.60% of missing measurements over ocean (western african coast)
12/05/2016 22:44:59 → 22:52:23	C009	AMR Cold Sky calibration maneuver
16/05/2016 10:00:00 → 10:16:15	C009	Due to Poseidon3B instrument CAL2 calibration, data gap over land on pass 248
17/05/2016 02:34:00 → 19/05/2016 03:34:16	C010	Due to Poseidon3B instrument CAL2 calibration (5 sequences), data gaps over land on passes 31, 64, 38, 12, and 44
12/07/2016 04:26:36 → 04:34:00	C015	AMR Cold Sky calibration maneuver
05/09/2016 04:24:44 → 04:32:08	C021	AMR Cold Sky calibration maneuver
07/11/2016 22:21:30 → 22:28:54	C027	AMR Cold Sky calibration maneuver
27/11/2016 06:15:00 to 06:46:58	C029 / P159, 160	Due to CNG calibration, parts of passes 159 and 160 are missing (mostly over land). Pass 159 has 54.73% of missing measurements (10.54% over ocean).
10/01/2017 16:37:35 → 16:44:59	C034	AMR Cold Sky calibration maneuver
23/02/2017 11:35:00 → 12:06:59	C038	Poseidon3B instrument CNG calibration
26/02/2017 17:13:07 → 17:20:31	C038	AMR Cold Sky calibration maneuver

Date	Jason-3 Cycle/Pass	Reason
27/04/2017 04:13:16 → 04:20:40	C044	AMR Cold Sky calibration maneuver
03/06/2017 from 15:46:00 to 16:17:59	C048 / P159	Due to CNG calibration, pass 159 has 56.55% of missing data mostly over land (10.54% over ocean)
28/06/2017 05:10:04 → 05:17:28	C051	AMR Cold Sky calibration maneuver
14/08/2017 05:57:05 → 06:04:29	C055	AMR Cold Sky calibration maneuver
30/08/2017 12:07:15 to 14:10:33	C057 / P123-125	Due to DEM upload: • Pass 123 has 23.91% of missing measurement (15.44% over ocean). • Pass 124 is missing • Pass 125 has 96.16% of missing measurement (100% over ocean).
31/08/2017 14:22:58 to 16:26:10	C057 / P151-153	Due to DEM upload: • Pass 151 has 12.40% of missing measurement (8.57% over ocean). • Pass 152 has 100% of missing measurement over ocean • Pass 153 has 98.40% of missing measurement (100% over ocean).
31/08/2017 21:33:00 to 22:04:59	C057 / P159	Due to CNG calibration, pass 159 has 56.17% of missing measurement (10.54% over ocean).
04/09/2017 17:32:09 → 17:39:33	C058	AMR Cold Sky calibration maneuver
14/09/2017 from 16:54:56 to 17:52:18	C059 / P005	Due to Gyro calibration, pass 5 has 47.22% of missing measurements (0.07% over ocean)
14/10/2017 15:30:11 → 15:37:35	C062	AMR Cold Sky calibration maneuver
02/11/2017 02:05:23 → 02:12:47	C063	AMR Cold Sky calibration maneuver

Date	Jason-3 Cycle/Pass	Reason
02/12/2017 02:30:00 → 03:01:59	C066 / P235	Due to CNG calibration, pass 235 has 57.16% of missing measurement (8.33% over ocean).
16/12/2017 02:03:45 → 02:11:09	C068	AMR Cold Sky calibration maneuver
26/12/2017 23:03:32 → 23:06:25	C069	Pass 110 has 5.88% of missing measurement (5.66% over ocean) probably due to connection to Usingen anomaly.
05/01/2018 20:45:36 → 20:53:00	C070	AMR Cold Sky calibration maneuver
04/02/2018 16:46:42 → 16:54:06	C073	AMR Cold Sky calibration maneuver
26/02/2018 02:36:17 → 02:43:41	C075	AMR Cold Sky calibration maneuver
01/03/2018 08:17:00 → 08:48:59	C075 / P235	Due to CNG calibration, pass 235 has 57.03% of missing measurement (8.33% over ocean).
07/04/2018 23:25:16 → 23:32:40	C079	AMR Cold Sky calibration maneuver
25/04/2018 20:34:10 → 20:41:34	C081	AMR Cold Sky calibration maneuver
29/05/2018 14:05:00 → 14:36:59	C084 / P235	Due to CNG calibration, pass 235 has 57.00% of missing measurement (8.33% over ocean).
30/05/2018 13:08:34 → 13:17:02 14:41:24 → 14:42:47	C085 / P006-007	Due to BDR update: • Pass 6 has 15.31% of missing measurement (10.80% over ocean). • Pass 7 has 2.84% of missing measurement (4.86% over ocean).
10/06/2018 00:41:29 → 00:48:53	C086	AMR Cold Sky calibration maneuver
07/07/2018 19:27:47 → 19:35:10	C088	AMR Cold Sky calibration maneuver
31/07/2018 01:05:47 → 01:13:11	C091	AMR Cold Sky calibration maneuver

Date	Jason-3 Cycle/Pass	Reason
22/08/2018 01:25:28 → 01:32:52	C093	AMR Cold Sky calibration maneuver
29/08/2018 19:00:00 → 19:31:59	C094 / P057	Due to CNG calibration, pass 057 has 57.00% of missing measurement (12.67% over ocean).
02/10/2018 18:53:50 → 19:01:14	C097	AMR Cold Sky calibration maneuver
21/10/2018 14:35:37 → 14:40:19	C099	AMR Cold Sky calibration maneuver
01/12/2018 00:25:00 → 00:56:59	C103 / P159	Due to CNG calibration, pass 159 has 56.43% of missing measurement (10.54% over ocean).
04/12/2018 01:36:39 → 01:44:03	C103	AMR Cold Sky calibration maneuver
25/12/2018 18:48:13 → 18:55:37	C106	AMR Cold Sky calibration maneuver
22/01/2019 15:56:15 → 16:03:39	C108	AMR Cold Sky calibration maneuver
12/02/2019 22:04:38 → 22:12:02	C111	AMR Cold Sky calibration maneuver
24/02/2019 09:57:16→ 06/03/2019 08:44:21	C112 P050 / C113 P061	Safe Hold Mode. Passes 050 to 254 of cycle 112 and passes 001 to 060 of cycle 113 are missing.
07/03/2019 14:30:00 → 15:25:00	C113 / P093 and 094	Due to Gyro calibration, passes 093 and 094 have respectively 19.2% and 23.9% of missing measurements (all over ocean)
27/03/2019 02:53:30 → 03:00:54	C115	AMR Cold Sky calibration maneuver
06/04/2019 23:17:22→ 12/04/2019 02:20:01	C116	Safe Hold Mode. Passes 108 to 245 are completely missing and pass 246 has 16.37% of missing measurement (15,46% over ocean).
30/04/2019 07:43:45 → 07:47:01	C118	Due to PLTM gaps, pass 199 has 26 non-continuous missing points over ocean.
29/05/2019 05:50:23 → 05:57:47	C121	AMR Cold Sky calibration maneuver

Date	Jason-3 Cycle/Pass	Reason
31/05/2019 11:10:00 → 11:41:59	C121 / P235	Due to CNG calibration, pass 235 has 59.96% of missing measurement (8.00% over ocean).
11/06/2019 → 13/06/2019	C123	Due to PLTM gaps, passes 021 and 071 have 47 and 33 non-continuous missing points over ocean.
18/06/2019 18:36:47 → 18:44:11	C123	AMR Cold Sky calibration maneuver
18/07/2019 00:15:34 → 00:22:58	C126	AMR Cold Sky calibration maneuver
08/08/2019 21:00:06 → 21:07:30	C128	AMR Cold Sky calibration maneuver
18/08/2018 18:58:00 → 19:29:59	C129 / P235	Due to CNG calibration, pass 235 has 55.42% of missing measurement (7.98% over ocean).
20/09/2019 20:18:57 → 20:26:21	C133	AMR Cold Sky calibration maneuver
09/10/2019 15:58:18 → 16:05:42	C135	AMR Cold Sky calibration maneuver
04/11/2019 22:08:50 and 22:14:46	C137	Due to PLTM gaps, pass 204 has 2.63% of missing points over ocean.
21/11/2019 19:38:16 → 19:45:40	C139	AMR Cold Sky calibration maneuver
25/11/2019 22:42:00 → 23:13:59	C139 / P235	Due to CNG calibration, pass 235 has 57.19% of missing measurement (8.40% over ocean).
13/12/2019 20:13:34 → 20:20:58	C141	AMR Cold Sky calibration maneuver
09/01/2020 20:51:16 → 20:58:40	C144	AMR Cold Sky calibration maneuver
31/01/2020 04:51:17→ 05/02/2020 09:37:14	C146 P153 / C147 P033	Safe Hold Mode. Passes 154 to 254 of cycle 146 and passes 001 to 032 of cycle 147 are missing.
05/02/2020 21:00:53→ 13/02/2020 08:42:44	C147 P044-237	Safe Hold Mode. Passes 045 to 236 of cycle 147 are missing.

Date	Jason-3 Cycle/Pass	Reason
04/03/2020 02:28:00 → 02:29:59	C149 / P235	Due to CNG calibration, pass 235 has 55.42% of missing measurement (8.08% over ocean).
14/03/2020 02:27:18 → 02:34:42	C150	AMR Cold Sky calibration maneuver
01/04/2020 16:30:06 → 16:37:30	C152	AMR Cold Sky calibration maneuver
15/05/2020 23:40:30 → 23:47:54	C157	AMR Cold Sky calibration maneuver
29/05/2020 09:05:00 → 09:36:59	C158 / P159	Due to CNG calibration, pass 159 has 51.21% of missing measurement (10.11% over ocean).
06/06/2020 01:44:40 → 01:52:04	C159	AMR Cold Sky calibration maneuver
15/06/2020 21:50:42→ 19/06/2020 07:32:46	C160 P100-187	Safe Hold Mode. Passes 101 to 186 of cycle 160 are missing.
04/07/2020 01:20:01 → 01:27:25	C162	AMR Cold Sky calibration maneuver
26/07/2020 01:40:45 → 01:48:09	C164	AMR Cold Sky calibration maneuver
12/08/2020 17:15:00 → 17:46:59	C166 / P057	Due to CNG calibration, pass 057 has 55.44% of missing measurement (11.62% over ocean).
01/09/2020 13:03:18 → 03/09/2020 14:13:40	C168 / P053-109	Due to DEM upload: • Pass 083 has 14.06% of missing measurement (9.27% over ocean). • Pass 109 has 3.35% of missing measurement (1.72% over ocean).

Date	Jason-3 Cycle/Pass	Reason
27/10/2020 13:23:01→ 29/10/2020 11:36:00	C173 P222 / C174 P017	Due to DORIS anomaly: • Pass 222 of cycle 173 has 90.30% of missing measurement (88.77% over ocean). • Passes 223 of cycle 173 to 016 of cycle 174 are entirely missing. • Pass 017 of cycle 174 has 42.78% of missing measurement (52.00% over ocean).
26/11/2020 19:50:00 → 20:21:59	C176 / P235	Due to CNG calibration, pass 235 has 55.67% of missing measurement (2.78% over ocean).
29/11/2020 17:23:41 → 17:31:05	C177	AMR Cold Sky calibration maneuver
27/12/2020 16:32:49 → 16:40:13	C180	AMR Cold Sky calibration maneuver
17/01/2021 16:46:07 → 16:53:31	C182	AMR Cold Sky calibration maneuver
24/02/2021 01:35:00 → 02:06:59	C186 / P235	Due to CNG calibration, pass 235 has 56.9% of missing measurement (2.54% over ocean).
19/03/2021 23:06:47 → 23:14:11	C188	AMR Cold Sky calibration maneuver
02/04/2021 20:46:22 → 21:12:41	C189	Ground control segment anomaly
02/05/2021 06:05:37 → 06:13:01	C192	AMR Cold Sky calibration maneuver
22/05/2021 02:02:41 → 02:10:05	C194	AMR Cold Sky calibration maneuver
24/05/2021 07:22:00 → 07:53:59	C194 / P235	Due to CNG calibration, pass 235 has 56.9% of missing measurement (2.46% over ocean).
22/06/2021 06:27:41 → 06:35:05	C197	AMR Cold Sky calibration maneuver

Date	Jason-3 Cycle/Pass	Reason
12/07/2021 23:14:40 → 23:22:04	C199	AMR Cold Sky calibration maneuver
02/08/2021 11:32:28 → 11/09/2021 03:26:35	C202 to C205	**Caution :** Altimeter calibrations wrongly planned over ocean
27/08/2021 23:43:32 → 23:50:56	C204	AMR Cold Sky calibration maneuver
28/08/2021 11:57:00 → 12:28:59	C204 / P235	Due to CNG calibration, pass 235 has around 55% of missing measurement (around 2% over ocean).
12/09/2021 03:21:30 → 03:28:54	C206	AMR Cold Sky calibration maneuver
26/10/2021 20:13:41 → 20:21:05	C210	AMR Cold Sky calibration maneuver
16/11/2021 14:44:21 → 14:51:45	C212	AMR Cold Sky calibration maneuver
28/11/2021 16:55:00 → 17:26:59	C213 / P235	Due to CNG calibration, pass 235 has 56.43% of missing measurement (2.62% over ocean).
15/12/2021 16:05:29 → 16:12:53	C215	AMR Cold Sky calibration maneuver
05/01/2022 22:02:23 → 22:09:47	C217	AMR Cold Sky calibration maneuver
20/01/2022 19:25:51 → 21:13:32	C219 / P46,47,48	Ground segment anomaly (Pass 46 has 84% of missing measurements and pass 47 has 100% of missing measurements over ocean)
04/02/2022 06:18:20 → 07:14:33	C220 / P188,189	Ground segment anomaly (Pass 188 has 100% of missing measurements over ocean)
19/02/2022 20:42:05 → 20:49:29	C222	AMR Cold Sky calibration maneuver
25/02/2022 22:40:00 → 23:11:59	C222 / P235	Due to CNG calibration; pass 235 has 2.3% of missing measurements over ocean
08/03/2022 17:27:52 → 17:35:16	C224	AMR Cold Sky calibration maneuver
23/04/2022 13:05:48 → 13:13:12	C300	AMR Cold Sky calibration maneuver

Date	Jason-3 Cycle/Pass	Reason
28/04/2022 15:55:45 → 22:07:50	C300	AMR Reset
09/05/2022 02:05:32 → 02:12:56	C301	AMR Cold Sky calibration maneuver
27/05/2022 03:45:00 → 04:16:59	C303	Due to CNG calibration; pass 209 has 11% of missing measurements over ocean
10/06/2022 01:17:54 → 01:25:18	C305	AMR Cold Sky calibration maneuver
31/08/2022 08:18:00 → 08:49:59	C313	Due to CNG calibration; pass 133 has 10% of missing measurements over ocean
01/09/2022 20:54:57 → 21:02:21	C313	AMR Cold Sky calibration maneuver
27/09/2022 07:02:00 → 07:48:00	C316 / P61-113	Due to DEM upload: • Pass 087 has 16% of missing measurements over ocean • Pass 111 has 7% of missing measurements over ocean • Pass 112 has 100% of missing measurements over ocean • Pass 113 has 77% of missing measurements over ocean
13/10/2022 23:50:51 → 23:58:15	C317	AMR Cold Sky calibration maneuver
03/11/2022 14:47:43 → 14:55:07	C320	AMR Cold Sky calibration maneuver
28/11/2022 14:05:00 → 14:36:59	C322	Due to CNG calibration; pass 133 has 11% of missing measurements over ocean
03/12/2022 20:21:44 → 20:29:08	C323	AMR Cold Sky calibration maneuver

Table 4 – List of missing Jason-3 passes

3.1.2. Over ocean

The behaviour of Jason-3 over ocean is excellent and conform to what is observed with Jason-2 during

Jason-3 validation and cross calibration activities (Annual report 2022)

Nomenclature : SALP-RP-MA-EA-23597-CLS   Page : 39

Document version: 1.1   Date : January 23, 2022
. . . .

tandem phase (on the same ground track, with 80 seconds of difference), and even after on interleaved groundtrack.

Looking at data over ocean, Jason-3 is always available (ocean is fully covered) out of specific events (see figure 8).

. In addition, due to the median tracker mode used for the acquisition after the orbit change, a few missing points over ocean are to be found in each cycle (particularly over high latitudes). Moreover, over cycles 315, 319, and 322, the switch in the acquisition mode (see 2.3.) leads to some missing measurements over ocean (around 70 each time) near the French coast. Both phenomenas can be observed in figure 7.
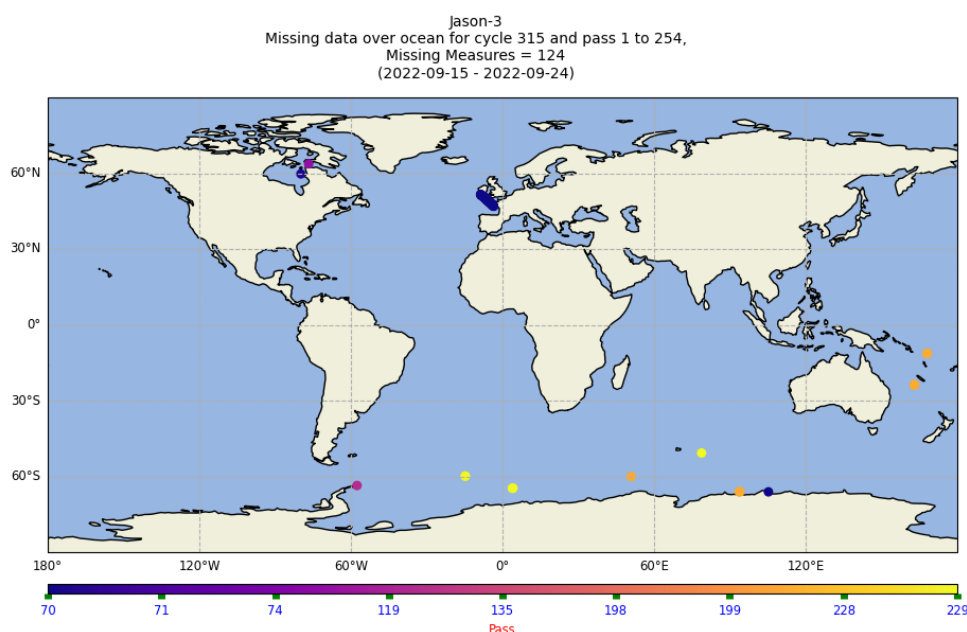

Figure 7 – Missing measures over ocean for cycle 315

Note that Jason-2 missing measurements reason until end of 2017 is detailed in Jason-2 2017 annual report [17].
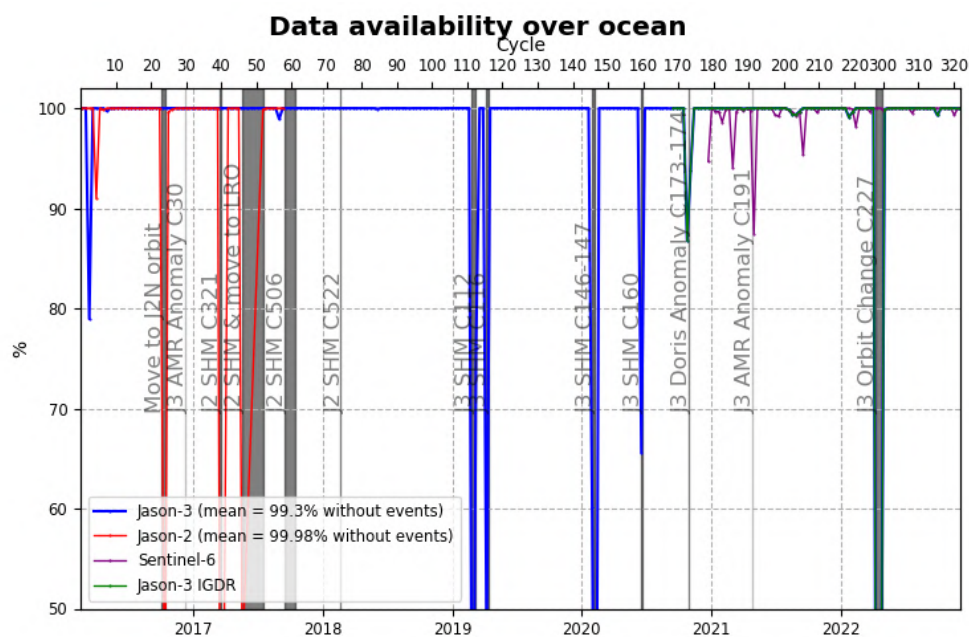
Figure 8 – Jason-2 and Jason-3 GDR data availability over ocean (per cycle)

3.2. Edited measurements

Editing criteria allow to select only measurements considered as valid over ocean. This editing process is structured in 4 main steps:

1. Measurements over land are removed, only measurements over ocean and lakes are kept

2. Measurements over ice are removed

3. Threshold criteria are applied on altimeter, radiometer and geophysical parameters as described in the following table 5. Except for the dual frequency ionosphere correction, only Ku-band measurements are used in this editing procedure, as they mainly represent the end user dataset.

4. A spline criterion is applied to remove the remaining spurious data.

3.2.1. Global editing

The percentage of total edited measurements is monitored on a cyclic basis. The average of total edited measurements is 37.6% (see Figure 9). A small annual cycle is visible due to ice coverage signal (see dedicated part 3.2.2.): the total percentage is slightly lower during March/April/May (30-35%), then increasing during May to July and remains around 38-42%, and start to slowly decrease in mid-September. This expected behaviour is related to sea ice coverage, and was already observed on previous altimetry missions such as OSTM/Jason 2. The peak detected on cycle 30 is due to an AMR anomaly that occured from 08/12/2016 04:36:34 to 09/12/2016 12:58:47. The second peak visible on cycle 112 is due to edited data before SHM (see details about SHM in 2019 Annual report [18]). The peak visible on cycle 147 is due to SHM (not significant figure as there are less than 2 days for this cycle). The peak visible on cycle 191 is due to a radiometer yellow alarm which brought a data gap.

When superimposing both editing levels between Sentinel-6 and Jason-3, it is shown that the editing is consistent between both missions (see Figure 9).
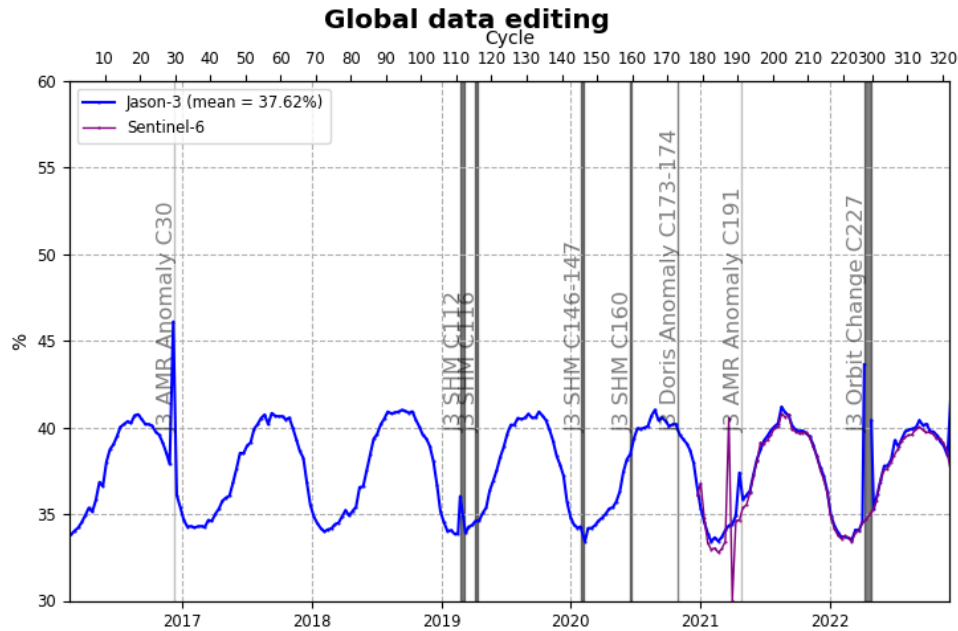

Figure 9 – Jason-3 and Sentinel-6 data editing average by cycle.

3.2.2. Flagging quality criterion: Ice flag

The ice flag (from GDR) is used to remove the ice and sea ice data. Figure 10 shows cycle per cycle percentage of measurements edited by this criterion in comparison with Jason-2 (only ocean and big lakes measurements are kept). Jason-2 and Jason-3 ice flag show similar features while on repetitive orbit. The number of measures flagged according to this criterion is higher with standard "F" than with standard "D", this is due to a change in the surface classification between both standards (see [5]).
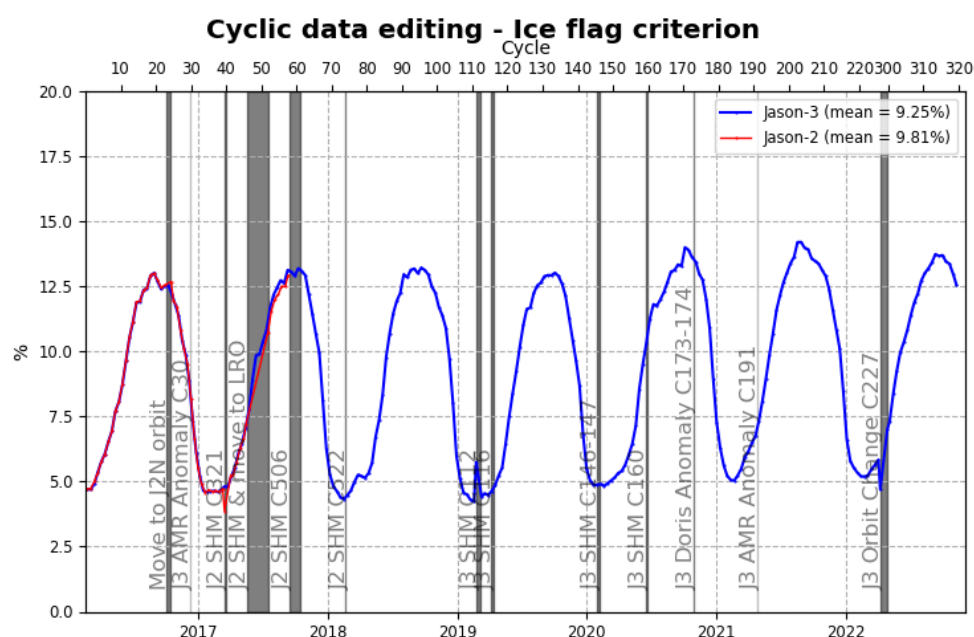

Figure 10 – Cycle per cycle monitoring of the percentage of edited measurements by ice flag criterion.

Over the shown period, no anomalous trend is detected but the nominal annual cycle is visible. Indeed, the maximum number of points over ice is reached during the southern winter (i.e. July - September). As Jason-3 takes measurements between 66° north and south, it does not detect thawing of sea ice (due to global warming), which takes place especially in northern hemisphere over 66°N.

3.2.3.   Flagging quality criterion: Rain flag

Though the altimeter rain flag is available in GDR, it is not used hereafter during the editing procedure. The percentage of measurements where rain flag is set to 1 is plotted in figure 11 top pannel. Using the altimeter rain flag would lead to edit 1.36% of additional measurements compared to recommanded editing procedure (see figure 11 bottom pannels for comparison). This is way less than the 5.85% of flagged with the standard "D" (see [5]).
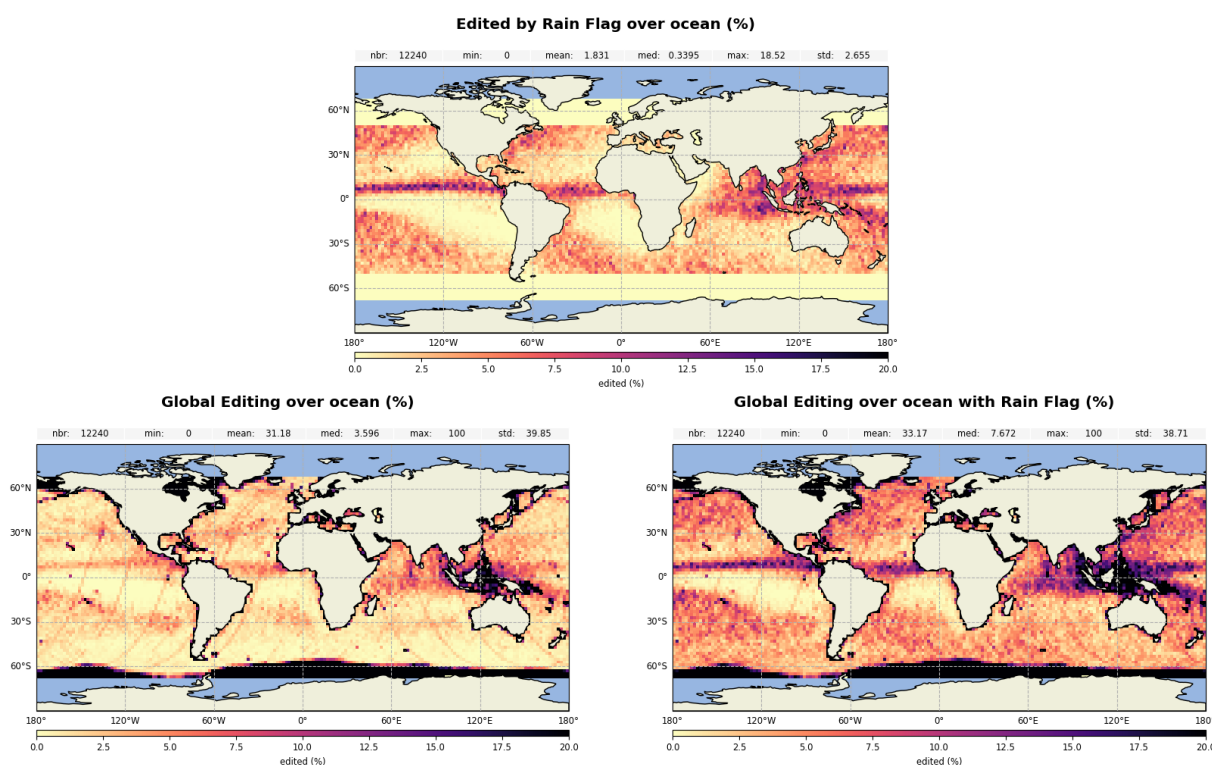

Figure 11 – Top: Percentage of edited measurements by altimeter rain flag criterion. Bottom left: Map of global edited measurements without considering the rain flag. Bottom right: Map of global edited measurements using all criteria and considering the rain flag. All figures are computed over ocean and from cycle 209 to 319.

3.2.4.   Editing on thresholds criteria

After quality flag analysis, instrumental parameters have also been analyzed from comparison with thresholds. The average of total edited measurements following threshold criterion is around 3.38% (Figure 12). For each criterion, cycle percentage of edited measurements is monitored (detailed from part 3.2.4.1. to 3.2.4.11.). This allows detection of anomalies in the number of removed data, which could have instrumental, geophysical or algorithmic origins. In particular, note that no measurement is edited by the following corrections (these parameters are only verified in order to detect data at default values, which might happen during a processing anomaly):

  – dry troposphere correction,

  – inverted barometer correction (including DAC),

  – equilibrium tide,

  – earth tide,

  – pole tide.

Threshold criteria applied on altimeter, radiometer and geophysical parameters are described in the following table 5. The last column represents the mean of rejected data on each criterion over GDR cycles 1 to 319.

Parameter	Min thresholds	Max thresholds	Mean edited
Sea surface height	$-130\,m$	$100\,m$	0.83%
Sea level anomaly	$-2.0\,m$	$2.0\,m$	1.51%
Number measurements of range	10	*Not applicable*	1.1%
Standard deviation of range	0	$0.2\,m$	1.4%
Squared off-nadir angle	$-0.2\,deg^2$	$0.64\,deg^2$	0.66%
Dry troposphere correction	$-2.5\,m$	$-1.9\,m$	0.00%
Inverted barometer correction	$-2.0\,m$	$2.0\,m$	0.00%
AMR wet troposphere correction	$-0.5m$	$-0.001\,m$	0.2%
Ionosphere correction	$-0.4\,m$	$0.04\,m$	0.91%
Significant wave height	$0.0\,m$	$11.0\,m$	0.66%
Sea State Bias	$-0.5\,m$	$0.0\,m$	0.59%
Number measurements of Ku-band Sigma0	10	*Not applicable*	1.09%
Standard deviation of Ku-band Sigma0	0	$1.0\,dB$	2.14%

Parameter	Min thresholds	Max thresholds	Mean edited
Ku-band Sigma0	$7.0\,dB$	$30.0\,dB$	0.64%
Ocean tide	$-5.0\,m$	$5.0\,m$	0.01%
Equilibrium tide	$-0.5\,m$	$0.5\,m$	0.00%
Earth tide	$-1.0\,m$	$1.0\,m$	0.00%
Pole tide	$-15.0\,m$	$15.0\,m$	0.00%
Altimeter wind speed	$0\,m.s^{-1}$	$30.0\,m.s^{-1}$	1.09%
All together	-	-	3.45%

Table 5 – Editing criteria over cycles 1 to 319

The peak detected on cycle 30 (Figure 12) is due to an AMR anomaly that occured from 08/12/2016 04:36:34 to 09/12/2016 12:58:47. The second peak in located on cycle 112, where occured SHM. Before going into SHM, data is rejected by several parameters out of threshold (square off nadir angle, rms of range, backscattering coefficient, significant wave height, altimeter ionosphere, sea state bias, wind speed, sea surface height, sea level anomaly). The third pic is due to an AMR anomaly that occured from 24/04/2021 17:18:33 to 25/04/2021 01:21:54. A small peak is visible for cycle 307, it is attributed to a small AMR anomaly from 03/07/2022 00:00:12 to 02:36:07. A last peak is slightly visible for cycle 323, it is due to an AMR anomaly occuring from 10/12/2022 17:40:09 to 11/12/2022 06:26:14 and lead to the editing of several passes. Except those anomalies the rate of rejected by thresholds data is quite stable.
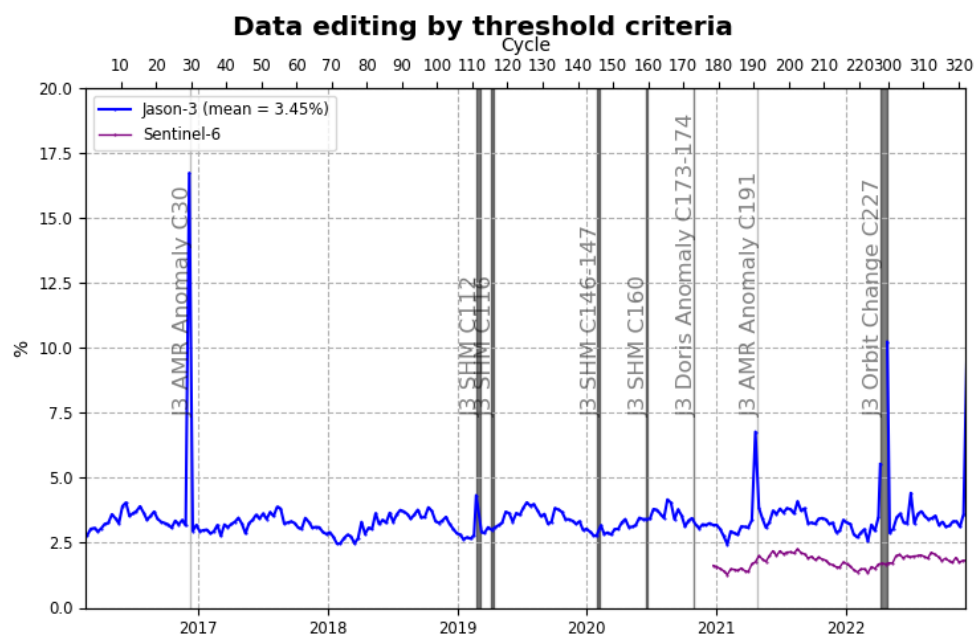

Figure 12 – Jason-3 data editing by threholds average by cycle.

3.2.4.1. Threshold criteria: 20-Hz range measurements number and standard deviation

1Hz range measurements computed with less than 10 full resolutions (20Hz, 20 measurements/seconds) are removed. Indeed they are considered as not consistent to compute 1Hz resolution range. Such situation usually occurs in regions with disturbed sea state or heavy rain, as shown on Figure 13 top right. Indeed waveforms are distorted by rain cells, which makes them often meaningless for SSH calculation. As a consequence, edited measurements due to several altimetric criteria are often correlated with wet areas.

For Jason-3, the average percentage of removed measurements using this criterion is 1.1% whereas it is 1.04% for Jason-2. The two missions provide very close values (Figure 13 top right).

Using the threshold editing on 20Hz measurements standard deviation (Figure 13 bottom), 1.4% of data are removed in average for Jason-3, which is very close to Jason-2 (1.41%). An annual signal appears here for both missions. As for 20Hz range measurements number, edited measurements are correlated with wet areas.
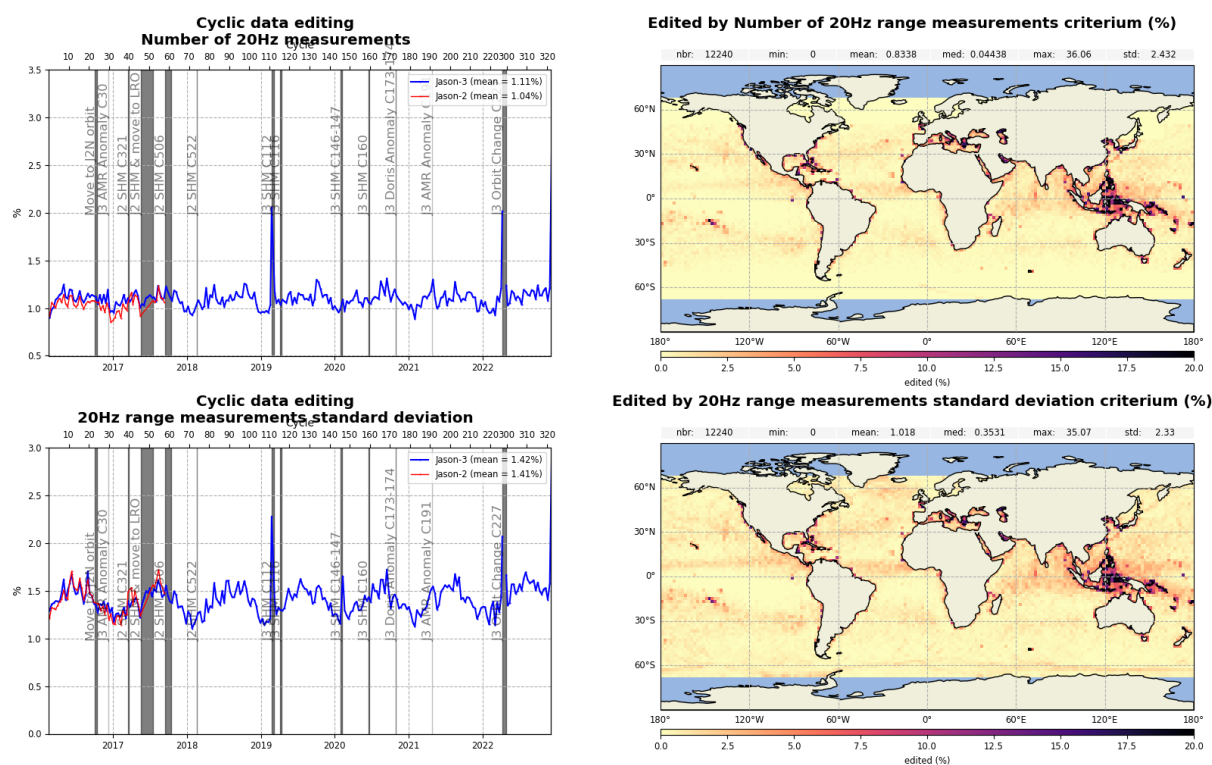

Figure 13 – Percentage of edited measurements by 20Hz range measurements threshold criterion (top) and by 20Hz range measurements standard deviation threshold criteria (bottom). Cycle per cycle monitoring compared with Jason-2 (left) and Jason-3 averaged map from cycle 209 to 319 (right).

3.2.4.2. Threshold criteria: Significant wave height (swh)

The percentage of edited measurements due to significant wave heights criterion is represented on Figure 14, and is about 0.66%. They are mostly due to set to default values data, and are located near coasts, in the equatorial regions and in circumpolar areas. The percentage of edited measurements slightly increases after the orbit change, this is also the case for the backscatter coefficient and is directly linked to the interleaved orbit properties.
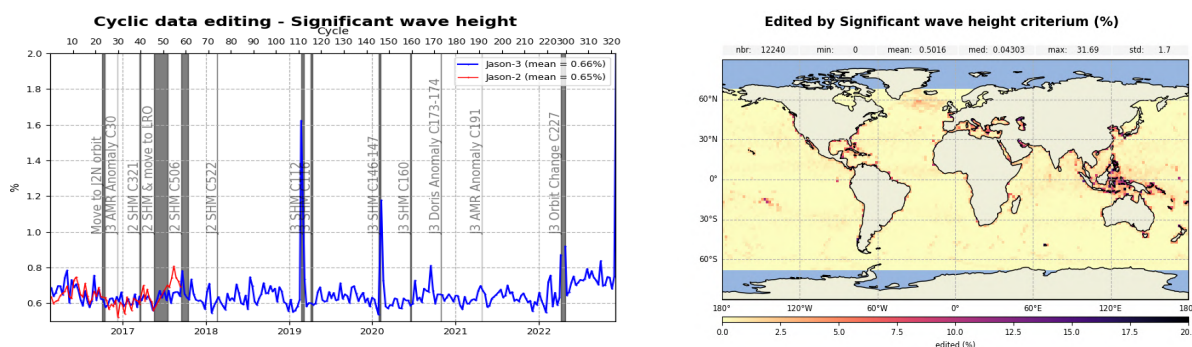
Figure 14 – Percentage of edited measurements by SWH threshold criterion. Left: Cycle per cycle monitoring compared with Jason-2 (Jason-2 DEM cycle in cyan. Jason-3 median tracker cycles in purple.) Right: Jason-3 averaged map from cycle 209 to 319 .

3.2.4.3. Threshold criteria: Backscatter coefficient (sigma0)

The percentage of edited measurements due to backscatter coefficient criterion is represented on top of Figure 15. It is about 0.64%, compared to 0.61% for Jason-2. The bottom part of Figure 15 shows again close values between the two missions for the 20Hz sigma0 standard deviation criterion. However, there are more rejected measurements with this criterion on Jason-3 (2.14%) than Jason-2 (1.95%). The number of measures flagged according to this criterion is higher with standard "F" than with standard "D", this is due to a change in the surface classification between both standards (see [5]). In addition differences seem to be linked to acquisition modes:

- For Jason-3 cycles 1 to 5, 7-8, 10, and 20, both missions are using median tracker: rejected data rate on this criterion are equivalent for both missions.

- For almost all cycles, Jason-2 uses median tracker and Jason-3 uses Diode/DEM automatic switch: there are less data removed for Jason-2 than for Jason-3.

- For Jason-2 cycle 311 (over Jason-3 cycles 30 and 31), both missions are in Diode/DEM mode: the results are quite equivalent.

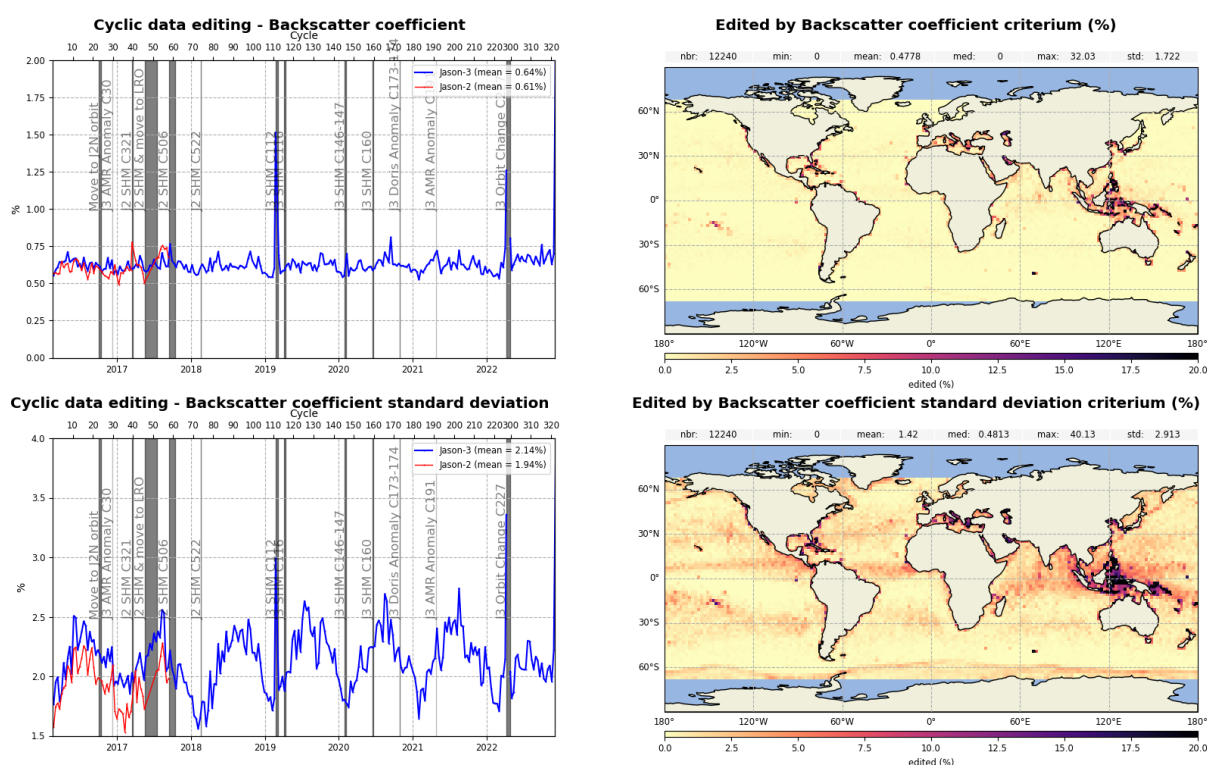Edited measurements are especially found in regions with disturbed waveforms, as shown on the maps.

Figure 15 – Percentage of edited measurements by backscatter coefficient threshold criterion (top) and by 20Hz backscatter coefficient standard deviation threshold criteria (bottom). Cycle per cycle monitoring compared with Jason-2 (left, Jason-2 DEM cycle in cyan. Jason-3 median tracker cycles in purple) and Jason-3 averaged map from cycle 209 to 319 (right).

3.2.4.4. Threshold criteria: Radiometer wet troposphere correction

The percentage of edited measurements due to radiometer wet troposphere correction criterion is represented in figure 16. It is about 0.2%. When removing cycles which experienced problems, percentage of edited measurements drops to 0.08%. For some cycles, the percentage of edited measurements is higher than usual. For cycle 30, this unusual value (13.85%) is due to an AMR anomaly that occured from 08/12/2016 04:36:34 to 09/12/2016 12:58:47. For cycle 191, the edited measurements (3.4%) correspond to another AMR anomaly occuring from 24/04/2021 17:18:33 to 25/04/2021 01:21:54. Compared to Jason-2 values, they are within the same order of magnitude, except specific events or anomalies (Jason-2 AMR anomalies during cycle 285 and cycle 326, that correspond respectively to Jason-3 cycle 5 and cycle 45 datation).
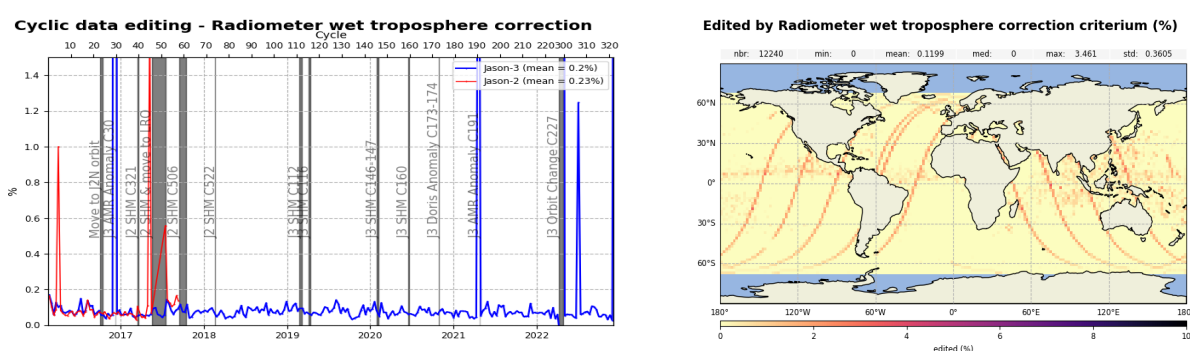
Figure 16 – Percentage of edited measurements by radiometer wet troposphere correction threshold criterion. Left: Cycle per cycle monitoring compared with Jason-2. Right: Jason-3 averaged map from cycle 209 to 319.

3.2.4.5. Threshold criteria: Ionospheric correction

The mean percentage of edited data by threshold criterion on ionospheric correction is 0.91%. It is much lower than Jason-2 mean (1.18%) and this gain is explained by the filtered version of the ionospheric correction used in the standard "F" (see [5] and [12]). The map on figure 17 shows that measurements edited by filtered dual frequency ionosphere correction are mostly found near coasts and at ice frontiers.
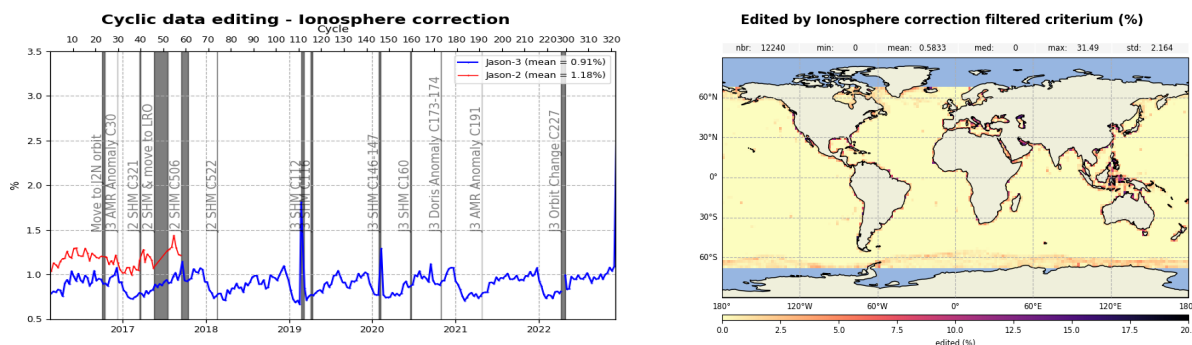

Figure 17 – Percentage of edited measurements by ionospheric correction threshold criterion. Left: Cycle per cycle monitoring compared with Jason-2. Right: Jason-3 averaged map from cycle 209 to 319.

3.2.4.6. Threshold criteria: Altimeter wind speed

The percentage of edited measurements due to altimeter wind speed criterion is represented on figure 18. It is about 1.09%, and in accordance with Jason-2 (1.03%). Measurements are usually edited because of default values. This is the case when sigma0 itself is at default value, or when it shows very high values (higher than 25 dB), which occurs during sigma bloom situations and also over sea ice. Indeed, the wind speed algorithm (which uses backscatter coefficient and significant wave height) can not retrieve values for sigma0 higher than 25 dB.

Wind speed is also edited when it includes negative values, which can occur in GDR products. Nevertheless, sea state bias is available even for negative wind speed values. Therefore, the percentage of edited altimeter wind speed data is higher than the percentage of edited sea state bias data (see 3.2.4.7.).

The map 18 showing percentage of measurements edited by altimeter wind speed criterion is correlated with maps 14 (swh) and 19 (ssb).
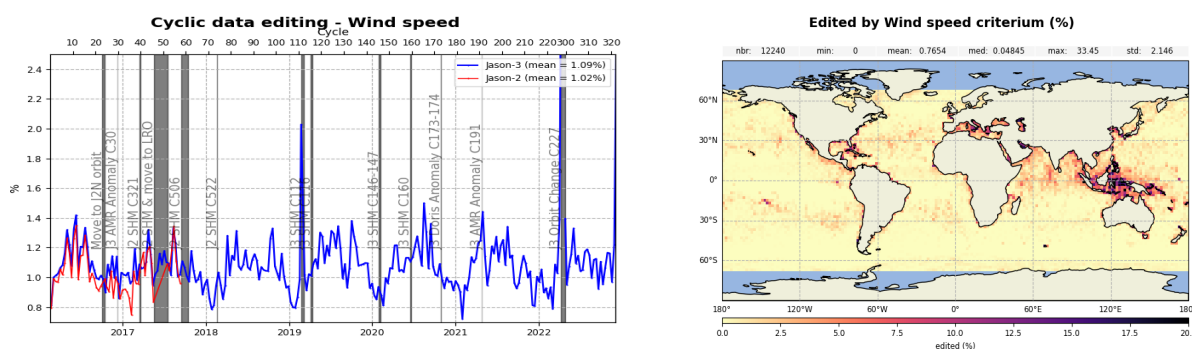

Figure 18 – Percentage of edited measurements by wind speed threshold criterion. Left: Cycle per cycle monitoring compared with Jason-2. Right: Jason-3 averaged map from cycle 209 to 319.

3.2.4.7. Threshold criteria: Sea State Bias

Regarding the sea state bias criterion, the percentage of Jason-3 edited measurements is about 0.59% and 0.63% for Jason-2. The difference can also be observed on the sigma0 and the significant wave height threshold criteria (which are both used for SSB computation).
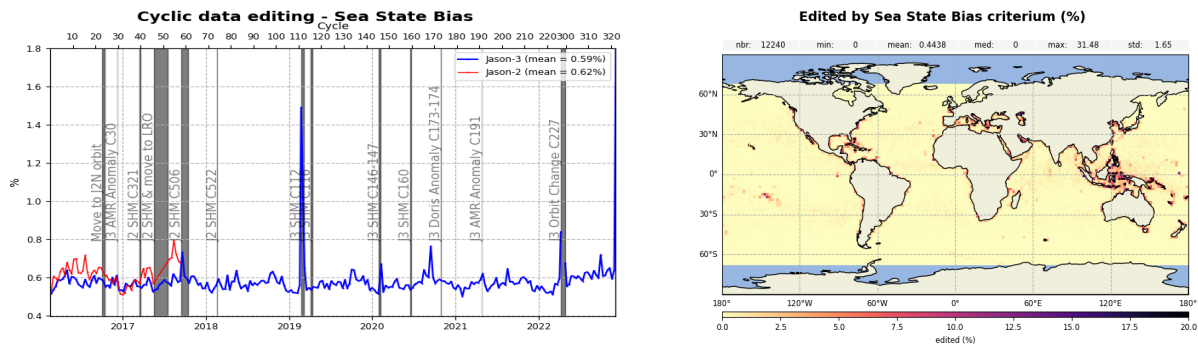

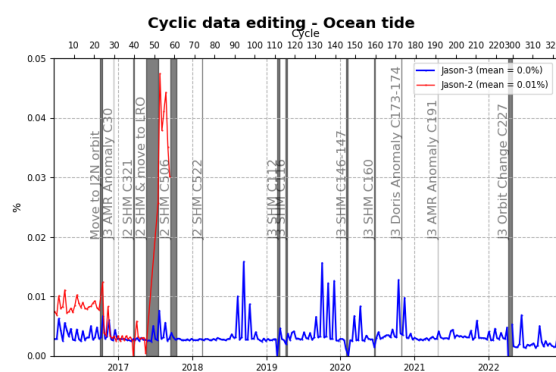*Figure 19 – Percentage of edited measurements by sea state bias threshold criterion. Left: Cycle per cycle monitoring compared with Jason-2. Right: Jason-3 averaged map from cycle 209 to 319.*

3.2.4.8. Threshold criteria: Ocean tide

The percentage of edited measurements due to ocean tide is lower than 0.01% for both missions. The ocean tide correction is a model output, there should therefore be no edited measurement. Indeed there are no measurements edited in open ocean areas, but only very few near coasts (Alaska, Kamchatka, Labrador). These measurements are mostly at default values. The level of edited measurements decreases or increases with move of orbit for Jason-2 : this is related to the new ground track, which no longer overflows the same areas. Two different models are used for both missions : Jason-3 uses the FES14B model while Jason-2 uses the GOT4.8.

Figure 20 – Percentage of edited measurements by ocean tide threshold criterion. Cycle per cycle monitoring compared with Jason-2.

3.2.4.9. Threshold criteria: Square off nadir angle

The percentage of edited data is a little higher for Jason-3 (0.66%) than it is for Jason-2, this is due to the difference in the surface type mask as explained in [5] (part 3.2.3). An increase in Jason-2 edited measurements is observed from July 2017 after Jason-2 move to drifting orbit. The map 21 shows that edited measurements are mostly found in coastal regions and regions with disturbed waveforms.
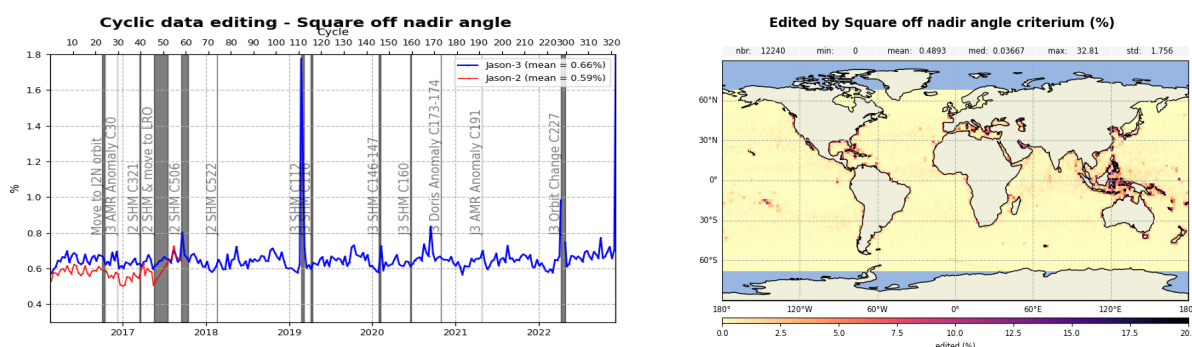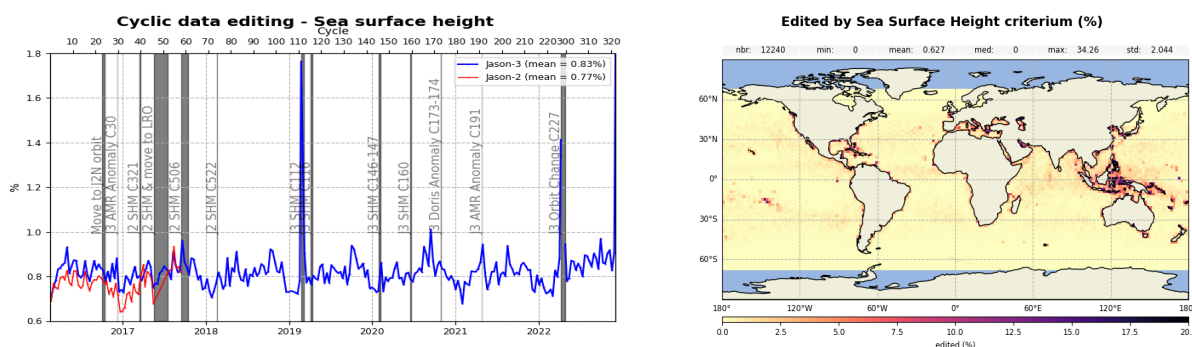

Figure 21 – Percentage of edited measurements by square off nadir angle threshold criterion. Left: Cycle per cycle monitoring compared with Jason-2. Right: Jason-3 averaged map from cycle 209 to 319.

3.2.4.10. Threshold criteria: Sea surface height

Sea surface height represents the difference between the orbit and the altimeter range in Ku band. Figure 22 summarizes the editing resulting from the sea surface height threshold criterion. It removes in average 0.83% of data for Jason 3 whereas it removes 0.77% of data for Jason 2. The editing is usually due to range measurements at default values near coast in equatorial and mid-latitude regions, as well as regions with low significant wave heights.

Figure 22 – Percentage of edited measurements by sea surface height threshold criterion. Left: Cycle per cycle monitoring compared with Jason-2. Right: Jason-3 averaged map from cycle 209 to 319.

3.2.4.11. Threshold criteria: Sea Level Anomaly

The percentage of edited data by threshold criterion is 1.51% for Jason-3. As the wet tropospheric correction is used in the SLA computation, percentage of edited SLA measurement presents the same peak on cycle 30. In the same way edited data due to derive from altimeter corrections before SHM at cycle 112 are rejected for this criterion (second peak in february 2019). The radiometer yellow alarm from cycle 191 also produces another lack of wet tropospheric correction which results in a SLA editing as well, this event is seen in the figure 23 over of a few tracks. When removing these cycles, the percentage of edited measurements drops to lower than 1%. The rate of rejected data for Jason-3 is a little higher than for Jason-2 (0.93%), this is due to the special editing of the filtered ionospheric corrrection in coastal areas (see [5] part 3.2.1 and 3.2.4). As in Jason-3, higher points on Jason-2 monitoring are mainly due to Jason-2 wet troposphere contribution, where AMR was unavailable during cycle 285 (Jason-3 cycle 5), cycle 326 (Jason-3 cycle 45), and for restart after SHM, leading to an increase of the quantity of edited data (point out of plot scale).
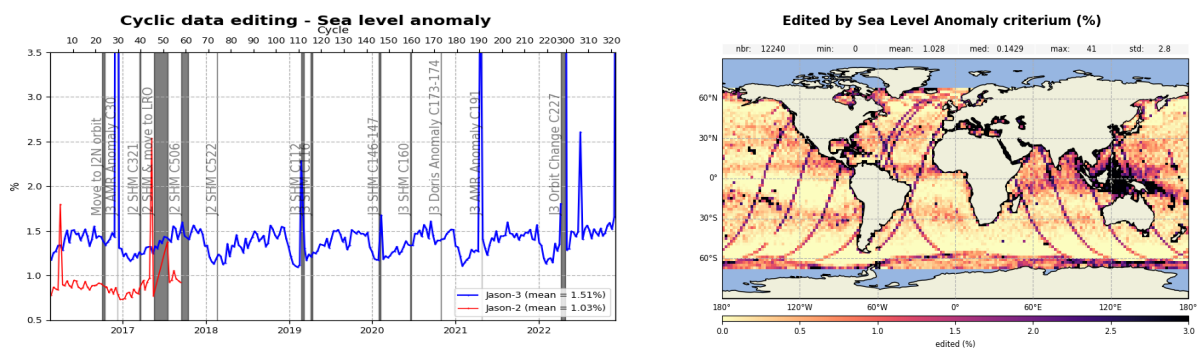
Figure 23 – Percentage of edited measurements by sea level anomaly threshold criterion. Left: Cycle per cycle monitoring compared with Jason-2. Right: Jason-3 averaged map from cycle 209 to 319.

4.   Monitoring of altimeter and radiometer parameters

4.1.   Methodology

Mean and standard deviation of Jason-3 main parameters have both been monitored since the beginning of the mission.

4.2.   20 Hz range measurements

The monitoring of the number and standard deviation of 20 Hz elementary range measurements used to derive 1 Hz data is presented here. These two parameters are computed during the altimeter ground processing. For both Jason-2 and Jason-3, before performing a regression to derive the 1 Hz range from 20 Hz data, a MQE (mean quadratic error) criterion is used to select valid 20 Hz measurements. This first step of selection consists in verifying that the 20 Hz waveforms can be approximated by a Brown echo model (Brown, 1977 [14]) (Thibaut et al. 2002 [15]).

Then, through an iterative regression process, elementary ranges too far from the regression line are discarded until convergence is reached. Thus, monitoring the number of 20 Hz range measurements and the standard deviation computed among them is likely to reveal changes at instrumental level.

4.2.1.   20 Hz range measurements number in Ku-Band and C-Band

Jason-3 number of elementary 20 Hz range measurements starts with values slightly higher than Jason-2 until cycle 3. During cycle 3, new calibration (CAL2) filter turned the square off-nadir angle to zero, which implies the absence of waveform mispointing, a higher MQE and a smaller number of elementary measurements. Then from cycle 4 onwards, Jason-3 number of elementary 20 Hz range measurements is very similar to Jason-2 with an average of 19.61 versus 19.60 in Ku-band (left of figure 24) and 19.24 versus 19.25 in C-band (right of figure 24).
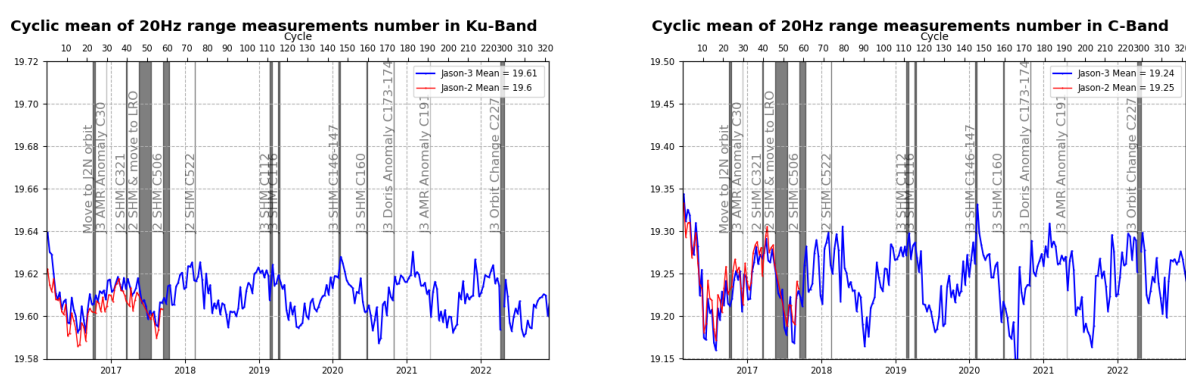

Figure 24 – Cyclic monitoring of number of elementary 20 Hz range measurements for Jason-2 and Jason-3 in both frequency bands (Ku and C)

Elementary number of measurements used to compute a 1Hz measurement is correlated to significant wave height (4.5.): figure 25 shows less elementary range measurements around Indonesia, the Mediterranean Sea and close to coasts, which are all regions of low significant wave heights.
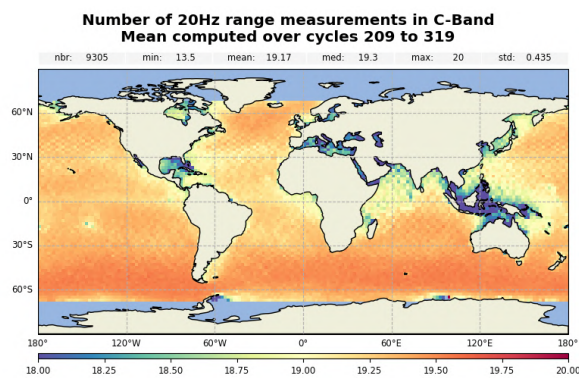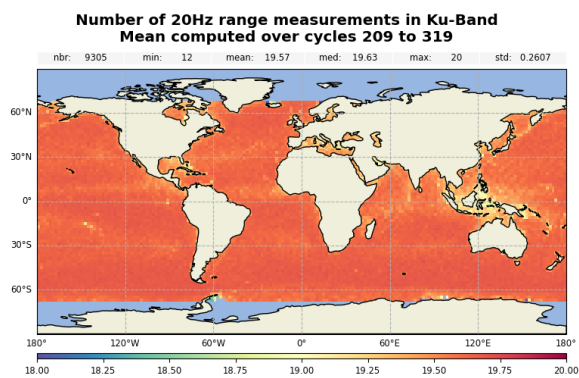
Figure 25 – Map of number of 20 Hz range measurements for Jason-3 averaged over cycles 209 to 319, in Ku-band (left) and in C-band (right).

4.2.2. 20 Hz range measurements standard deviation in Ku-Band and C-Band

Figure 26 shows the monitoring of Jason-3 and Jason-2 20 Hz range measurements standard deviation, in Ku-band (left) and C-band (right). Jason-3 standard deviation of the 20 Hz measurements is 8.00 cm for Ku-Band and 17.57 cm for C-Band. It is similar to Jason-2 data (8.00 cm in Ku-Band and 17.44 cm in C-Band). 20 Hz range measurements standard deviation is higher on C-band than on Ku-band due to the onboard averaging that is performed over less waveforms (onboard averaging of 90 measurements for each 20 Hz Ku-band value, against 15 in case of C-band), which leads to an increased noise.
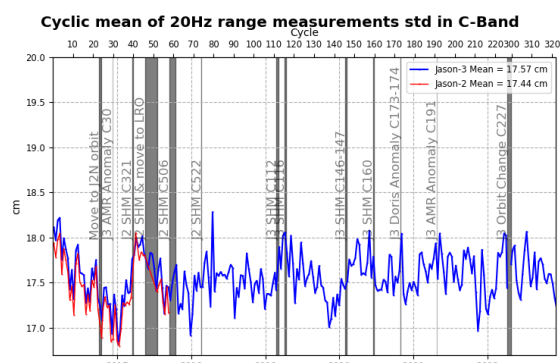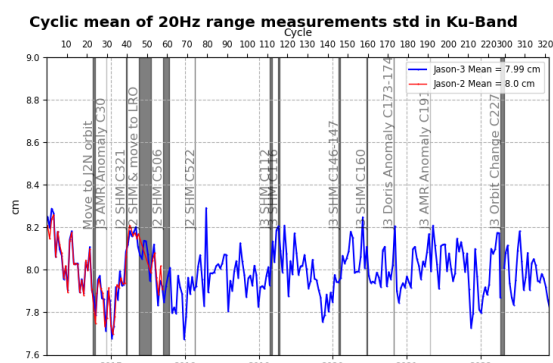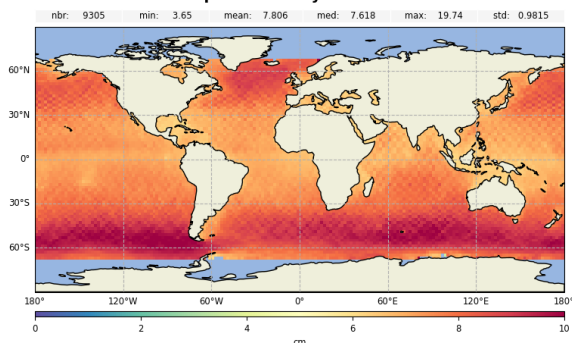

Figure 26 – Cyclic monitoring of number of elementary 20 Hz range measurements standard deviation for Jason-2 and Jason-3 in both frequency bands (Ku and C)

Standard deviation of measurements is correlated to significant wave height (swh dedicated part: 4.5.).
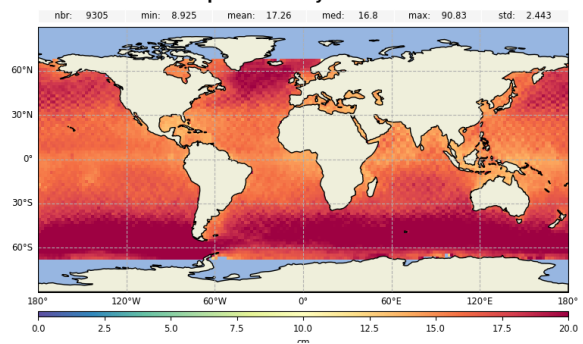
Figure 27 – Map of 20 Hz range measurements standard deviation for Jason-3 averaged over cycles 209 to 319, in Ku-band (left) and in C-band (right).

4.3. Off-Nadir Angle from waveforms

The off-nadir angle is derived from the slope of the trailing edge of the waveform during the altimeter processing: it can either be caused by real platform mispointing or by backscattering properties of the surface. The square of the off-nadir angle, averaged on a cyclic basis (taking into account valid measurements only), has been plotted for Jason-3 and Jason-2 on figure 28.

At the beginning of the mission, Jason-3 altimeter mispointing was deeply analysed to understand the negative values observed from cycle 3 after GPS upload. Mispointing is actually related to CAL2 filter shapes, which depends on automatic gain control settings for Jason-3. During the first cycles, the in-flight calibration (CAL2) filters were measured using a different Automatic Gain Control code than the one used during waveform acquisition over ocean, in order to optimize the CAL2 measurement numerical accuracy (quantification optimization). It has however an impact on the filter slope and fully explains the observed mispointing negative values. The filter slope was modified during cycle 14 (June 26th, 2016) and explains the jump to zero on the IGDR curve. This correction was applied during GDR production, which explains the difference between red and green curves between cycles 4 and 14, so that GDR mispointing has been close to zero from cycle 4.
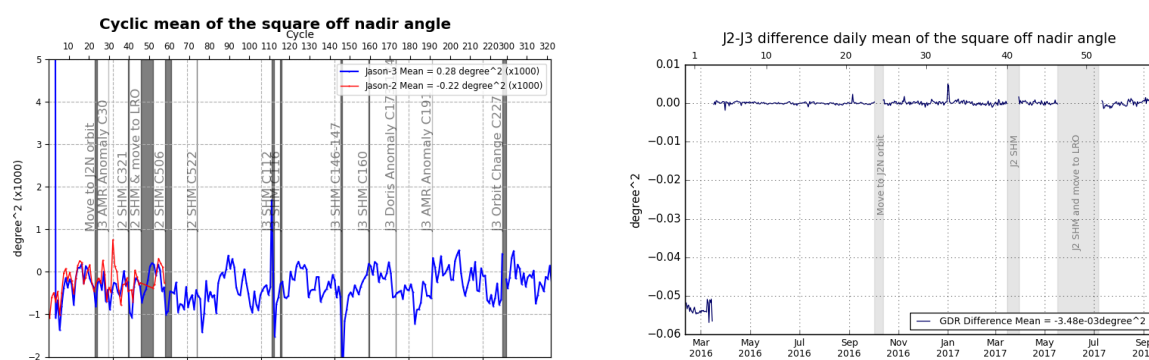

*Figure 28 – **Left:** Cyclic monitoring of the square off-nadir angle for Jason-2 and Jason-3 for GDRs (blue and red curves) and Jason-3 IGDRs (product IGDR for cycles 1 to 41, and IGDR L2P from cycle 25 to 132 in green). **Right:** Jason-2 - Jason-3 difference daily monitoring of the square off-nadir angle (Note that the figure on right panel was computed using GDR-D data for both Jason-3 and Jason-2.).*

Except round SHM in 2019 and 2020, no mispointing event occured on Jason-3 over the considered period. The map figure 29 is generally slightly negative, except for regions around Indonesia, and close to coasts.
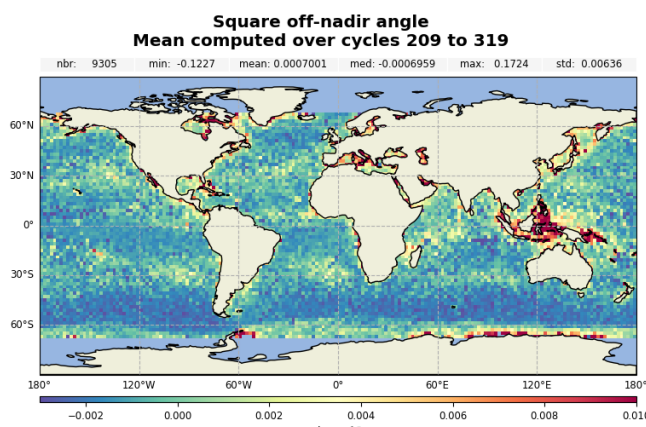
Figure 29 – Map of the square off-nadir angle for Jason-3 averaged over cycles 209 to 319.

Without taking into account the first three cycles, square off-nadir angle is monitored year by year on the left part of figure 30, highlighting a small annual signal (global mean is higher during summer). Also, a small higher value of square off-nadir angle is visible before SHM at cycle 112 and just after SHM at cycle 147. Square off-nadir angle slighly depends on significant wave height as shown on right part of figure 30: considering this monitoring for swh between 2m and 6m, slope is -0.0004 deg^2/m.
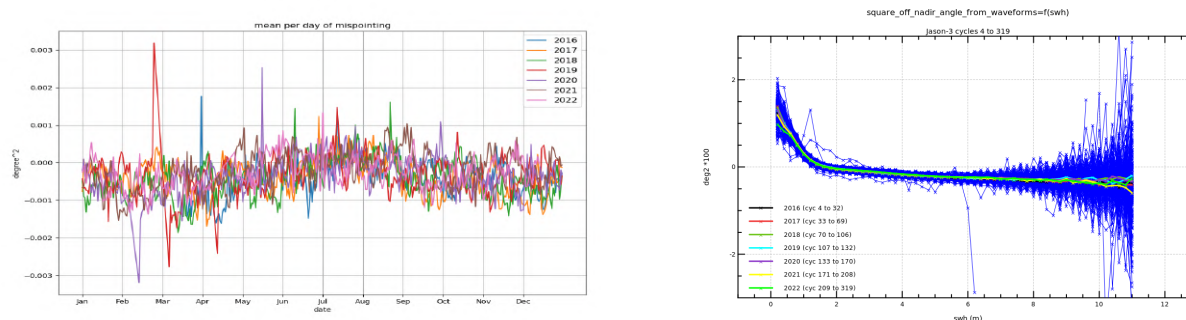

*Figure 30 – **Left:** Mean per day of mispointing for Jason-3 from cycle 4. **Right:** Square off nadir angle against swh.*

4.4. Backscatter coefficient

The Jason-3 Ku-band and C-band backscatter coefficients show good agreement with Jason-2 as visible on cyclic monitoring (figure 32). Jason-3 backscatter coefficient is about 13.69 dB for Ku-band (15.39 dB for C-band) while for Jason-2 it is about 13.51 dB (15.40 dB). The difference between the two missions is about -0.25 dB (-0.11 dB) and presents a good stability. However, this was different from cycle 0 to cycle 4, where slight mispointing on Jason-3 caused a higher difference of sigma0 between missions.

During the tandem flight, Jason-3 sigma0 was modified with a new altimeter characterization file, an update of the Look Up Tables (LUT, Patch 6) and a new CAL2 filter (cycle 14, June 26th , 2016). All of them where applied on all GDR cycles. As a consequence, there is a bias between backscatter coefficient in GDR and IGDR products until cycle 14. In addition, a new AMR calibration file is applied for IGDR cycle 17 (see part 4.7.), so that IGDR and GDR sigma0 are slightly different until cycle 17 due to atmospheric attenuation applied to sigma0 (as the atmospheric attenuation is derived from radiometer parameters).
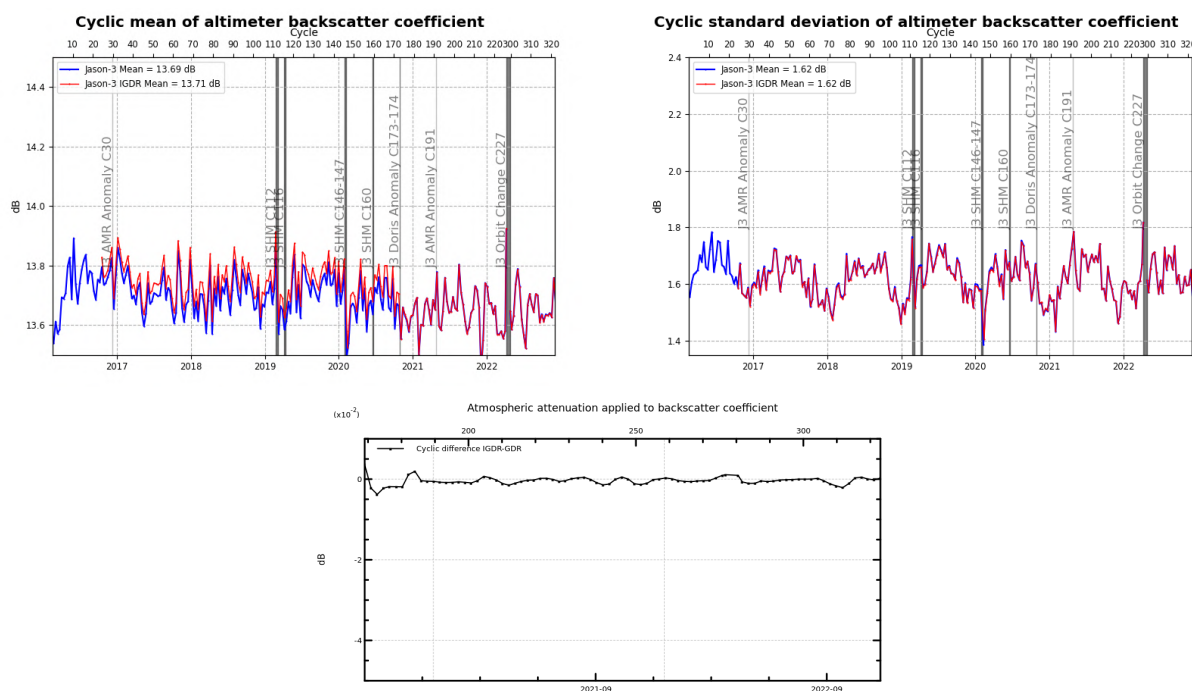

*Figure 31 – **Top:** Cyclic monitoring of backscatter coefficient for Jason-3 (Ku-band) textcolorVertIG-DRIGDR/GDR. **Bottom:** difference of atmospheric attenuation applied to sigma0 between IGDR and GDR products.*
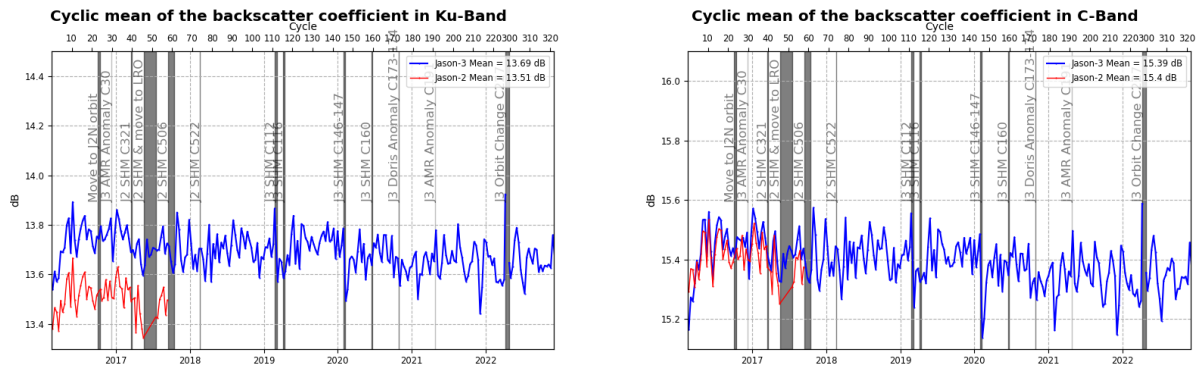
Figure 32 – Cyclic monitoring of backscatter coefficient for Jason-2 and Jason-3 for Ku-band (left) C-band (right)
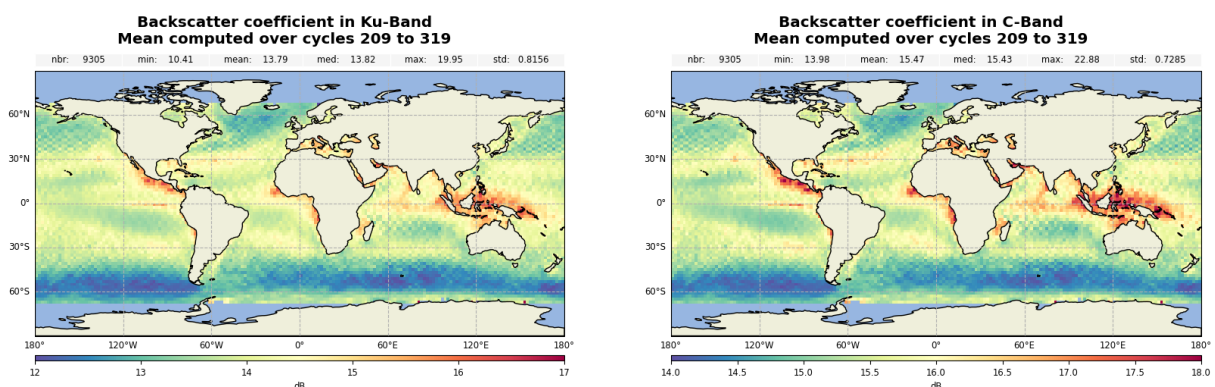

Figure 33 – Map of backscatter coefficient for Jason-3 averaged over cycles 209 to 319, in Ku-band (left) and in C-band (right).

4.5. Significant wave height

As for sigma0 parameter, a very good consistency between both Jason-2 and Jason-3 significant wave height is shown (see figure 35). In addition, until Jason-3 cycle 23 (tandem phase, observing the same ocean with only 1'20" apart), Jason-2 and Jason-3 measurements are identical. After Jason-2 move to interleaved orbit, the two missions are not as close as during tandem phase and measured swh are slightly different, but there is still no bias between Jason-2 and Jason-3 measured wave height in average (see bottom of figure 35).
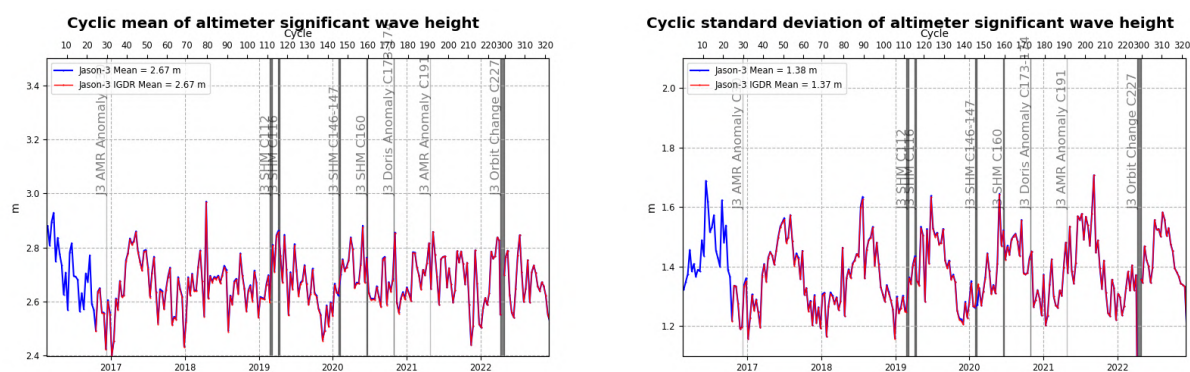

Figure 34 – Cyclic monitoring of significant wave height for Jason-3 (Ku-band) IGDR/GDR.
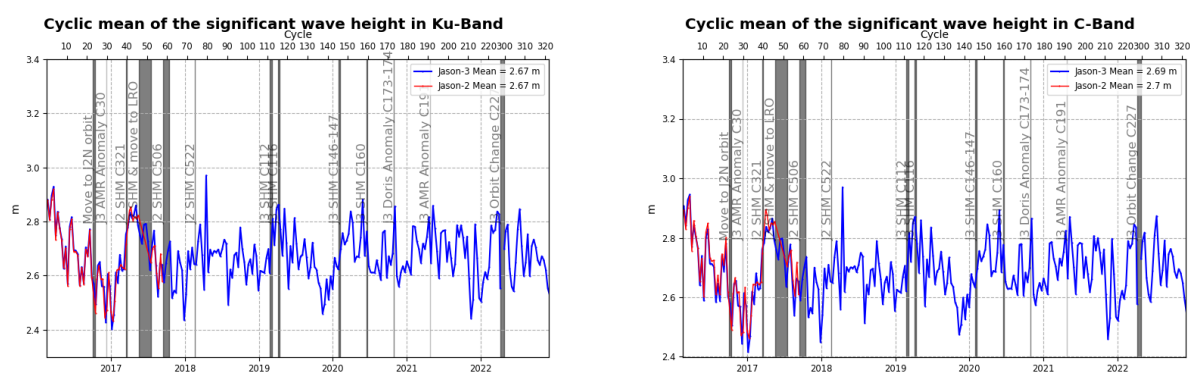

Figure 35 – Cyclic monitoring of significant wave height for Jason-2 and Jason-3 for Ku-band (left) and for C-band (right).
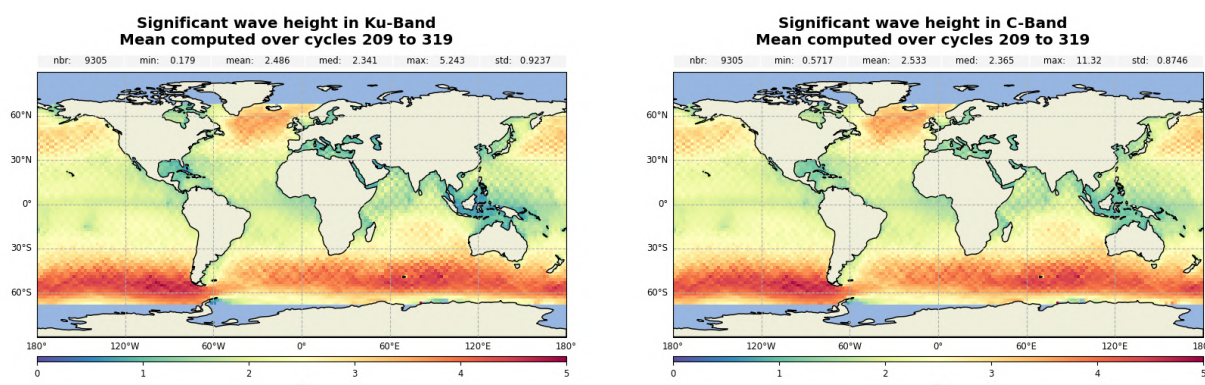
Figure 36 – Map of significant wave height for Jason-3 averaged over cycles 209 to 319, in Ku-band (left) and in C-band (right).

4.6. Dual-frequency ionosphere correction

The dual frequency ionosphere corrections derived from the Jason-3 and Jason-2 altimeters show a mean difference of about 0.87 cm (figure 37), with cycle to cycle variations lower than 1 mm.

Until the LUT changes that occurred during cycle 14 (for O/IGDRs), the mean bias between the two missions was 1 cm (for O/IGDRs). It turns then to 0.55 cm following "jumps" of Ku range (5 mm), C Range (1.5 cm) and sea state bias (0.1 mm). This event has an impact on Sea Level Anomalies retrieved from OGDRs and IGDRs products. For GDR products, the same LUT was used for the whole mission period, hence the absence of jump (see bottom and right of figure 37).

Note that as IGDR are produced following standard F, a filtered solution of altimeter ionospheric correction has been available in the products from IGDR cycle 174 onwards (see [12]). The maps were produced with the bifrequency ionospheric correction and not the filtered one.
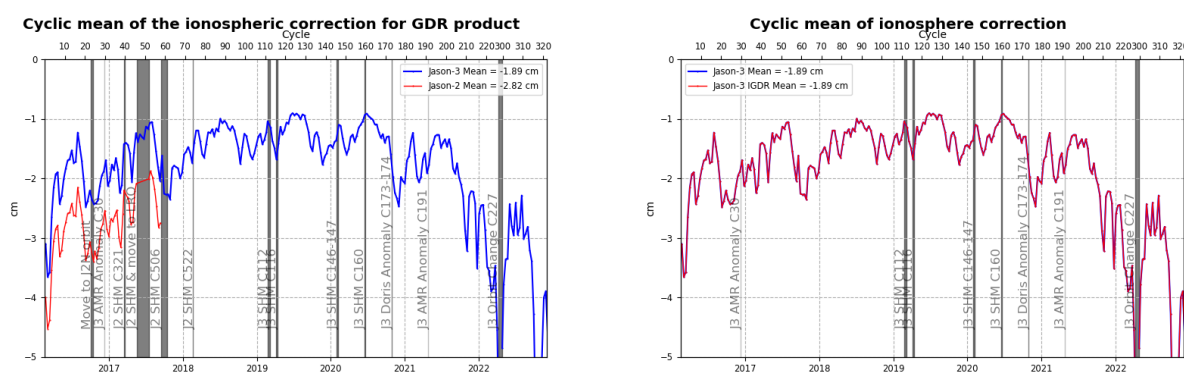

*Figure 37 – Cyclic monitoring of ionospheric correction for Jason-2 and Jason-3. (**left**). Cyclic monitoring of Jason-3 ionospheric correction for IGDR and GDR data (**right**).*
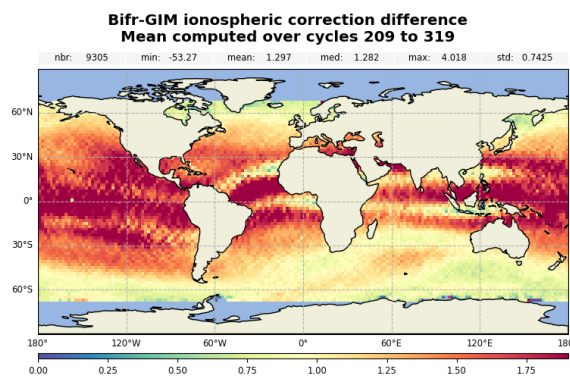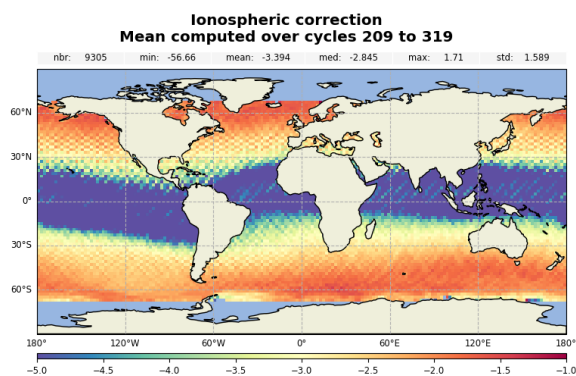
*Figure 38 – **Left:** Map of ionospheric correction for Jason-3 averaged over cycles 209 to 319. **Right:** Map of dual-frequency minus GIM ionospheric correction solutions.*

When comparing altimeter ionosphere correction to GIM correction (figure 39), mean as well as standard deviation of this difference present same variation for both missions.
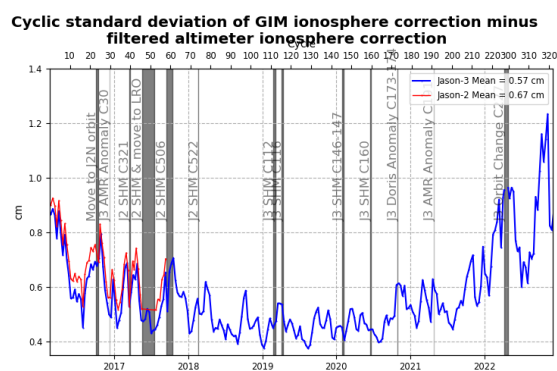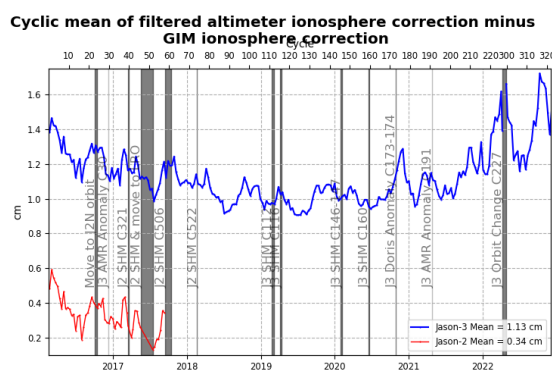

Figure 39 – Cyclic monitoring of GIM ionosphere correction minus filtered altimeter ionosphere correction for Jason-2 and Jason-3. Left: mean, right: standard deviation.

4.7.   AMR Wet Troposphere Correction

4.7.1.   Overview

In order to evaluate radiometer wet troposphere correction, liquid water content, water vapor content and atmospheric attenuation, Jason-3 uses a three-frequency AMR radiometer (18.7, 23.8 and 34.0 GHz), similar to the one used on Jason-2.

Note that the 23.8 GHz channel is the primary water vapor sensing channel, meaning a higher water vapor concentration leads to larger 23.8 GHz brightness temperature values. As a consequence, top right and bottom right parts of figure 40 are correlated. Moreover, the 34 GHz channel and the 18.7 GHz channel, which have less sensitivity to water vapor, facilitate the removal of the contributions from cloud liquid water and excess surface emissivity of the ocean surface due to wind, which also act to increase the 23.8 GHz brightness temperature.
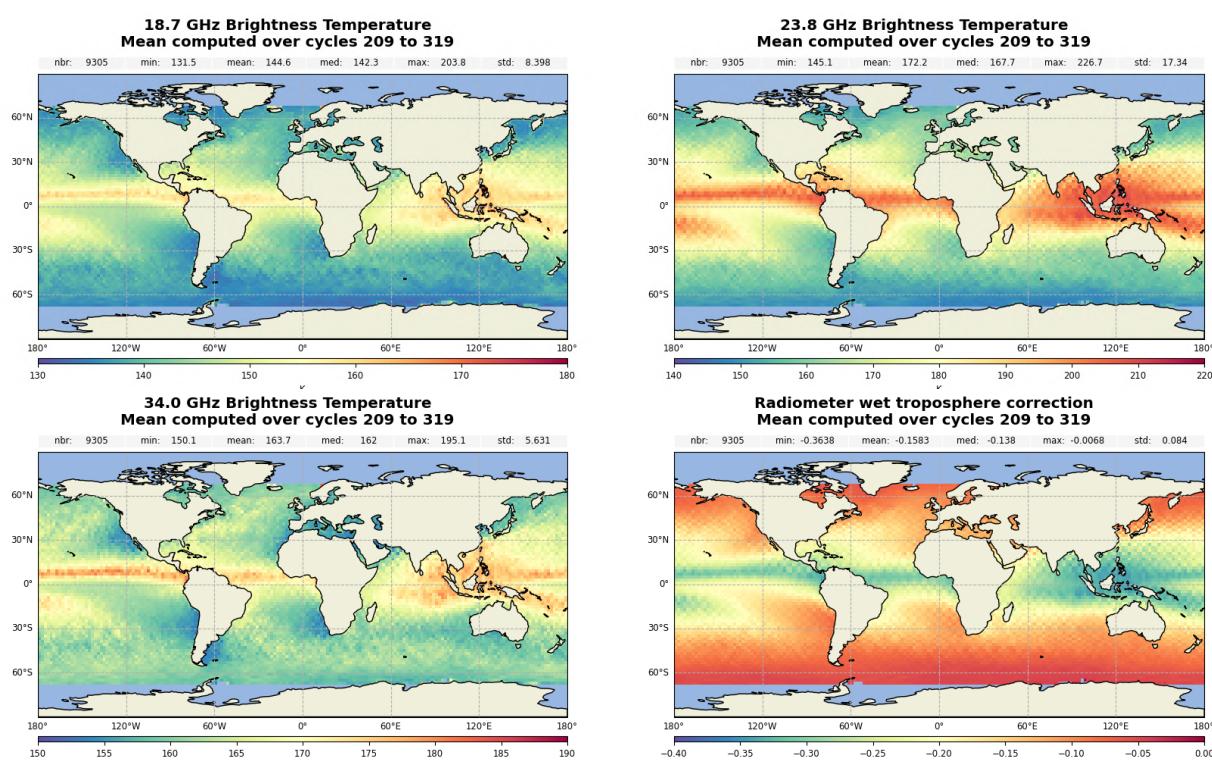

Figure 40 – Map of Jason-3 brightness temperatures averaged over cycles 209 to 319: 18.7 Ghz channel (top left), 23.8 Ghz channel (top right) and 34.0 Ghz channel (bottom left). Map of AMR wet troposphere correction for Jason-3 averaged over cycles 209 to 319 (bottom right)

4.7.2.   Comparison with the ECMWF model

The wet troposphere correction computed from ECMWF model data has been used to check the Jason-2 and Jason-3 radiometer corrections. The cross-comparison between all radiometers and models available is necessary to analyze the stability of each wet troposphere correction. An overview of the wet troposphere correction importance for mean sea level is given in Obligis et al. [16]. The difference between AMR and model data is computed on a daily basis and is plotted on figure 42 for Jason-3 IGDR and GDR, and Jason-2 GDR for comparisons. As observed, Jason-3 AMR correction has a drift of more than half a millimetre per cycle for IGDRs (and OGDRs, not shown). Such behaviour is routinely monitored by JPL instrument expert team. Impact of drift is corrected through ground calibration (ARCS, Autonomous Radiometer Calibration System), also accounting for cold sky calibrations. The first ARCS calibration occured at the end of cycle 17 and is visible on IGDR monitoring. As regards GDR data, AMR radiometer correction is calibrated at each cycle and the calibration coefficients are modified if necessary. It allows to correct the drift for GDR data (red curve on figure 42), nevertheless small drifts and jumps persist of up to 2 mm amplitude.

Due to an ECMWF model change of version on June 6th 2019, a jump is visible in the monitoring of radiometer minus model wet tropopshere correction mid-2019.
Due to an ECMWF model change of version on September 2021, a jump is visible in the monitoring of radiometer minus model wet tropopshere correction in October 2021.

Due to the change of version for O/IGDR products for standard "F" on 29th October 2020, an expected jump of about -6.4mm is visible on IGDR data. Note that the jump between 24/11/2020 and 30/11/2020 on IGDR data (seen on figure 41) is due to the use of a wrong AMR calibration file for the product generation.

In GDR, Jason-3 AMR-ECMWF model daily difference is about 0.2 mm and about 5.3 mm for Jason-2. Though Jason-3 radiometer wet troposphere correction is more stable for GDRs, Jason-3 and Jason-2 do not have exactly the same behaviour, with an inflexion point around cycle 13 and another one after Jason-2 moved to its new interleaved groundtrack on October 2016. With 2017 Safe Hold Modes, Jason-2 shows some jumps that are known to occur after restart. The jump visible on January 2020 on Jason-3 is due to the SHM that occurs over cycle 143.
Standard deviation of radiometer minus model wet troposphere correction is equivalent around 1.2 cm for Jason-2 and around 1,1 cm for Jason-3 (right of figure 42).
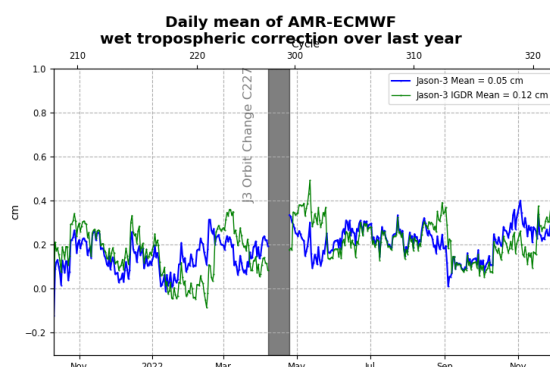

Figure 41 – Daily monitoring of AMR minus ECMWF model wet tropospheric correction over one year.
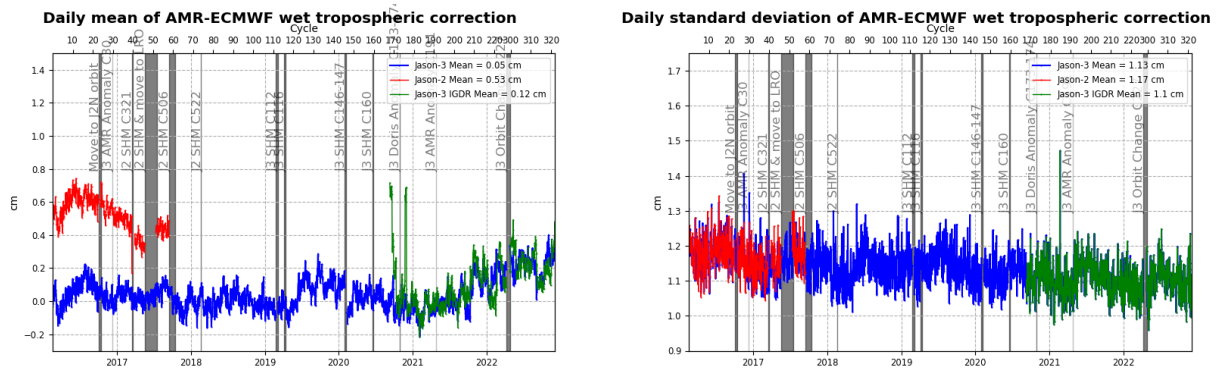
*Figure 42 – Daily monitoring of AMR minus ECMWF model wet tropospheric correction. mean (**left**) and standard deviation (**right**)*

4.7.3. Investigations regarding a drift of the instrument

An investigation was performed in the scope of the MSL activities over 2021 to assess a potential drift trend of the radiometer instrument. This was adressed in Jason-3 2021 Annual Report (see [7]).

Over 2022, further investigations were conducted to confirm this trend. This process is still on and might lead to minor changes in the wet tropospheric correction currently available.

4.8. Altimeter wind speed

Jason-3 and Jason-2 present very close results in terms of wind speed. Jason-2 provides lower wind values than Jason-3 (7.80 vs 7.98 m.s^{-1}, figure 43). The evolution frm GDR-D to GDR-F wind speed computation is detailed in [5] part 5.4.4. The difference between the two missions is 0.23 m.s^{-1} and can be separated in two phases: before and after 16-03-2016. The uploading of updated parameters for STR1 and gyros to correct misalignments occurred on March, 16th 2016 (Cycle 3) and corrected the square off nadir angle, i.e. the mispointing of the platform. Then from the restart of data production (March 18th) mispointing was set to value close to zero, which increases the sigma0 and decreases the wind speed.
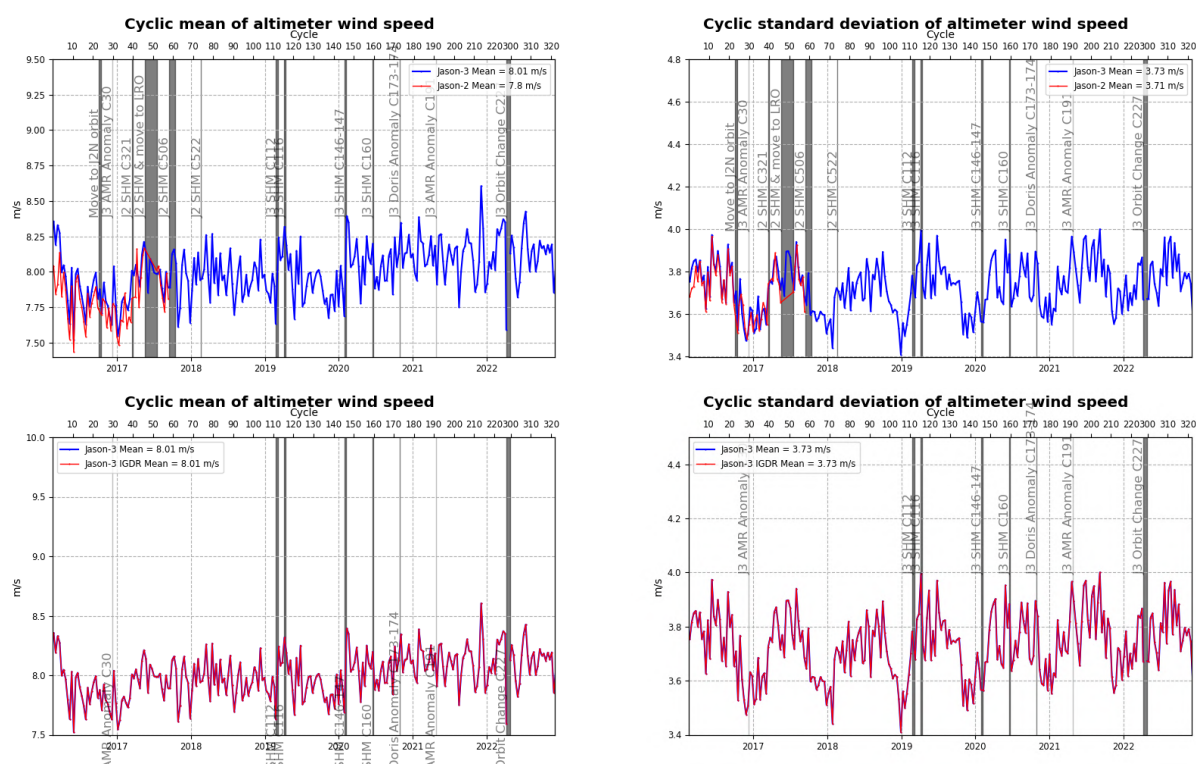

Figure 43 – Cyclic monitoring of altimeter wind speed mean (left) and standard deviation (right). **Top:** *for Jason-2 and Jason-3.* **Bottom:** *for Jason-3 GDR and IGDR data.*

Due to the change of version for IGDR products for standard "F" on 29th October 2020, an expected jump is visible on IGDR data (bottom left of figure 43). An adjustment is done before computing wind speed values (bias on sigma0) so that wind speed values in standard "F" are more coherent with ERA5 model distribution as seen on figure 44 and detailed in [5].
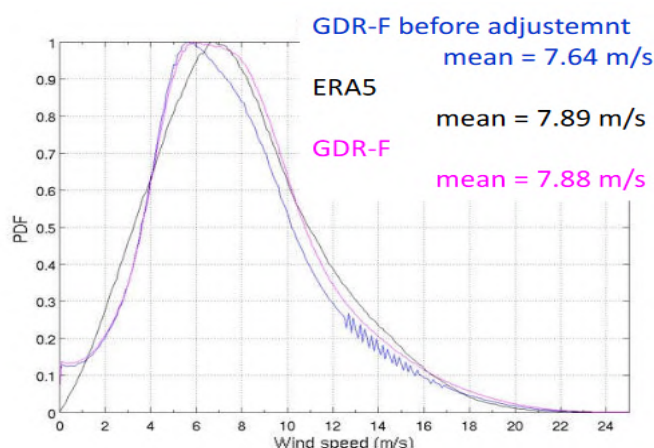
Figure 44 – Wind speed comparison product and ERA5 model

4.9. Sea state bias

GDR Sea state bias (SSB) in Ku band from Jason-3 (-10.34 cm) and Jason-2 (-8.46 cm) present an excellent agreement both in average and in standard deviation (5.02 and 4.61 cm for Jason-3 and Jason-2 respectively).

Due to the change of version for IGDR products for standard "F" on 29th October 2020, an expected jump of about -1.9cm is visible on IGDR data (figure 45).
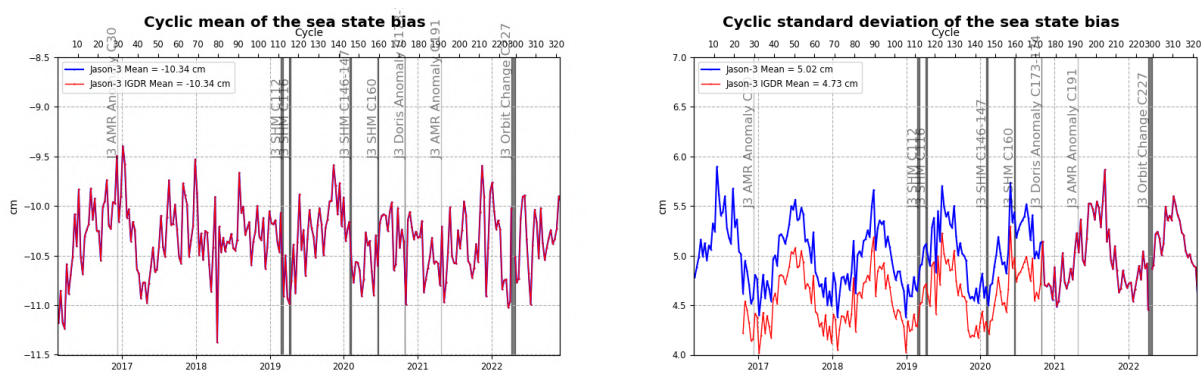

Figure 45 – Cyclic monitoring of the sea state bias mean and standard deviation for Jason-3 IGDR/GDR.
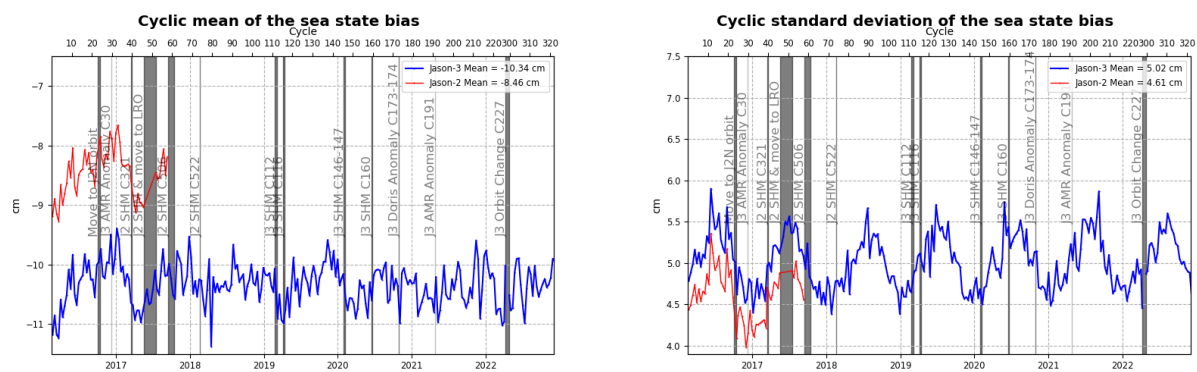
Figure 46 – Cyclic monitoring of the sea state bias mean and standard deviation for Jason-2 and Jason-3

5. SSH crossover analysis

5.1. Overview

SSH crossover differences are the main tool to estimate the whole altimetry system performances. They allow to analyze the SSH consistency between ascending and descending passes: it should not be significantly different from zero. More importantly, special care is given to the geographical homogeneity of the mean difference at crossovers. However in order to reduce the impact of oceanic variability, we select crossovers with a maximum time lag of 10 days. Mean and standard deviation of SSH crossover differences are computed from the valid dataset to perform maps or a cycle by cycle monitoring over all the altimeter period. In order to monitor the performances over stable surfaces, additional editing is applied to remove shallow waters (bathymetry above -1000m), areas of high ocean variability (variability above 20 cm rms) and high latitudes ($> |50|deg$). SSH performances are then always estimated with equivalent conditions. The main SSH calculation for Jason-3 (and Jason-2) are defined below.

$$SSH = Orbit - Altimeter\ Range - \sum_{i=1}^{n} Correction_i$$

with $Jason-3\ Orbit = CNES\ orbit$ for GDR products, and

$$
\begin{aligned}
\sum_{i=1}^{n} Correction_i \quad = \quad & Non\ parametric\ sea\ state\ bias\ correction \\
+ \quad & Dual\ frequency\ ionospheric\ correction\ (filtered) \\
+ \quad & Radiometer\ wet\ troposphere\ correction \\
+ \quad & Dry\ troposphere\ correction \\
+ \quad & Dynamical\ atmospheric\ correction \\
+ \quad & Ocean\ tide\ correction\ (including\ loading\ tide) \\
+ \quad & Internal\ tide\ correction \\
+ \quad & Earth\ tide\ height \\
+ \quad & Pole\ tide\ height
\end{aligned}
$$

In this part, performance indicators from IGDR input products or IGDR L2P (used in DUACS system) are presented. L2P updates that are then applied (ocean tide correction, mean sea surface model, mog2d dynamical atmospheric correction) are detailed in [21]. Note that comparisons between Jason-3 and Jason-2 have been done from Jason-3 cycle 1 to 58 only (Jason-2 cycles 281 to 506).

5.2. Mean of SSH crossover differences

The cycle by cycle mean of SSH differences is plotted in figure 47 for Jason-3 for IGDRs and GDRs. Mean of SSH differences at crossovers for Jason-3 IGDR products has noticeable negative values in average (-0.09cm for IGDR versus -0.01cm for GDR): mainly link to negative values over IGDR in standard D period.
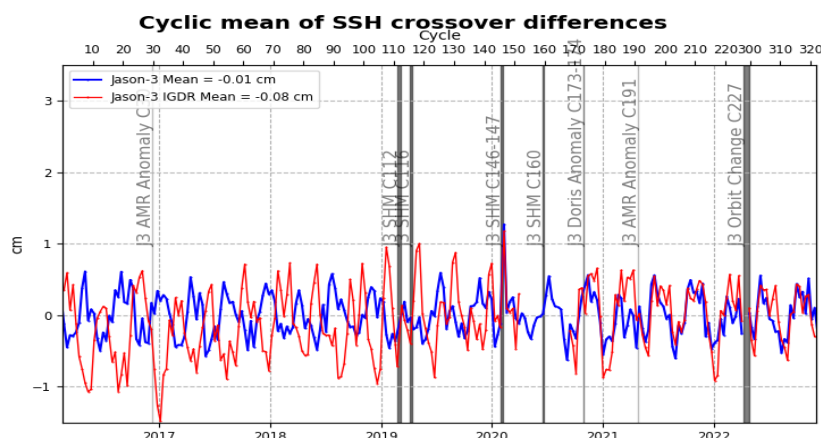

Figure 47 – Monitoring of mean of Jason-3 SSH crossover differences for IGDRs and GDRs. Only data with $|latitude| < 50°$, bathymetry < -1000m and low oceanic variability were selected. (ocean_tide_fes = FES14B is used in SSH computation)

The maps of mean SSH crossover differences on figure 48 were calculated using GDR-F products for Jason-3 *(left)* and Jason-2 GDR-D *(right)*. These maps highlight reduced small geographic patterns for Jason-3 compared to Jason-2 (see [5] part 4.1).
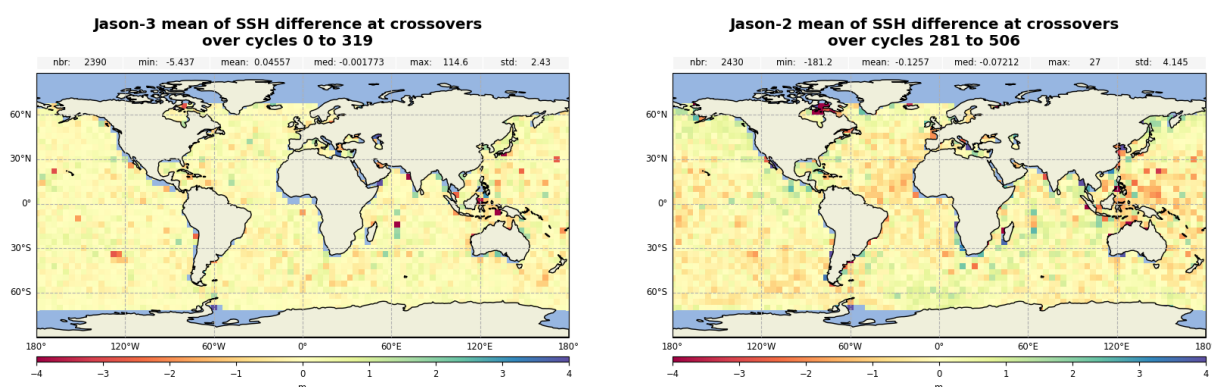

Figure 48 – Map of SSH crossovers differences mean for Jason-3 cycle 0 to 319 (left) and for Jason-2 cycle 281 to 506 (right)

Dual-mission crossover performances are computed between Jason-3 GDR-D and Jason-2 GDR-D and presented figure 49. Mean SSH differences at Jason 3/Jason 2 crossovers is quite stable and around 3 cm in average. The geographical pattern indicates some hemispheric biases, positive to the west, negative to the east. It corresponds to orbital signatures observed on sea surface height (right side of figure 49). Note that these 3 cm are due to processing differences as colocated Jason-2 minus Jason-3 non-corrected SLA (orbit - range - MSS) differences averaged over the period of tandem phase (cycle 001 to 023) shows an equivalent
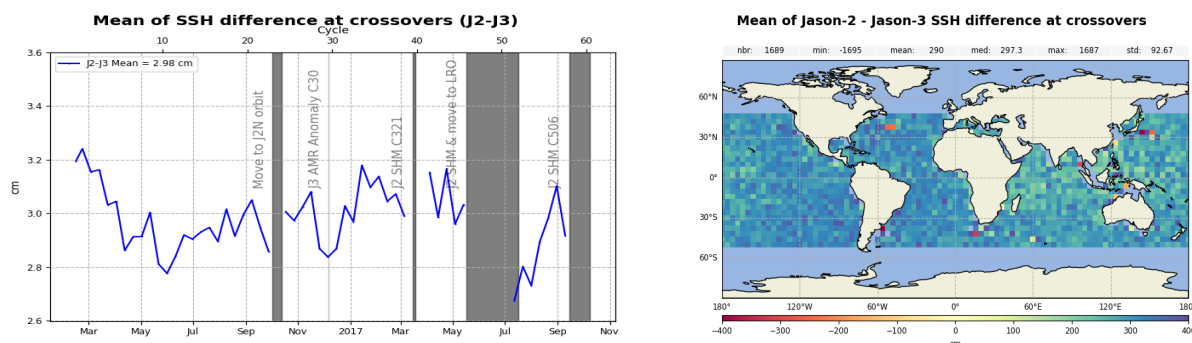
bias (left side of figure **??**).

Figure 49 – Cyclic monitoring of Jason-2 - Jason-3 SSH crossover differences mean (left) and map over cycle 1 to 58 (right). Only data with $|latitude| < 50°$, bathymetry $< -1000m$ and low oceanic variability were selected (for both missions, GDR-D data are used for these figures).

5.3. Standard deviation of SSH crossover differences

The cycle by cycle standard deviation of SSH crossovers differences are plotted for Jason-3 and Jason-2 in figure 50 after applying geographical criteria (bathymetry, latitude, oceanic variability). This metric allows to estimate the system noise by dividing by $\sqrt{2}$ (which leads to 3.48 cm for Jason-2 GDR-D and 3.39 cm for Jason-3 GDR-F). Both missions show very good performances, very similar and stable in time. No anomaly is detected. Thanks to GDR-F reprocessing, this indicator is significantly reduced for Jason-3 with regards to Jason-2 (and particularly the use of the filtered ionospheric correction, see part 4.1.1 of [5]).
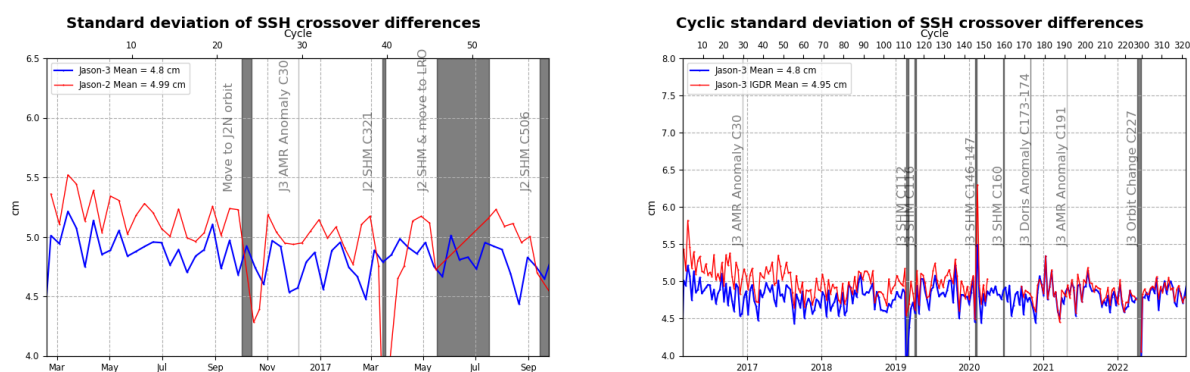

*Figure 50 – Cycle by cycle standard deviation of SSH crossover differences for Jason-2 and Jason-3 (**left**), and for Jason-3 using OGDRs, IGDRs and GDRs (**right**). Only data with $|latitude| < 50°$, bathymetry $< -1000m$ and low oceanic variability were selected.*

5.4. Estimation of pseudo time-tag bias

The pseudo time tag bias (α) is found by computing at SSH crossovers a regression between SSH and orbital altitude rate ($\dot{H}$), also called satellite radial speed: $SSH = \alpha \dot{H}$.

This empirical method allows us to estimate the potential real time tag bias but it can also absorb other errors correlated with $\dot{H}$. Therefore it is called "pseudo" time tag bias. The monitoring of this coefficient estimated at each cycle is performed for Jason-2 and Jason-3 in figure 51. Both curves are very similar highlighting an almost 59-day signal with almost no bias (close to -0.01 ms for Jason-3). Both missions present 59 and 117 day signals. Thanks to POE-F and FES14B ocean tide, there is a significant reduction of the 59-days signal and a small reduction of the 117 days signal (compared to previous version GDRD). The 90-days signal is slightly observed with GOT ocean tide but not with FES.
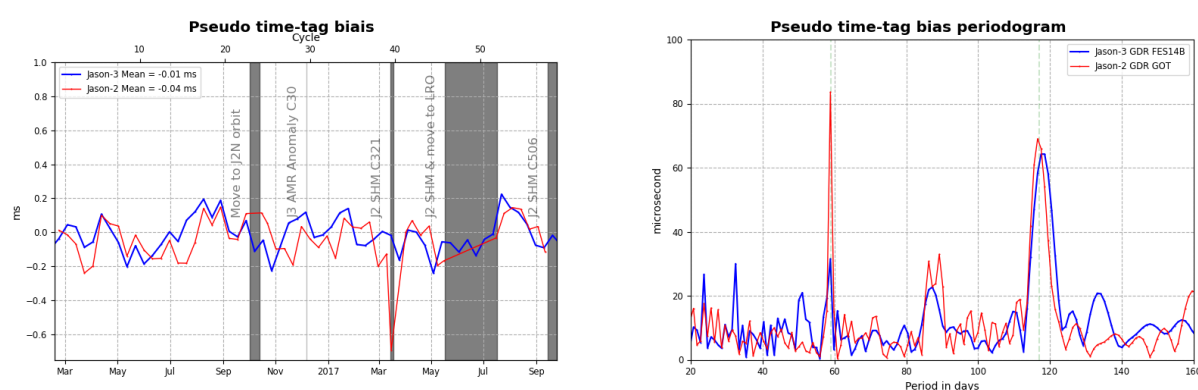

Figure 51 – Monitoring (left) and periodogram (right) of pseudo time-tag bias estimated cycle by cycle from GDR products for Jason-2 and Jason-3

6. Sea Level Anomalies (SLA) Along-track analysis

6.1. Overview

The Sea Level Anomalies (SLA) are computed along track from the substraction of the mean sea surface to the SSH, with the SSH calculated as defined in previous section 5.1. : $SLA = SSH - MSS$. SLA analysis is a complementary indicator to estimate the altimetry system performances. It allows to study the evolution of SLA mean (detection of jump, abnormal trend or geographical correlated biases), and also the evolution of the SLA variance highlighting the long-term stability of the altimetry system performances. In order to take advantage of the Jason-3/Jason-2 tandem flight (cycles 1 to 23), we performed direct SLA comparisons between both missions during this period.

6.2. Mean of SLA for Jason-3 and Jason-2

The daily monitoring of mean SLA for Jason-2 and Jason-3 is computed on figure 52. During this period, both types of curves are very similar and stable in time with variations close to 1 mm rms, except that they are spaced out by a 0.75 cm bias (0.61 cm when using ECMWF model wet troposphere correction). This bias can result from differences between Jason-3 and Jason-2 sea state bias model used, and to a small amount due to ionosphere correction differences. The global average SSH bias is close to 2.98 cm using SSH corrections (2.84 cm when using ECMWF instead of radiometer wet troposphere correction) and 2.23 cm without. However, the most crucial point for scientific applications was to ensure that there is no drift between both missions, since the global bias can be corrected a fortiori.
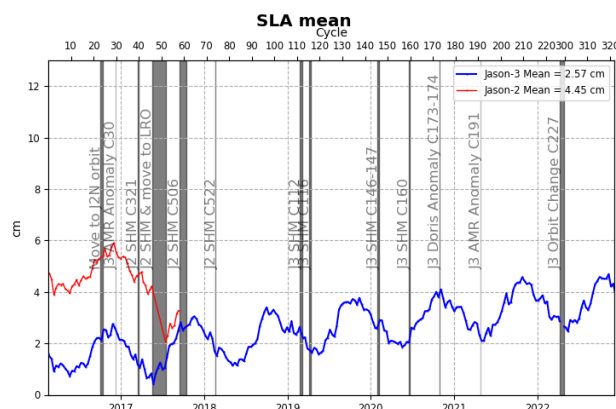

Figure 52 – Daily monitoring of SSH bias between Jason-2 and Jason-3 before Jason-2 moved to interleaved ground-track in October 2016 (using GDRD data for Jason-2 only).

6.3. Standard deviation of SLA for Jason-3 and Jason-2

The monitoring of SLA standard deviation has been computed for both missions (figure 53).

Note that this metric is very dependant to the MSS reference solution used to compute SLA.

Standard deviation of SLA from L2P products (Jason-2 and Jason-3 figure) are lower than with IGDR or GDR thanks to L2P updates that include a change from product MSS referenced on 7 years to a solution referenced on 20 years.

The figure aligning IGDR and GDR data for Jason-3 shows an almost perfect superposition all over 2022 due to the common standard "F" over this period.

Cartography of standard deviation of spatial Jason-3 minus Jason-2 SLA differences (not shown here) does not show any anomaly. It varies indeed in function of noise on measurements, which depends on significant wave height. Therefore, standard deviation of SLA differences is higher in regions with important significant wave heights.

Jason-3 in standard "F" is homogeneous with the CNES/CLS15 MSS and the filtered ionospheric correction, this reduces the along-track SLA std compared to standard "D" (see [5] part 4.2).
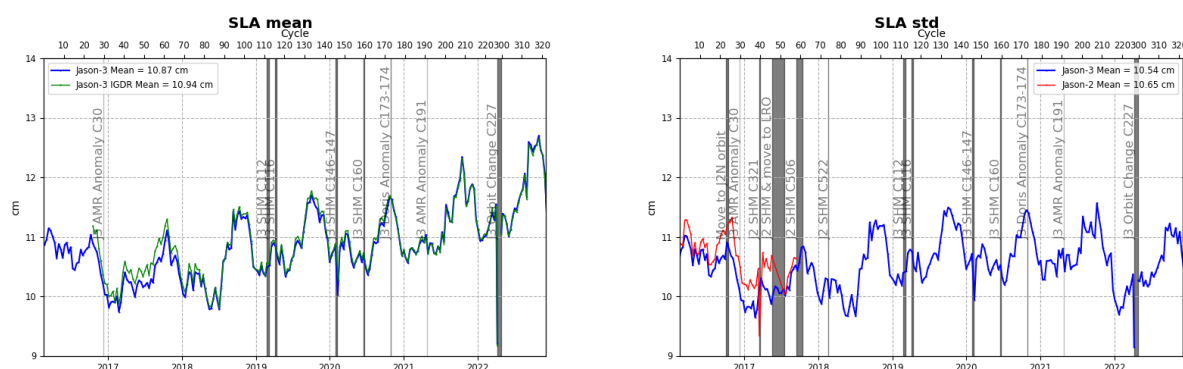

*Figure 53 – Cyclic monitoring of along-track SLA standard deviation. Jason-3 IGDRs and GDRs (**left**). Jason-2 and Jason-3 GDRs residuals (=interpolated over theorical ground track)(**right**)*

6.4.   Sea level seasonal variations

From Sea Level Anomalies computed relative to the Mean Sea Surface CNES/CLS15, the surface topography seasonal variations have been mapped in table 6 for the overall Jason-3 data set. Major oceanic signals are shown clearly by these maps: it allows us to assess the data quality for oceanographic applications.

The most important changes are observed in the equatorial band with the development of La Niña. The map of SLA over Winter 2021 echoes the one over Winter 2018 with a signature of height diminution over the Pacific Ocean (but a little bit weaker in 2021).
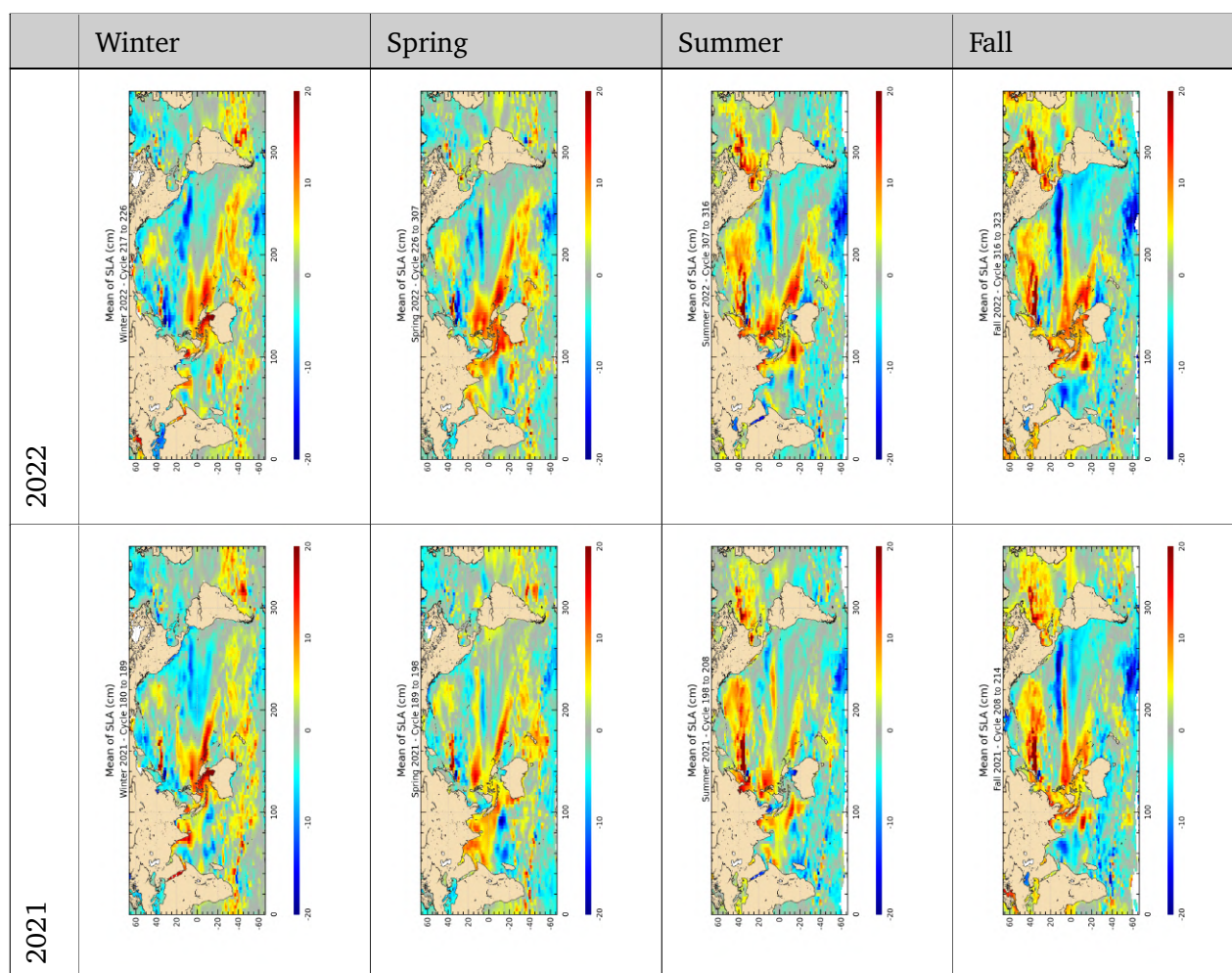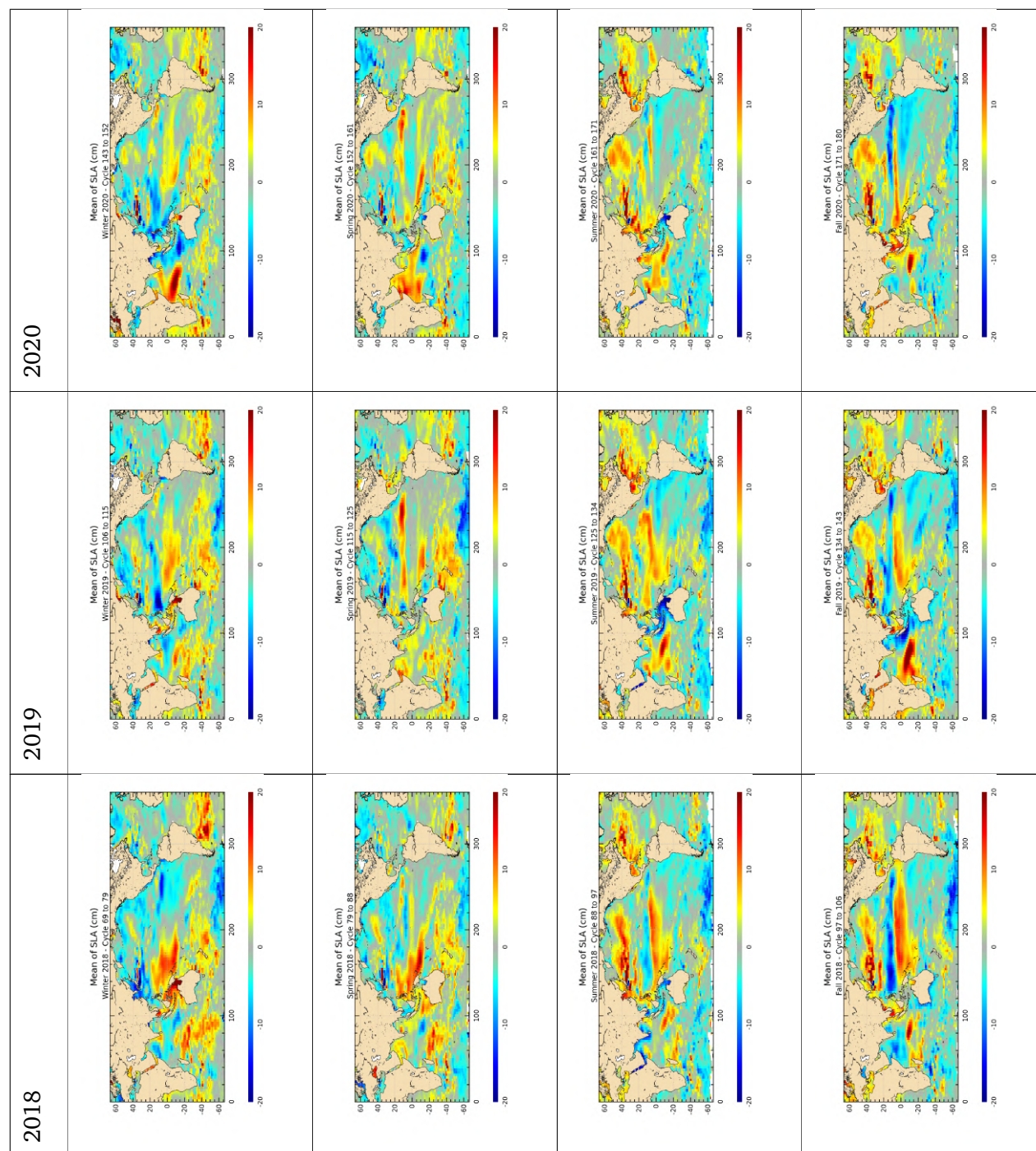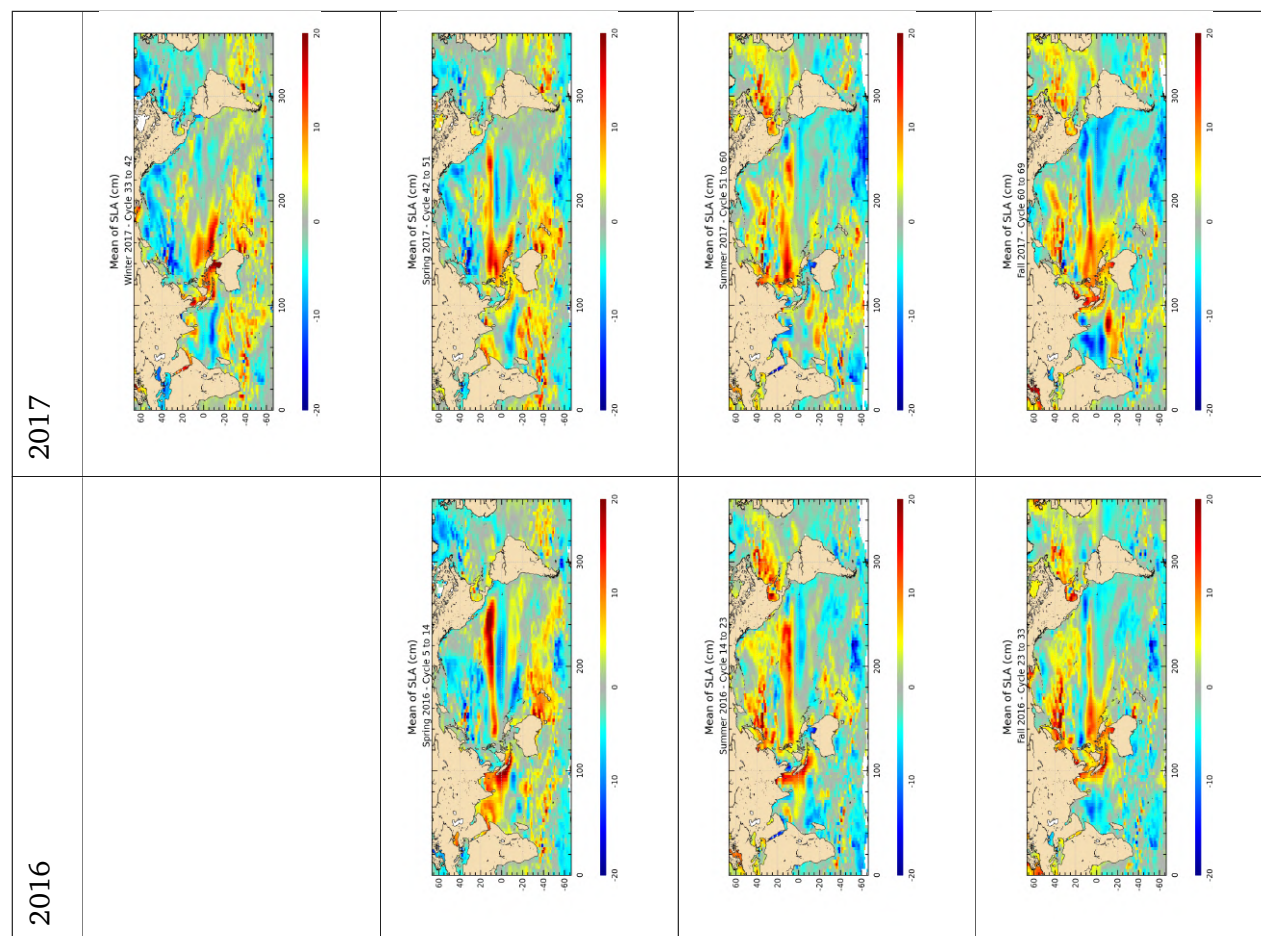
Table 6 – Seasonal variations of Jason SLA (cm) for years 2016 to 2022
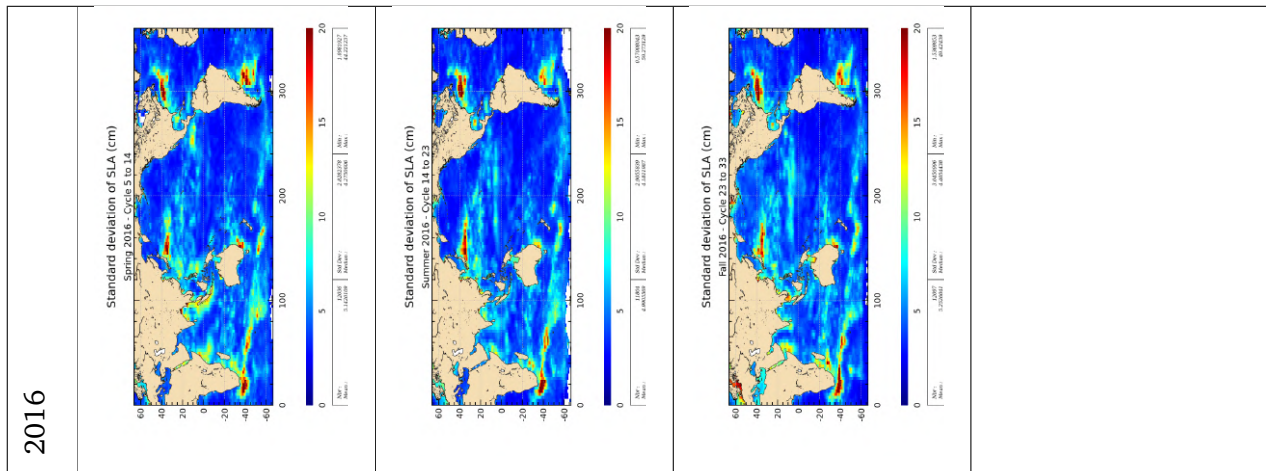
	Winter	Spring	Summer	Fall
2022				
2021				
2020				
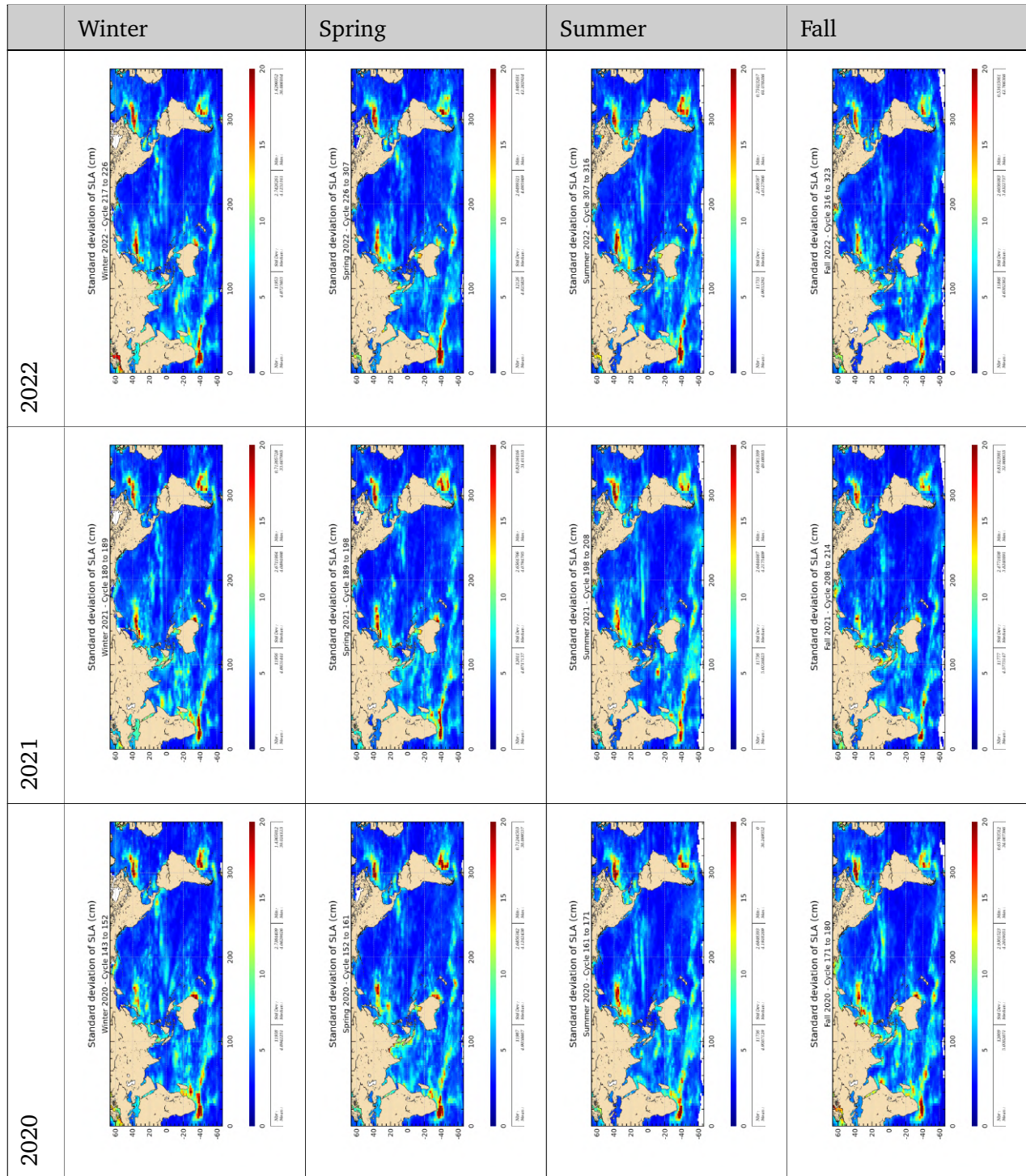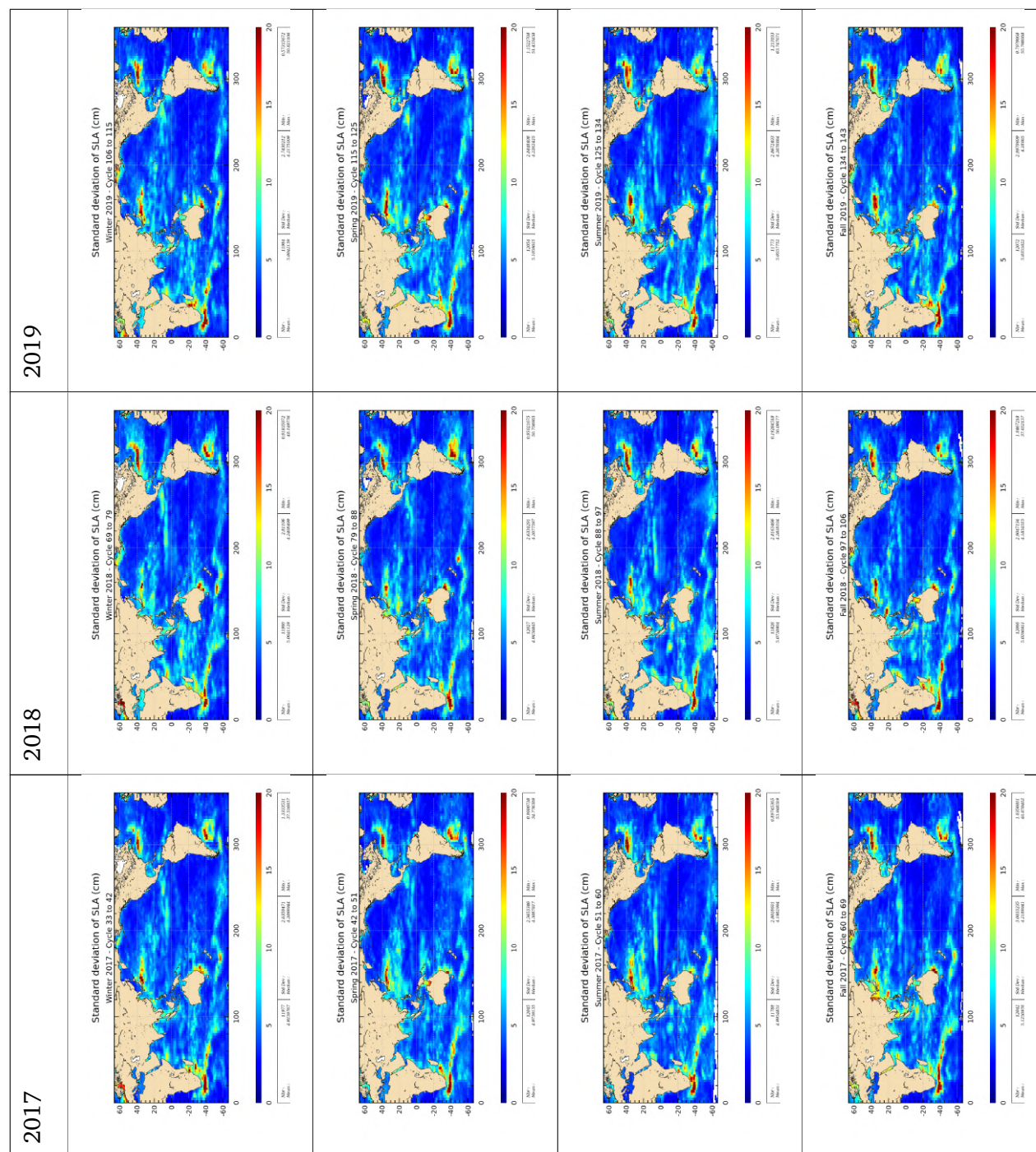
Table 7 – Seasonal variations of Jason SLA standard deviation (cm) for years 2016 to 2022

7. Mean Sea Level (MSL) trends

7.1. Computation of the Mean Sea Level

For more details about Mean Sea Level (MSL) studies method, see the dedicated annual report of activities [?] on MSL Aviso Website: http://www.aviso.altimetry.fr/msl. This report includes the description of the Mean Sea Level indicator, the comparisons between altimetry and tide gaudes measurements, the comparisons between altimetry and *ARGO+GRACE* measurements and specific studies linked to MSL activities.

Data from Jason-3 mission were introduced in DUACS system end of September 2016 (when Jason-2 moved to its new interleaved orbit). Over the tandem phase of Jason-3 (till cycle 023), both Jason-2 and Jason-3 satellites flew on the same ground track, only 1mn20s apart. They therefore measured the same features, allowing to calibrate Jason-3. This allowed to link precisely the MSL time series of Jason-2 and Jason-3. The uncertainty of the bias value between the two time series is less than 1 mm. The evolution of the ocean MSL can therefore be precisely observed on a continual basis since 1993 thanks to the 4 reference missions: TOPEX/Poseidon, Jason-1 (from may 2002 to october 2008), Jason-2 (from october 2008 to may 2016) and now Jason-3 (since june 2016).

Wet troposphere correction, inverse barometer correction, GIA (-0.3 mm/yr) are applied to calculate the MSL and the data series are linked together accurately thanks to the tandem flying phases. The following global bias are applied: 1.16 cm between T/P&Jason-1, 0.23 cm between Jason-1/Jason-2 and -2.97 cm between Jason-2/Jason-3. An exhaustive overview over possible errors impacting the MSL evolution is given in [?]. Furthermore, annual and semi-annual signals are removed from the time serie and a 2-month filter is applied. For more details, see MSL Aviso Website: http://www.aviso.altimetry.fr/msl.

Though mean sea level trend is globally positive, it is inhomogeneous distributed over the ocean: locally, sea level rise or decline up to ±10 mm/yr are observed on right panel of figure 54 (note that this map of regional MSL trends is estimated from multi-mission grids (Ssalto/DUACS products) in order to improve spatial resolution).
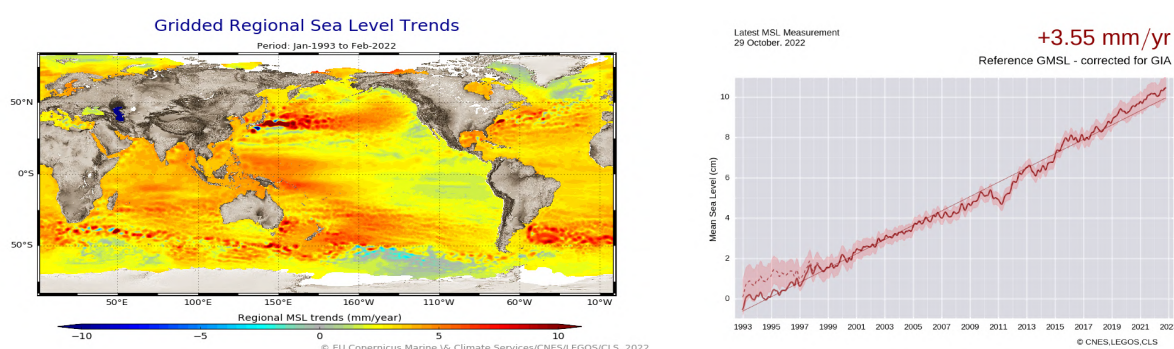

Figure 54 – Global (right) and regional (left) MSL trends from 1993 onwards.

8. Particular points and investigations

8.1. Change to the interleaved orbit

From the 7th of April to the 22nd of April 2022, Jason-3 moved from its reference orbit to the interleaved position. This operation was successful and the Poseidon altimeter had to be shut down during the whole maneuver. After the maneuver, all radiometer and altimeter parameters had to be assessed.

8.1.1. Data availability

The altimeter was switched back on on the 25th of April (cycle 300 pass 159). Over the first passes, the amount of missing points per pass was higher than the usual, especially in the Southern Hemisphere.
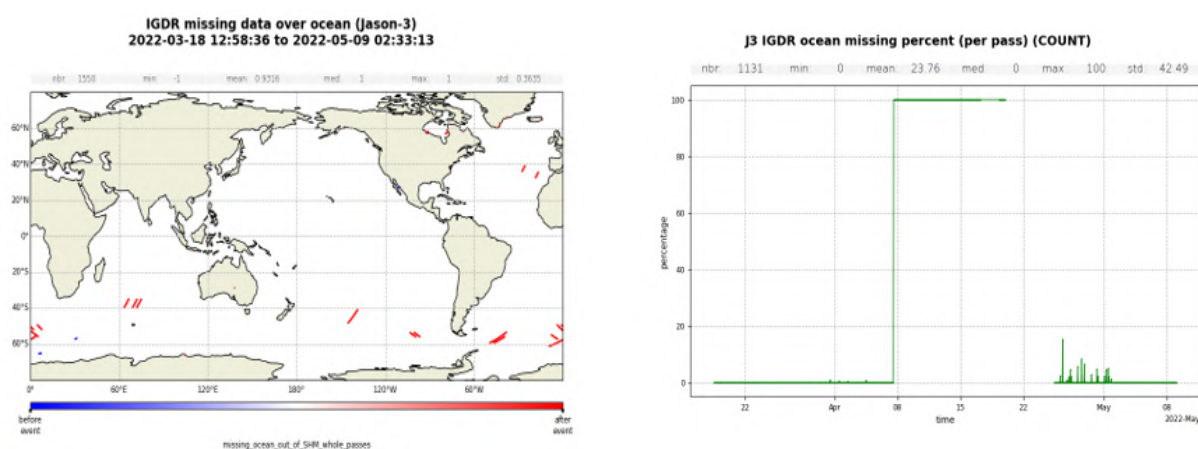

Figure 55 – IGDR data. Map and plot of Jason-3 IGDR missing data before and after the orbit change.

8.1.2. Edited data

The radiometer was not switched off during the whole orbit change but the first passes showed a strong pattern of rejected points on threshold for the wet troposphere criterion. For this reason, a reset of the radiometer was performed between 28/04/2022 15:55:45 and 28/04/2022 22:07:50. After the reset, the level of wet troposphere correction measurements fell back to what was previously observed.

8.1.3. SLA validity

When looking at the stability of the SLA measurements, the orbit change had no impact on the instruments' performances as seen in figure 57.

These diagnostics validated the good performance of all on-board instruments in the new orbit, permitting to start a new use phase of the Jason-3 satellite.
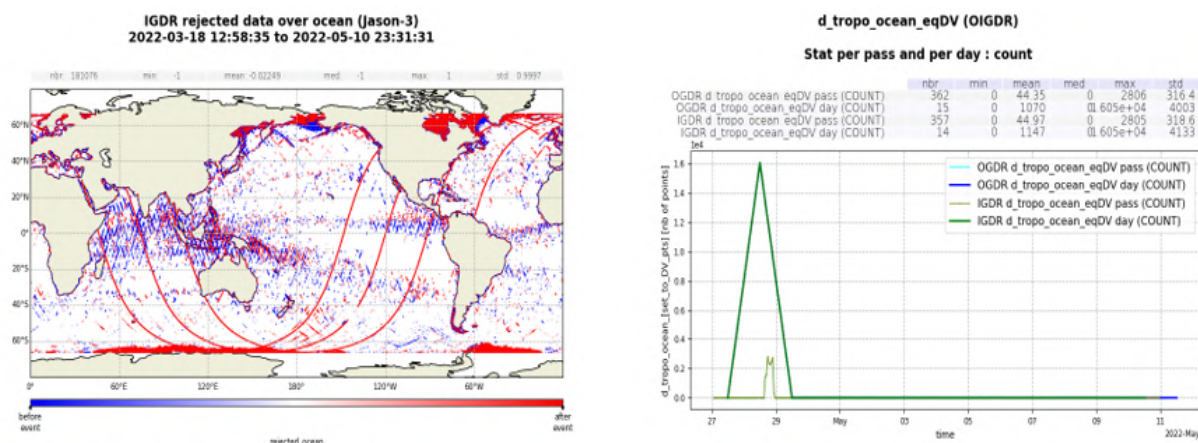
Figure 56 – IGDR data. Map and plot of Jason-3 edited data due to wet troposphere correction before and after the orbit change.
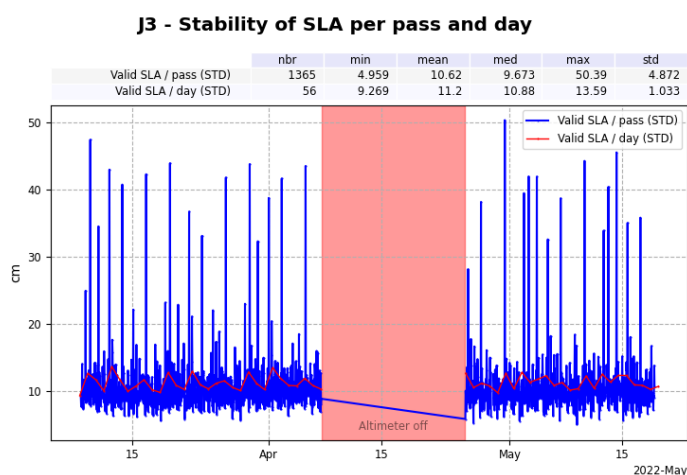

Figure 57 – GDR data. Evolution of the standard deviation of the SLA before and after the orbit change.

8.2. Orbit anomalies over Hawaii

Over the second semester of 2022, numerous jumps in the orbit measurements were measured when flying over Hawaii. This was identified as a DIODE beacon anomaly.

8.2.1. Orbit signal difference
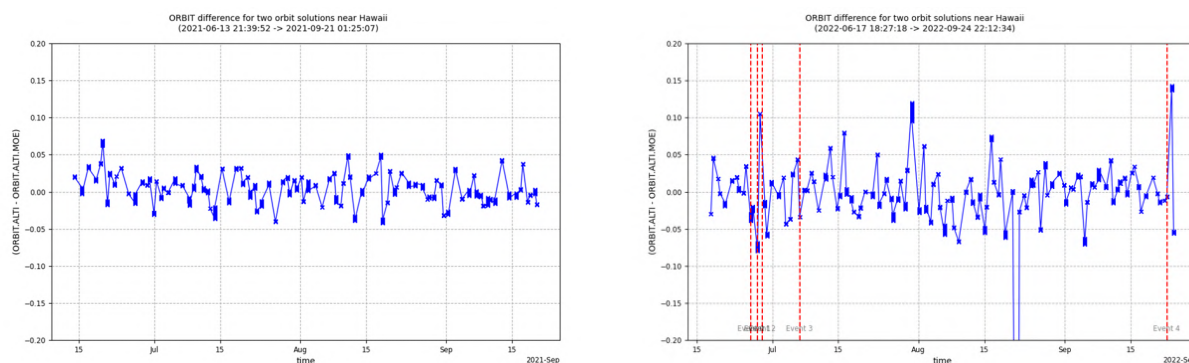
Figure 58 – Plot of orbit solution difference over Hawaii (left=2021, right=2022).

From figure 58, it appears that these peaks started over 2022 and are visible when comparing the DIODE orbit solution to the MOE. This confirms that this anomaly is only due to the DIODE data above Hawaii and are therefore due to the Hawai DIODE beacon.

8.2.2. Impact over SLA

As seen in figure 59, the SLA is almost not impacted by these orbit solution peaks as these occur in coastal areas which are edited for the SLA data. Yet, one peak is visible for cycle 307 (07/07/2022) and some others might occur in the future. For this reason, the DIODE beacon is to be replaced.

Figure 59 – SSHA O/IGDR data over Hawai between June and September 2022.

9. Conclusion

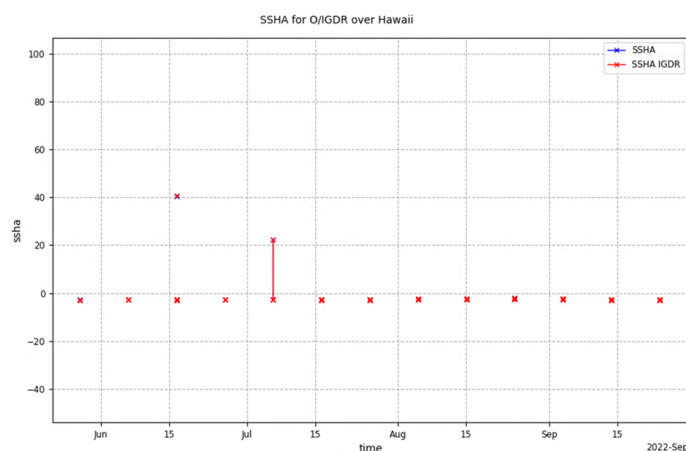Jason-3 was launched on January 17th, 2016. Since February 12th, Jason-3 was on its operational orbit following Jason-2 with 80 seconds delay on the same ground track. OGDR/IGDR products were opened to users end of June 2016, whereas the GDR products were available from November 2016 onwards.

The verification phase allowed extensive analysis and validation of the data, as both satellites observed the same geophysical phenomena until October 2nd 2016 when Jason-2 was moved to its interleaved ground track. This tandem flight phase has shown that Jason-3 data quality is excellent, at least of the same order as the Jason-2 one.

The main points of the performance assessment are summarized below:

- Ocean data availability is excellent and similar between Jason-3 and Jason-2 with a percentage greater than 99.9% after removing specific events.

- Data quality is also very good with less than 4% of measurements not consistent with altimeter and radiometer parameters threshold criterion. Jason-2 presents an equivalent percentage of edited data.

- The altimetry parameters analysis highlights a similar behaviour compared to Jason-2. Some biases exist as between dual-frequency ionosphere correction, but they are stable.

- At crossovers, Jason-3 shows performance similar to Jason-2 with a standard deviation lower than 5 cm. However mean difference analysis highlights a 120-days signal, which is present for both missions but was reduced for Jason-3 using new standard "F".

- At crossovers between Jason-3 and Jason-2, SSH performance presents excellent results with an SLA biais of about 3 cm. The consistency between both SLA is good with a small geographically correlated signal (lower than 0.5 cm in GDR) due to orbit quality.

Thanks to these good results, Jason-3 became the reference mission to ensure the continuity of Global Mean Sea Level monitoring on September 2016.

This reference role was transmitted to Sentinel-6 in April 2022 after the end of Jason-3/Sentinel-6 tandem phase.

Data production has followed standards F for OGDR and IGDR from cycle 174 onwards, and has been entirely reprocessed in this new standard for GDR. The reprocessing in GDR-F, including the update of mean sea surface, pole tide, internal tides, ocean tides and sea state bias allowed to significantly improve the quality of Jason-3 products over all the mission data.

10. References

References

[1] Analysis of the Sentinel-6A SLA biais correction at https://www.aviso.altimetry.fr/fileadmin/documents/data/tools/bias_S6ASAR_L2PL3_forORR.pdf

[2] Jason-3 cyclic reports available at https://www.aviso.altimetry.fr/en/data/calval/systematic-calval/validation-reports/jason-3-gdr.html

[3] Jason-3 product description available at https://www.aviso.altimetry.fr/fileadmin/documents/data/tools/product_description_j3.pdf

[4] Jason-3 handbook available at https://www.aviso.altimetry.fr/fileadmin/documents/data/tools/hdbk_j3.pdf

[5] Jason-3 validation of GDR-F data over ocean https://www.aviso.altimetry.fr/fileadmin/documents/calval/validation_report/J3/SALP-RP-MA-EA-23480-CLS_Jason3_Reprocessing_Report_v1-2.pdf

[6] Mean Sea Level informations in AVISO. https://www.aviso.altimetry.fr/en/data/products/ocean-indicators-products/mean-sea-level.html

[7] Flamant B. Jason-3 validation and cross calibration activities (Annual report 2021). https://www.aviso.altimetry.fr/fileadmin/documents/calval/validation_report/J3/SALP-RP-MA-EA-23528-CLS_Jason3_AnnualReport_2021_v1-3.pdf

[8] Roinard H. Jason-3 validation and cross calibration activities (Annual report 2020). https://www.aviso.altimetry.fr/fileadmin/documents/calval/validation_report/J3/SALP-RP-MA-EA-23473-CLS_Jason-3_AnnualReport2020_v1-1.pdf

[9] P. Thibaut et al., "Benefits of the "Adaptive Retracking Solution" for the JASON-3 GDR-F Reprocessing Campaign," 2021 IEEE International Geoscience and Remote Sensing Symposium IGARSS, 2021, pp. 7422-7425, doi: 10.1109/IGARSS47720.2021.9553647. Available at https://www.aviso.altimetry.fr/fileadmin/documents/data/tools/NT-Thibaut_AdaptiveRetrackingForJason3GDRF.pdf

[10] Benefits of the Adaptive Algorithm for Retracking Altimeter Nadir Echoes: Results From Simulations and CFOSAT/SWIM Observations. IEEE Transactions on Geoscience and Remote Sensing. 2021-journal-article. DOI: 10.1109/TGRS.2021.3064236

[11] Ngan Tran (CLS, France), Gerald Dibarboure (CNES, France), Nicolas Picot (CNES, France). Improving the continuity of the Jason SSB time-series. https://meetings.aviso.altimetry.fr/fileadmin/user_upload/tx_ausyclsseminar/files/Poster_OSTST18_SSB_tran.pdf

[12] Nencioli Francesco, Roinard Hélène, Bignalet-Cazalet Francois. 2021. Filtering ionospheric correction from altimetry dual-frequencies solution. DOI 10.24400/527896/a02- 2021.001. Available at https://www.aviso.altimetry.fr/fileadmin/documents/data/tools/NT-Nencioli_FilteredIonosphericCorrection.pdf

[13] Roinard H.. Jason-3 validation and cross calibration activities (Annual report 2017). SALP-RP-MA-EA-23187-CLS. https://www.aviso.altimetry.fr/fileadmin/documents/calval/validation_report/J3/SALP-RP-MA-EA-23187-CLS_Jason-3_AnnualReport2017_v1-2.pdf

[14] Brown G.S., "The average impulse response of a rough surface and its application", *IEEE Transactions on Antenna and Propagation*, Vol. AP 25, N1, pp. 67-74, Jan. 1977.

[15] Thibaut, P. O.Z. Zanifé, J.P. Dumont, J. Dorandeu, N. Picot, and P. Vincent, 2002. Data editing: The MQE criterion. *Paper presented at the Jason-1 and TOPEX/Poseidon Science Working Team Meeting, New-Orleans (USA), 21-23 October*.

[16] Obligis, E., L. Eymard, M. Ablain, B. Picard, J.F. Legeais, Y. Faugere and N. Picot, 2010. The wet tropospheric correction for altimetry missions: A mean sea level issue.*Oral presentation at OSTST meeting, Lisbon, Portugal*. Available at http://www.aviso.oceanobs.com/fileadmin/documents/OSTST/2010/oral/19_Tuesday/OBLIGIS.pdf.

[17] H. Roinard, E. Cadier. Jason-2 validation and cross calibration activities (Annual report 2017). Reference: SALP-RP-MA-EA-23186-CLS. Available at https://www.aviso.altimetry.fr/fileadmin/documents/calval/validation_report/J2/SALP-RP-MA-EA-23186-CLS_Jason-2_AnnualReport2017_v1-2.pdf.

[18] Roinard H.. Jason-3 validation and cross calibration activities (Annual report 2019). SALP-RP-MA-EA-23399-CLS.

[19] DUACS/Aviso team 'A new version of SSALTO/Duacs products available in April 2014' http://www.aviso.altimetry.fr/fileadmin/documents/data/duacs/Duacs2014.pdf

[20] A. Guerou. SALP annual report (2021) of Mean Sea Level Activities. Reference: SALP-RP-MA-EA-23541-CLS.

[21] Updates available for DUACS products. https://www.aviso.altimetry.fr/en/data/product-information/updates-and-reprocessing/ssalto/duacs-product-changes-and-updates.html

[22] Ray, R. D. and Ponte, R. M.: Barometric tides from ECMWF operational analyses, Ann. Geophys., 21, 1897–1910, https://doi.org/10.5194/angeo-21-1897-2003, 2003.